Las Vegas Ozone Study (LVOS)

Final Report (MOU #CBE 602948-13)
Clark County Department of Air Quality

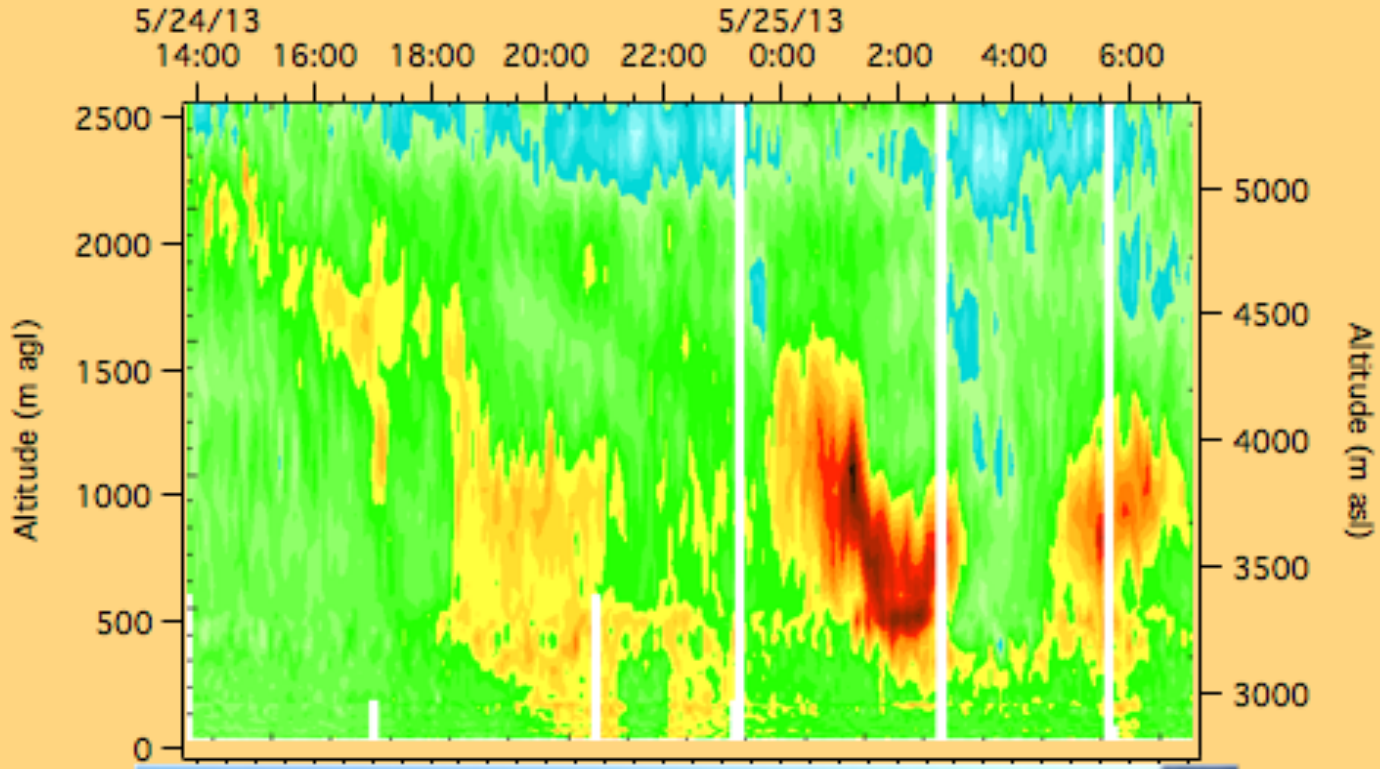

prepared by:
Dr. Andrew O. Langford
National Oceanic and Atmospheric Administration
Earth System Research Laboratory, Chemical Sciences Division

Disclaimer

The statements and conclusions in this Report are those of the author from the National Oceanic and Atmospheric Administration, and not necessarily those of the Clark County Department of Air Quality. The views, opinions, and findings contained in this report are those of the author(s) and should not be construed as an official National Oceanic and Atmospheric Administration or U.S. Government position, policy, or decision.

The mention of commercial products, their source, or their use in connection with material reported herein is not to be construed as actual or implied endorsement of such products.

July 25, 2014

This Report was submitted in fulfillment of the Memorandum of Agreement No. CBE 602948-13, between Clark County, Nevada and NOAA.

Cover: TOPAZ lidar truck and time-height curtain plot of ozone measured above Angel Peak on the night of May 24-25, 2013.

Acknowledgements

The successful execution of the Las Vegas Ozone Study (LVOS) required the efforts of many people. Personnel from the Boulder, Colorado based Chemical Sciences Division of the National Oceanic and Atmospheric Administration Earth System Research Laboratory (NOAA/ESRL/CSD) and from the Cooperative Institute for Research in Environmental Sciences (CIRES) at the University of Colorado conducted the measurement campaign. The TOPAZ lidar measurements were made possible by the hard work of Christoph Senff, Raul Alvarez, Scott Sandberg, Ann Weickmann, and Richard Marchbanks. John Holloway and Eric Williams provided the in situ CO and O_3 instrumentation and helped with the analysis, and Owen Cooper provided key satellite imagery. We are grateful to John Vimont of the U.S. National Park Service and Jessica Ward of Air Resource Specialists, Inc. for providing the 1-minute NPS ozone data. Mickey Turner and Andy Gagliardo from Clark County provided key logistical support to make the measurements at Angel Peak possible.

Interpretation of the LVOS measurements relied on the modeling efforts of Jerome Brioude of NOAA/ESRL/CSD and CIRES, Brad Pierce from the Center for Satellite Applications and Research at the Cooperative Institute for Meteorological Satellite Studies of NOAA and the University of Wisconsin, Patrick Reddy from the Colorado Department of Public Health and Environment, and Meiyun Lin from the NOAA Geophysical Research Laboratory and Princeton University Cooperative Institute for Climate Science. We would especially like to thank Zheng Li, Dennis Ransel, and their colleagues at the Clark County Department of Air Quality for their hospitality and support in the planning and execution of the Las Vegas Ozone Study (LVOS).

Finally, we would like to acknowledge additional support from the NOAA Health of the Atmosphere and Climate Programs and the NASA Tropospheric Ozone Lidar Network (TOLNet, http://www-air.larc.nasa.gov/missions/TOLNet/).

Executive Summary

The 2013 Las Vegas Ozone Study (LVOS) was conducted in the late spring and early summer of 2013 to assess the seasonal influence of stratosphere-to-troposphere transport (STT) and long-range transport from Asia (AS) on surface ozone (O_3) concentrations in Clark County, Nevada and to determine if these processes direct contribute to exceedances of the National Ambient Air Quality Standard (NAAQS) in Clark County. Secondary goals included characterization of local photochemical production and regional transport of O_3 from the Los Angeles Basin, and understanding the impacts of biomass burning (wildland fires) on O_3 concentrations in Clark County. In this report, we describe the LVOS campaign and summarize the results of the measurement and modeling efforts.

The LVOS measurements were made at a former U.S. Air Force radar station ~45 km northwest of Las Vegas on Angel Peak (~2.7 km above mean sea level, asl) in the Spring Mountains. The study consisted of two extended periods (May 19 - June 4 and June 22 - 28, 2013) with near daily 5-minute averaged lidar measurements of ozone and backscatter profiles from the surface to ~2.5 km above ground level (~5.2 km asl), and continuous in situ measurements (May 20 to June 28) of O_3, CO, (1-min) and meteorological parameters (5-min) at the surface. The measurement activities were guided by forecasts and analyses from the NOAA/ESRL/CSD FLEXPART particle dispersion model and the NOAA/NESDIS/CIMSS Real Time Air Quality Modeling System (RAQMS). Interpretation of the measurements was aided by support from the NOAA/ESRL/GFDL AM3 chemistry-climate model.

The 2008 NAAQS of 75 ppbv ozone for an 8-h average was exceeded by one or more of the regulatory monitors in Clark County on 6 different days during 2013, with 3 of those days occurring during the LVOS campaign (**Table** ES1). The LVOS measurements and supporting model analyses show that STT played a major role in 4 of these exceedances with transported pollution from Asia making

a small contribution to 3. The model analyses also suggest that wildland fires were partly responsible for the 3 high O_3 days that occurred before and after LVOS. Thus, our analyses suggest that all 6 of the O_3 exceedance days in Clark County during 2013 were influenced by transport from outside the county.

***Table** ES1: Exceedances of the 2008 NAAQS in Clark County during 2013.*

Date	Monitors	MDA8	STT (AM3)	Sources
May 4	6	84	23-34	STT, Asia, Springs Fire
May 21	**1**	**78**	**22-36**	**STT, Asia**
May 25	**4**	**76**	**28-33**	**STT**
June 21	**3**	**78**	**20-24**	**STT, Asia**
July 3	4	87	~2	Carpenter 1 Fire
July 20	1	76	~5	Mountain Fire

Exceedance days during LVOS are shown in **boldface**.

Our analyses also suggest that the role of STT, long-range transport, and wildland fires will become of even greater concern when the NAAQS is lowered below 75 ppbv. The mean surface MDA8 ozone in rural Clark County at Jean, NV was 67 ppbv during May and June of 2013, which is only 8 ppbv less than the 2008 NAAQS and greater than the 65 ppbv currently being considered (www.epa.gov/oaqps001/greenbk/hindex.html). The number of exceedance days in Clark County during the 43-day LVOS field campaign would have increased from 3 to 14 if the NAAQS had been 70 ppbv instead of 75 ppbv, and from 3 to 25 if the NAAQS had been 65 ppbv. In other words, exceedances of the NAAQS generated by natural sources would have occurred 60% of the time during LVOS, making these events the rule rather than the exception.

Table of Contents

List of Figures

Figure C2. RAQMS 310K distributions of O_3 and CO at 1200UT on June 25.

Figure C3. NCEP Reanalysis 500 hPa geopotentials hgts at 1200UT on June 29.

Figure C4. MDA8 O_3 at Clark County and NPS monitors during June 21-30.

Figure C5. 5-min O_3 in Clark County on June 27.

Figure C6. TOPAZ and in situ measurements from Angel Peak on June 27.

Definitions and Abbreviations

agl	above ground level
asl	above mean sea level
AS	Asian
BB	biomass burning
CC	Clark County
CIMSS	Cooperative Institute for Meteorological Satellite Studies
CIRES	Cooperative Institute for Research in Environmental Sciences
CSD	Chemical Sciences Division
DAQ	Department of Air Quality
ESRL	Earth System Research Laboratory
GFDL	Geophysical Fluid Dynamics Laboratory
LVOS	Las Vegas Ozone Study
LVV	Las Vegas Valley
MDA8	daily maximum 8-h average
NESDIS	NOAA's Satellite and Information Service
NOAA	National Oceanic and Atmospheric Administration
NPS	National Park Service
RAQMS	Realtime Air Quality Modeling System
NAAQS	National Ambient Air Quality Standard
ppbv	parts-per-billion-by-volume
SMYC	Spring Mountain Youth Camp
ST	stratospheric
STT	stratosphere-to-troposphere transport
TOPAZ	Tunable Optical Profiler for Aerosols and oZone
UT/LS	upper troposphere/lower stratosphere
WRCC	Western Regional Climate Center

1. Introduction

Surface ozone (O_3) has decreased dramatically across much of the eastern United States over the last two decades [*He et al.*, 2013; *Lefohn et al.*, 2010], largely as a result of stricter emission controls on stationary and mobile NO_x sources [*Butler et al.*, 2011; *EPA*, 2012]. More than 65% of the rural eastern U.S. sites surveyed in a recent study by *Cooper* et al. [2012] showed statistically significant decreases in median ozone during the summer with 43% also exhibiting significant decreases in the spring. In contrast, only 8% of the western U.S. rural sites examined showed similar summertime decreases, and more than 50% had significant springtime increases. These east-west differences have been partially attributed to increasing emissions of NO_x and other ozone precursors from industrial activities and development in East Asia [*Brown-Steiner and Hess*, 2011; *Jacob et al.*, 1999; *Zhang et al.*, 2011] and to a higher fraction of background ozone in the western U.S. due to stratospheric influence [*Lin et al.*, 2012a]

Much of the pollution emitted in East Asia is carried eastward across the North Pacific Ocean by the prevailing winds. The fastest transport occurs in the mid- and upper troposphere, often associated with Asian boundary layer pollution being entrained into the warm conveyer belts (WCB) of midlatitude cyclones, and these plumes can descend to the surface of western North America [*Brown-Steiner and Hess*, 2011; *Cooper et al.*, 2004b; *Liang et al.*, 2005; *Lin et al.*, 2012b; *Stohl*, 2001]. The high average elevation and deep boundary layers of the intermountain west increase the likelihood that some of this pollution may reach the surface as the plumes move inland and the transported pollution descends isentropically behind cold fronts [*Liang et al.*, 2004]. Asian pollution can also be transported to western North America at low altitude but only has a significant impact in summer [*Holzer and Hall*, 2007].

Stratosphere-to-troposphere transport (STT) also contributes to the relatively high background ozone in boundary layer air transported ashore from the north

Pacific during spring and can likewise lead to episodic increases at the surface [*Ambrose et al.*, 2011; *Langford et al.*, 2009; *Lefohn et al.*, 2011]. Direct transport of undiluted stratospheric air to the surface is uncommon, but some exchange of air between the upper troposphere and lower stratosphere occurs with all midlatitude cyclones [*Johnson and Viezee*, 1981] and a fraction of the ozone-rich air descending in the dry airstream (DA) may be entrained into the deep springtime boundary layers of the intermountain west. This descending air can also become interleaved with long-range transport layers in the WCB [*Cooper et al.*, 2004a; *Cooper et al.*, 2004b; *Stohl and Trickl*, 1999].

Several climatologies [*James et al.*, 2003; *Sprenger and Wernli*, 2003; *Wernli and Bourqui*, 2002] suggest that deep stratospheric intrusions (i.e. those penetrating to within ~3 km of the surface) are most likely to form near the exit of the east Pacific storm track above the Pacific Northwest with the deepest descent of stratospheric air near the coast of Southern California. These conclusions are consistent with measurements [*Langford et al.*, 2012] made during the 2010 California Research at the Nexus of Air Quality and Climate Change (CalNex) field study, and with analyses from the NOAA/GFDL AM3 global-high resolution (~50 x 50 km) chemistry–climate model. **Figure** 1 displays the mean contributions of (a) STT [*Lin et al.*, 2012a], and (b) transport from Asia [*Lin et al.*, 2012b] to the daily maximum 8-h average (MDA8) surface O_3 in the United States during May and June of 2010. These plots show the greatest impact of both transport processes to be in the Intermountain West with minimal contributions along the Gulf Coast and in the Southeastern United States. The striking similarity between the two plots reflects the primary role of midlatitude cyclones in both transport processes. The AM3 model shows the stratospheric contribution to surface ozone during May and June of 2010 to be roughly 3 times that of long-range transport.

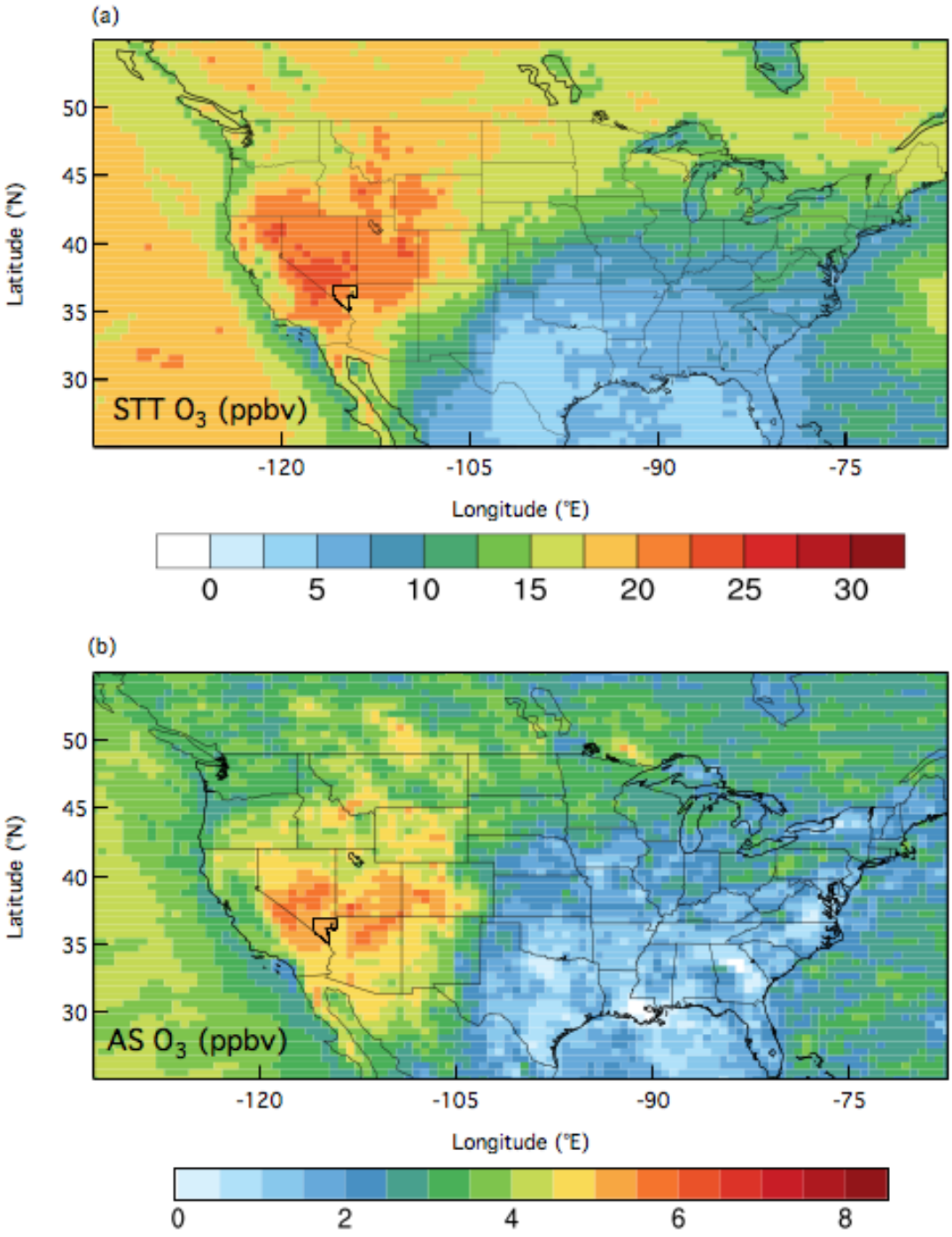

***Figure** 1. NOAA GFDL AM3 model mean contributions of (a) STT, and (b) Asian pollution, to MDA8 surface O_3 during May and June of 2010. The resolution is 50 km x 50 km. Note the different color scales. Clark County, NV is outlined in black. Adapted from Lin et al. [2012a, 2012b].*

Since the higher background concentrations and episodic increases associated with STT and Asian pollution are unaffected by local control strategies, these processes pose a serious challenge for air quality managers tasked with meeting the National Ambient Air Quality Standard (NAAQS) in the western United States. This is especially true in late spring when the contribution from local and regional photochemistry is also rapidly increasing. The problem will be compounded if the NAAQS is reduced from the current (2008) value of 75 parts-per-billion by volume (ppbv) for the MDA8 (http://www.epa.gov/oaqps001/greenbk/hindex.html). Although the U.S. EPA has established a provision (http://www.epa.gov/ttn/analysis/exevents.htm) to identify and exclude these "exceptional events", the shrinking margin between the NAAQS and increasing springtime background concentrations means that even modest episodic additions of 5 to 10 ppbv from STT or Asian pollution can potentially lead to exceedances of the NAAQS. Exceedance events will become increasingly frequent if the NAAQS is decreased to 70 ppbv or less, and the "exceptional events" approach may no longer be viable.

Concern about this problem and its implications for air quality management in Clark County, NV provided the motivation for the Las Vegas Ozone Study (LVOS) conducted in May and June of 2013. The primary goal of LVOS was to assess the seasonal contribution of stratosphere-to-troposphere transport (STT) and long-range transport to surface ozone in Clark County and to determine the magnitude of the direct contribution of these processes to exceedances of the National Ambient Air Quality Standard (NAAQS) in this area. Secondary goals included the characterization of local ozone production, regional transport from the Los Angeles Basin, and impacts from wildland fires. The work was funded primarily by the Clark County Department of Air Quality (CC/DAQ) and conducted by the NOAA Earth System Research Laboratory Chemical Sciences Division (ESRL/CSD).

2. Background

Clark County, Nevada (**Figure** 2) is home to the Las Vegas-Henderson-Paradise, NV Metropolitan Statistical Area (MSA), one of the fastest growing areas in the United States. The population of this MSA, which includes the cities of Las Vegas, Henderson, North Las Vegas, Boulder City, and Paradise, was slightly under 2 million in the 2010 U.S. Census or more than 70% of the total population of Nevada.

Nearly 40 million more people visit Las Vegas each year (http://www.lvcva.com/stats-and-facts/) and the 2011 National Emissions Inventory (http://www.epa.gov/ttn/chief/net/2011inventory.html) estimates that about 75% of the NO_x and 5% of the VOCs emitted in Clark County are derived from mobile sources. More than 90% of the emitted VOCs are derived from biogenic sources and about half of the remaining NO_x comes from one coal-fueled, and five natural gas-fueled power plants that provide about 5 MW of electricity for the area. Most of the population and development is confined to the Las Vegas Valley (LVV), a 1600 km^2 basin that lies between 500 and 900 m above mean sea level (asl) and is bounded on the west by the Spring Mountains and to the north by the Sheep Mountains, with the Muddy Mountains to the east and Black Mountains to the south. The I-15 corridor through the Mojave Desert and Cajon Pass links Las Vegas with the eastern Los Angeles Basin about 275 km to the southwest. The Cajon Pass and I-15 corridor is also a potential pathway for export of pollution from the Los Angeles Basin into the Mojave Desert and the Las Vegas Valley. The Clark County Department of Air Quality maintains a network of continuous ambient monitoring stations (CAMS) that measure surface ozone along with meteorological parameters and other trace gases (cf. **Figure** 2b).

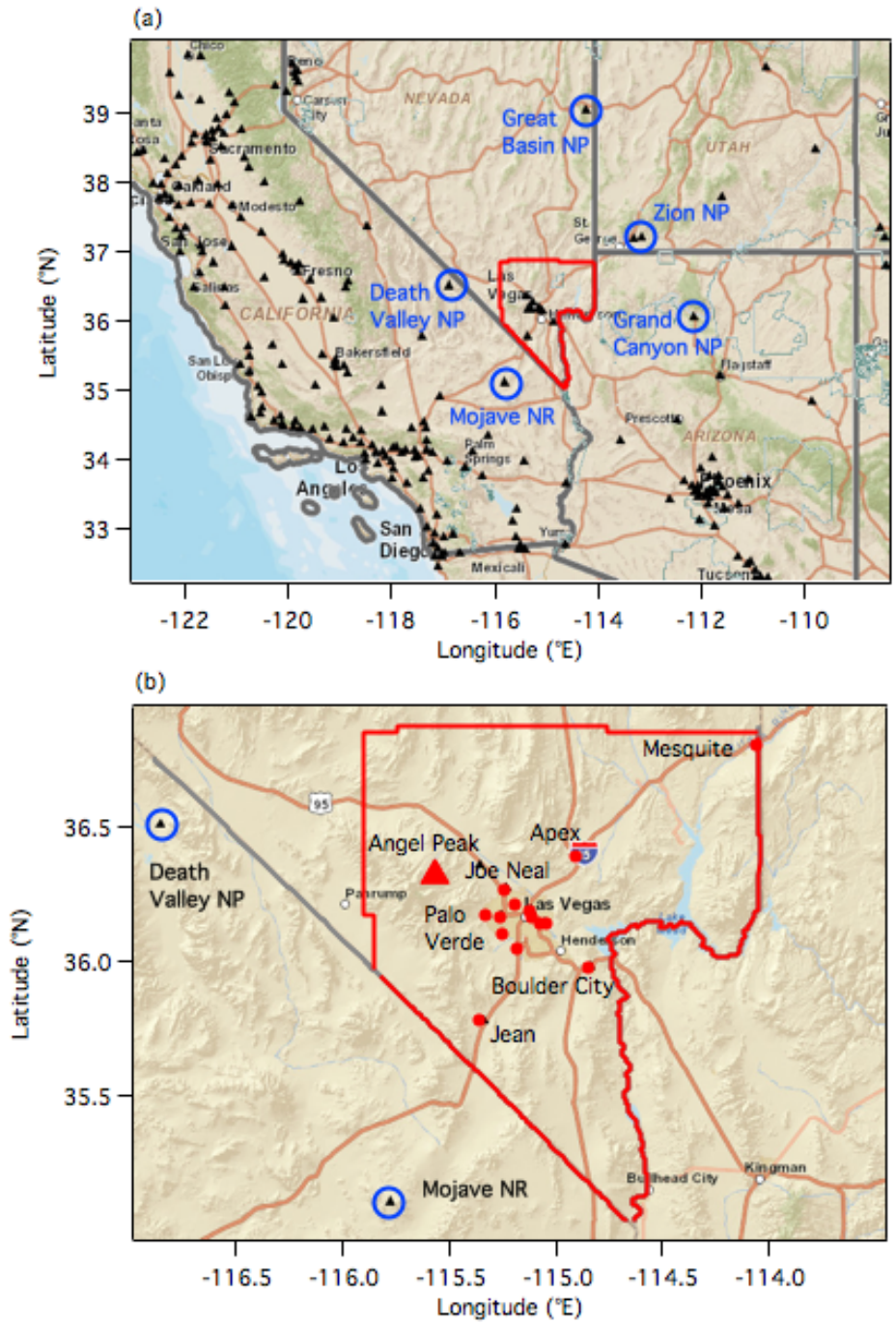

***Figure** 2. (a) Map of the southwestern U.S. showing regulatory O_3 monitors reporting to the U.S. EPA AirNow network (filled black triangles). The blue open circles identify regional monitors supported by the U.S. National Park Service. (b) Expanded view of Clark County with CC DAQ monitors represented by filled red circles. The large red triangle marks Angel Peak.*

Figure 3 plots the average MDA8 ozone measured at the monitoring station in Jean over the 3-yr period from 2010 to 2012. Jean is located along the I-15 corridor in the Mojave Desert about 45 km southwest of downtown Las Vegas at an elevation of 924 m asl. Since Jean is usually upwind of Las Vegas, but downwind of Los Angeles, it is the Clark County monitor least affected by local emissions, but most sensitive to transport from Southern California (Appendix A). **Figure** 3 also plots the corresponding time series from five monitors operated by the U.S. National Parks Service [2013] at remote locations surrounding Clark County (open circles in **Figure** 2a). The ozone seasonal cycle and the synoptic scale variability is very similar at all six sites with the highest concentrations in May and June or nearly two months before the maximum surface temperatures and greatest photochemical production. This suggests that it is primarily large-scale transport that determines the mean ozone at all six sites, although the influence of the LA Basin is seen in the slightly higher (1 to 4 ppbv) average concentrations at the Mojave National Reserve and at Jean during May and June. The sudden drop in ozone at all six sites in early July reflects the shift in the prevailing winds from southwesterly to southerly when the North American summer monsoon develops and the background concentrations are no longer determined by inflow from the Pacific.

Although Clark County is currently in attainment of the NAAQS (i.e. the 3-year average of the annual 4th highest measured MDA8 ozone concentration did not exceed 0.075 ppmv, parts-per-million by volume) based on data acquired between 2009 and 2011, the standard will be exceeded when more recent measurement periods are considered. The 3-year average (2010-2012) of the fourth highest MDA8 concentration was 0.075 ppmv or 75 ppbv at Jean, and 77 ppbv at Joe Neal, the northernmost monitor in the Las Vegas Valley (cf. **Figure** 2b). When the 2011-2013 data are used, the fourth highest value will still be 75 ppbv at Jean, but Joe Neal, Palo Verde, and two other Clark County monitors will be in exceedance.

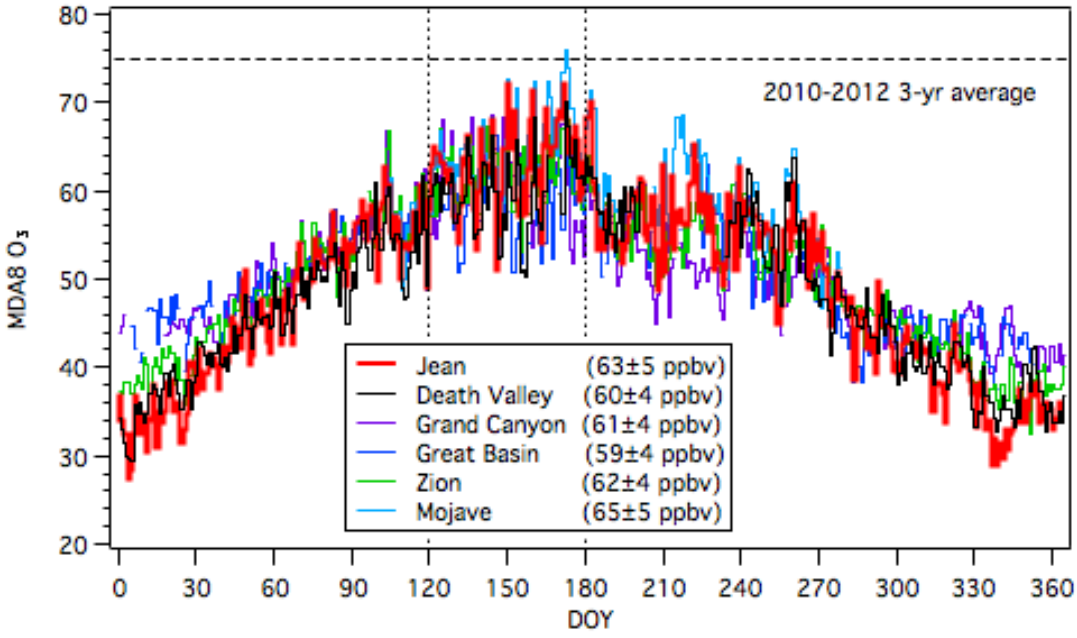

***Figure** 3. Mean MDA8 ozone measured by the CC/DAQ monitor at Jean, NV, Death Valley National Park, Great Basin National Park, Zion National Park, Grand Canyon National Park, and the Mojave National Reserve (seasonal) from 2010 to 2012. The mean values from each site during May and June (vertical dotted lines) are shown in the box. The horizontal dashed line indicates the 2008 8-h NAAQS of 75 ppbv.*

3. LVOS Measurement Campaign

3.1 Study location

The LVOS measurement campaign was conducted between May 19 and June 28, 2013 at a former U.S. Air Force General Surveillance Radar station atop Angel Peak (36.32 °N, 115.57 °W, 2,682 m asl) (**Figures** 4 and 5) about 45 km northwest of Las Vegas in the Spring Mountains and Toiyabe National Forest.

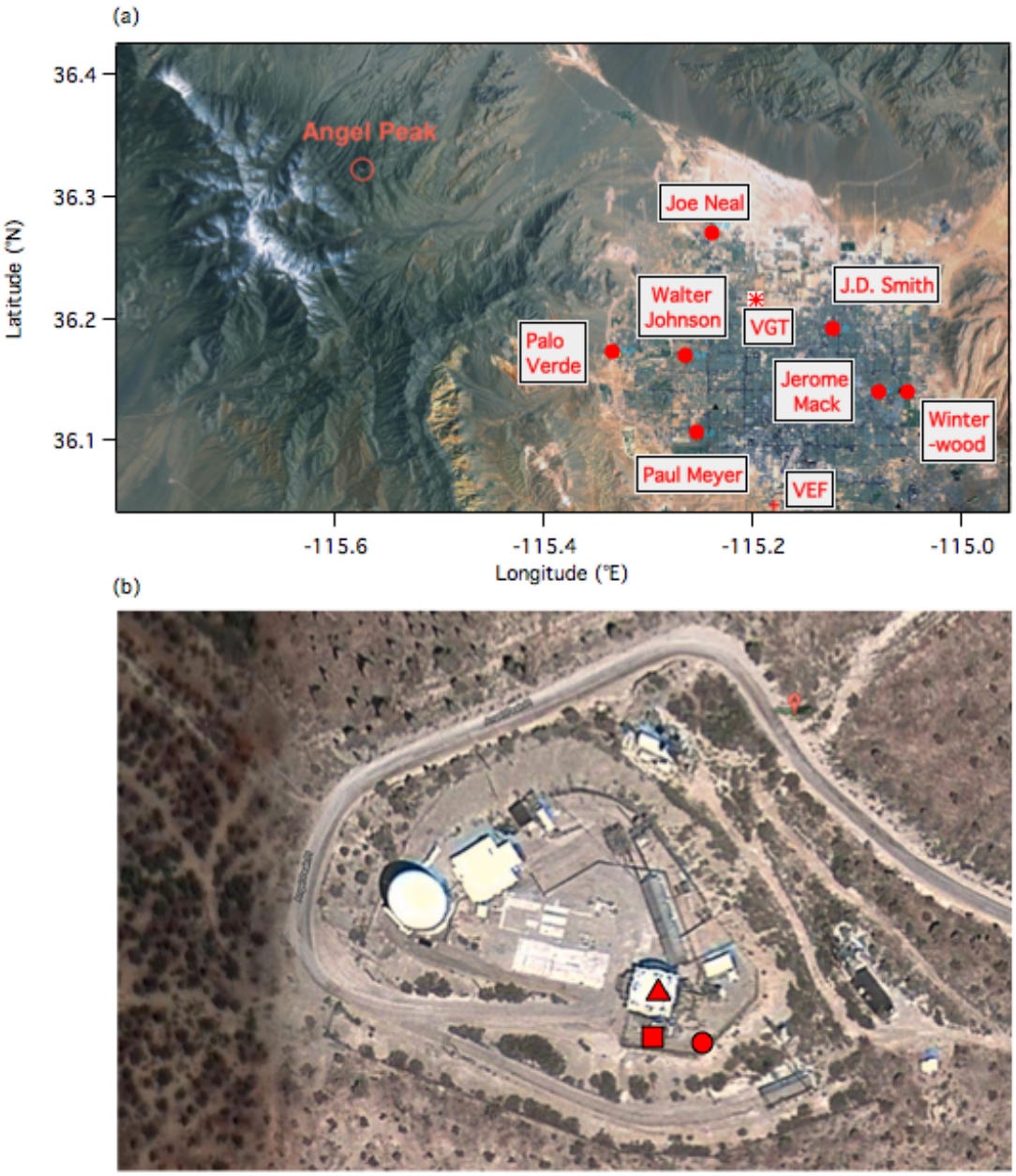

***Figure** 4. Satellite photographs from the U.S. EPA AirNow navigator showing (a) the location of Angel Peak relative to the Las Vegas Valley, and the CC/DAQ ozone monitors (filled circles) and airports (VEF, McCarran International Airport and VGT, North Las Vegas Airport). (b) Locations of TOPAZ (filled square), the in situ monitors (filled triangle), and the met station (filled circle) on the Angel Peak summit.*

***Figure** 5. Satellite photograph of the Angel Peak summit taken during the LVOS measurement campaign showing the TOPAZ truck parked next the former radome building.*

The radar station was decommissioned by the Air Force in 1969 and the property transferred to the Department of the Interior and to Clark County with the remaining operational radar system transferred to the Federal Aviation Administration (FAA). This limited-access site currently serves as a communications relay facility for Clark County and other state and federal agencies. The former cantonment area below the summit of Angel Peak was transferred to Clark County for operation as the Spring Mountain Youth Camp (SMYC). Angel Peak is relatively isolated from major emission sources and is usually exposed to free tropospheric air during the night. The summit overlooks

the Kyle Canyon drainage and the primary access road to the Las Vegas Valley to the southeast (**Figure** 6) and is frequently exposed to air transported from the Las Vegas Valley during late spring and summer when thermally driven upslope flows develop during the day and the mixed layer above the valley floor can grow to more than 4 km deep.

***Figure** 6. View from Angel Peak overlooking Kyle Canyon and the Las Vegas Valley to the southeast.*

The TOPAZ lidar truck was parked near the southeastern edge of the Angel Peak summit (**Figure** 7) at a fixed azimuth angle of 130° to overlook the Kyle Canyon drainage when the scanner was operated at low elevation angles (see below).

***Figure** 7. Views of the TOPAZ lidar truck at Angel Peak during LVOS.*

The in situ CO and O_3 instruments were installed within a temperature-regulated room in the former radar building nearest TOPAZ (cf. **Figures** 5 and 6), and sampled air at 1 standard liter per minute through 6 mm diameter and 30 m long PFA (polytetrafluoroethylene) lines. The inlets were equipped with 47 mm TFE (tetrafluroethylene) particulate filters and mounted ~2 m above the building roof or about 12 m above ground level (agl) (**Figure** 8a). The chemical measurements were complemented by a GPS-enabled weather station that recorded continuous 5-min averaged winds, temperature, and relative humidity

from a 3 m mast located near the southeastern edge of Angel Peak (**Figure** 8b). This position provided unobstructed fetch for wind directions between 45 and 270°, which occurred more than 75% of the time during the study. However, the anemometer was partially sheltered by the TOPAZ truck to the northwest and the building housing the in situ instruments to the north. Additional meteorological data and solar irradiance were obtained from the Western Regional Climate Center (WRCC) weather station (www.wrcc.dri.edu/weather/smyc.html) situated about 125 m lower in elevation and 800 m to the west of the summit at the SMYC.

***Figure** 8. Left: Sampling inlets for the in situ CO and O_3 monitors. Right: GPS-enabled weather station at Angel Peak.*

3.2 Meteorology during LVOS

The weather was mostly mild and dry during LVOS with clear skies or scattered fair weather cumulus on most days during the field campaign. The overall seasonal upward trend in temperature (**Figure** 9a) was punctuated by the passage of several cold fronts associated with deep upper level troughs or closed lows moving through the Pacific Northwest.

The passage of these troughs is seen in both the Angel Peak surface pressure and in the NCEP/CDAS Reanalysis 500 hPa geopotential heights averaged over a 5° x 5° box centered at 36°N, 115°W (**Figure** 9b). Strong SSW winds usually accompanied these systems (**Figure** 9c), and the descending air behind the fronts led to two extended periods (May 21-26, and June 13-18) with much drier air at the surface (**Figure** 9a). There were also two periods (June 4-9 and June 26-29) with strong ridging, warmer temperatures, and weak winds that led to regional stagnation and build up of O_3 from local photochemical production. These periods were accompanied by strong upslope flow at Angel Peak and afternoon fair weather cumulus (cf. **Figure** 9a). More extensive cloud cover occurred on May 21 and June 25. The yellow bars highlight the three days (May 21, 25, and June 21) when the 75 ppbv 2008 O_3 NAAQS was exceeded by one or more of the regulatory monitors in the Las Vegas Valley. These high ozone events will be discussed in more detail in Section 7.

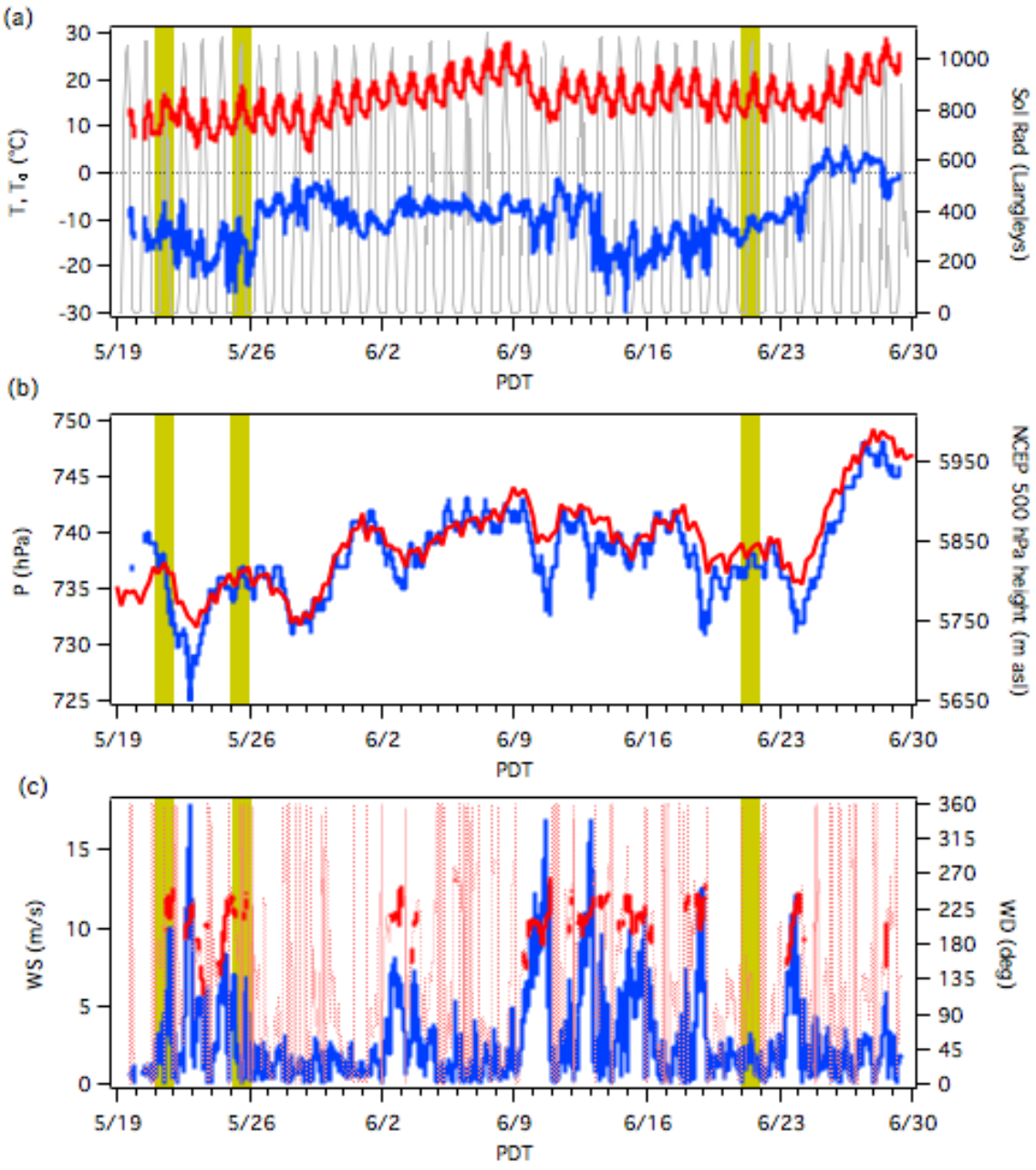

***Figure** 9. Time series of (a) solar radiation (gray) with surface temperature (red) and dew point (blue), (b) surface pressure (blue) and NCEP Reanalysis 500 hPa geopotential height (red), and (c) surface wind speed (blue) and direction (dotted red) from Angel Peak. The red points highlight the wind direction when the speeds were greater than 5 m/s. The yellow bands mark the O_3 exceedance days in Clark County.*

3.3 TOPAZ lidar measurements

The primary instrument used during LVOS was the TOPAZ (Tunable optical profiler for aerosols and ozone) 3-wavelength mobile differential absorption lidar (DIAL) system, which can profile ozone and aerosol layers from near the surface to ~2.5 km above ground level (agl). TOPAZ was reconfigured from the nadir-viewing aircraft-based version described previously [*Alvarez II et al.*, 2011; *A. O. Langford et al.*, 2010] and installed in the back of a truck for ground-based operations after the CalNex field campaign. The lidar is oriented in a zenith-viewing configuration with a large motorized vertically scanning mirror on top of the truck to permit line of sight measurements along elevation angles ranging from -6° (i.e. below the horizon) to 30° at a fixed azimuth direction. The mirror can also be moved completely out of the light path for zenith measurements.

TOPAZ uses near and far field detection channels to extend the dynamic range and can profile ozone over distances from about 400 m to 2.5 km during the day with the limits determined by the point of full overlap between the transmitter and receiver in the near field and the useful signal-to-noise cut off in the far field. The DIAL profiles are analyzed using a range resolution of 90 m, and a 450-m running average to smooth the resulting profiles. In normal operation, the scanning mirror is stepped through a series of angles to allow viewing at elevations of 2, 6, 20, and 90° above the horizon in a 5-min cycle with the backscatter returns averaged for 75 s at each angle. The resulting slant angle profiles are then projected along the zenith to create continuous vertical profiles down to about 15 m above the ground (**Figure** 10). The effective horizontal footprint of these blended profiles increases from about 11 meters near the top of the profile to about 900 m near the surface. For comparison, the horizontal sampling footprint associated with the 75 s integration time ranged from about 150 to 750 m for typical background winds of 2 to 10 m/s.

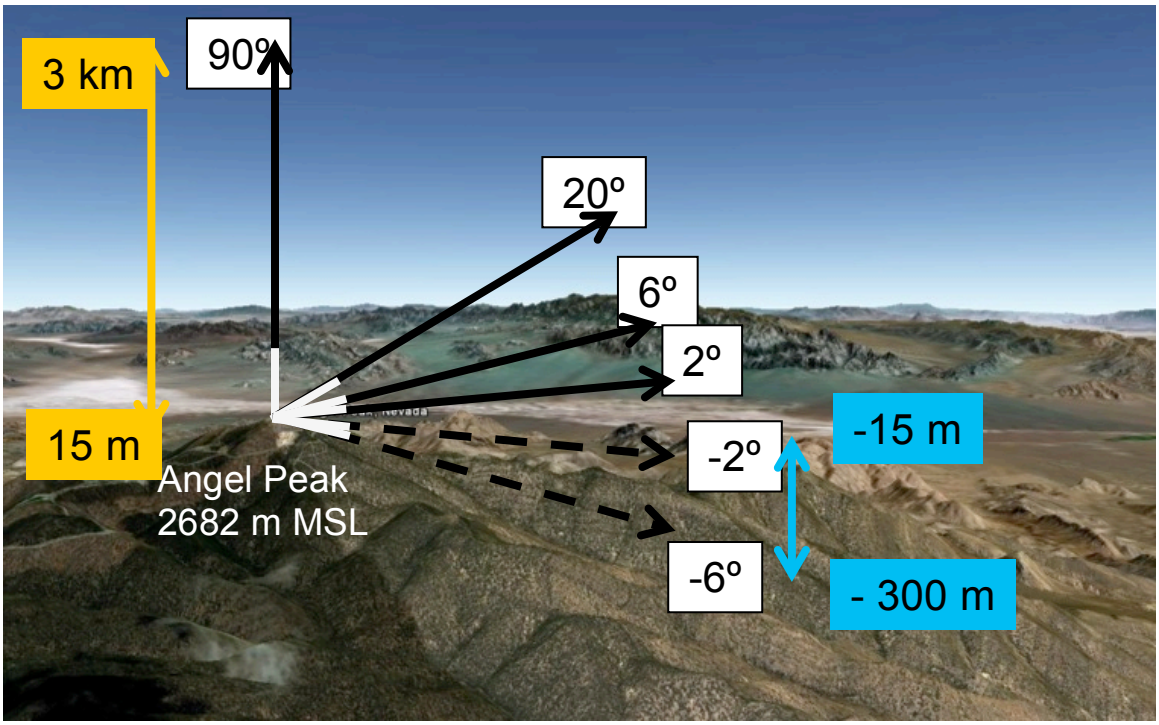

***Figure** 10. TOPAZ scan strategy during LVOS.*

TOPAZ is partially automated, but does not run autonomously and requires 1 to 2 operators. Each LVOS observing session consisted of 2 to 20 hours of nearly continuous 5-minute averaged ozone and backscatter profiles from the surface to ~2.5 km above ground level (~5.2 km above mean sea level). The system operated on 25 out of 43 possible days during LVOS, with a laser failure in mid-June dividing the data record into two intensive periods: May 19 to June 4, and June 22 to 28. **Figure** 11 displays a series of time-height color curtain plots showing the ozone concentrations measured by the TOPAZ lidar. The most striking features of these plots are the frequent layers with more than 100 ppbv of O_3 detected within a few km of the Angel Peak summit in late May. These layers were observed only under clear sky conditions and the backscatter profiles (not shown) indicate very low aerosol loadings associated with these layers consistent with a UT/LS origin. The McCarran soundings show that many of these filaments descended low enough to interact with the deep afternoon mixed layers. Note that these layered structures are qualitatively different from the

deep column of elevated O_3 and very high backscatter observed on June 2 when the plume from the 28000 acre Powerhouse Fire burning near Los Angeles engulfed Angel Peak (Appendix B). Another interesting feature of **Figure** 11 is the unusually low O_3 concentrations with relatively low backscatter seen extending well above Angel Peak on June 24-26. These low concentrations reflect a deep incursion of subtropical marine boundary layer air transported over the western U.S. by the counterclockwise circulation around an unusually large cyclone sitting over the Gulf of Alaska.

§§§

***Figure** 11. Time-height curtain plots of the ozone concentrations measured by TOPAZ during LVOS. The left axis shows the altitude above the surface of Angel Peak (2.68 km asl) and the right axis the corresponding altitude above mean sea level. The solid black lines show the normalized integrated backscatter from 15 to 2000 m agl. The "X" symbols show the mixing heights from the 0000 UT (1700 PDT) McCarran International Airport (VEF) soundings. Mixing heights greater than 5000 m asl are represented by "+" symbols and missing soundings by "0". The dotted gray curves show the normalized solar radiation measured at the nearby Spring Mountain Youth Camp (SMYC).*

§§§

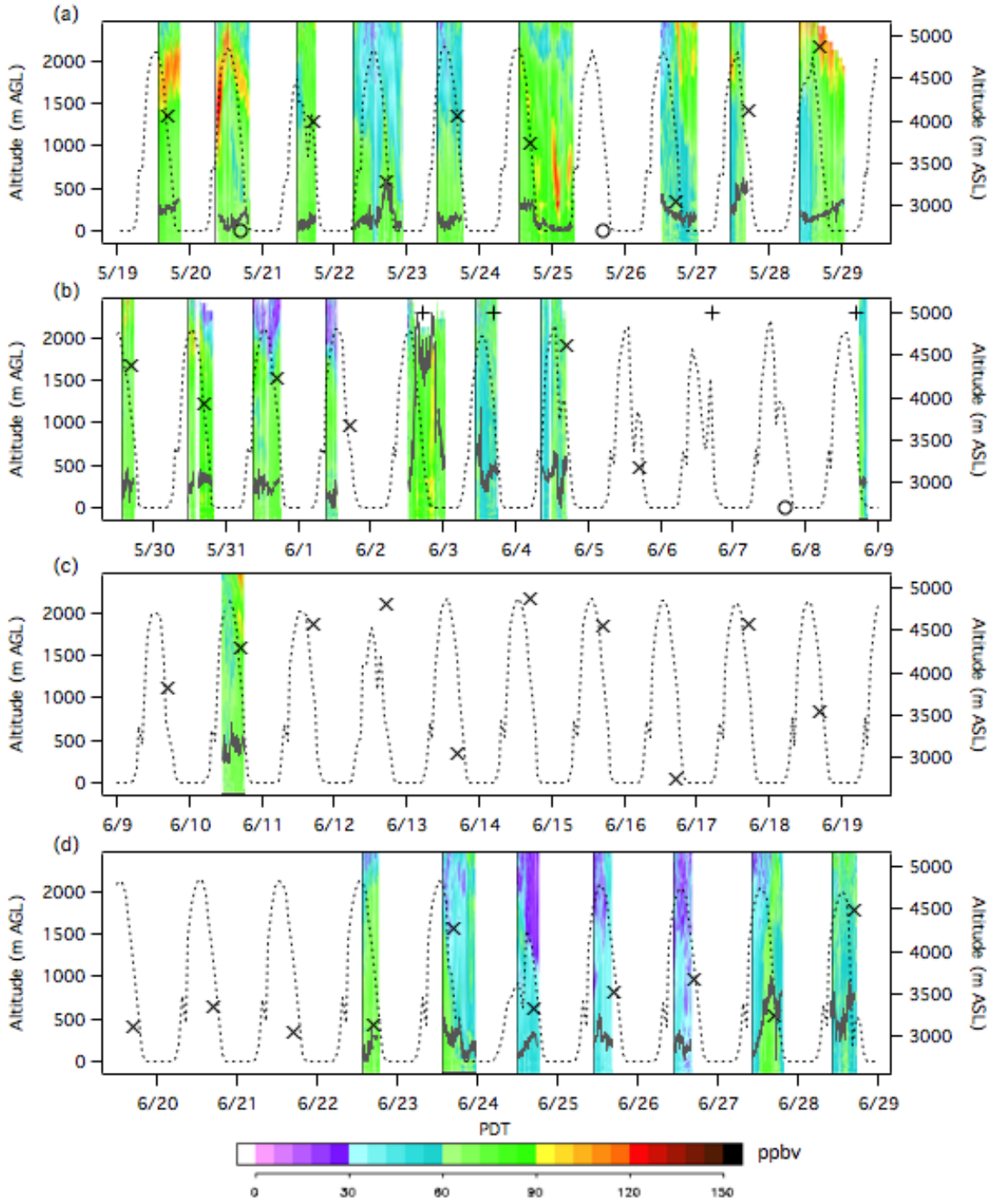
(a)
(b)
(c)
(d)
Altitude (m AGL)
Altitude (m ASL)
0
500
1000
1500
2000
3000
3500
4000
4500
5000
5/19
5/20
5/21
5/22
5/23
5/24
5/25
5/26
5/27
5/28
5/29
5/30
5/31
6/1
6/2
6/3
6/4
6/5
6/6
6/7
6/8
6/9
6/10
6/11
6/12
6/13
6/14
6/15
6/16
6/17
6/18
6/19
6/20
6/21
6/22
6/23
6/24
6/25
6/26
6/27
6/28
6/29
PDT
ppbv
0
30
60
90
120
150

Figure 11

3.4 In situ measurements

Surface O_3 and CO concentrations were measured continuously at Angel Peak from May 20 to June 29. Ozone concentrations were determined using a commercial UV-absorbance monitor with a detection limit of 1 ppbv for a 1-min integration time and an uncertainty of 2% [*Williams et al.*, 2006]. This instrument was calibrated against a reference standard in the laboratory prior to deployment. Carbon monoxide was measured using a modified commercial vacuum ultraviolet fluorescence [*Holloway et al.*, 2000] monitor with a detection limit below 1 ppbv for a 1-min integration time and an accuracy of 4%. This instrument was zeroed and calibrated hourly against a reference standard. Data from periods influenced by NO_x and CO emissions from vehicles, backup generator testing, and other local activities were identified and removed from the records.

Figure 12a plots the continuous 1-min in situ surface O_3 measurements from Angel Peak (blue line) together with the 15 to 2000 m agl average O_3 from TOPAZ (red symbols). The corresponding CO measurements are plotted in **Figure** 12b. The 8-h O_3 NAAQS was exceeded at Angel Peak on 8 days during LVOS (May 24, 25, 26, 30 and June 2, 17, 18). Background CO peaks in the springtime [*Kim et al.*, 2008] and the concentrations at Angel Peak accordingly declined slowly over the course of the campaign. The only large increases in CO beyond the daily 20 to 30 ppbv variations associated with the diurnal upslope flow coincided with the arrival of the Powerhouse Fire plume on June 2 when the concentrations nearly doubled, and on June 27 when polluted air from the Las Vegas Valley was transported to Angel Peak by strong upslope flow. The characteristics of the fire plume on June 2 contrast sharply with the relatively low CO and aerosol backscatter (cf. **Figure** 11) measured during the late May exceedance days. The concentrations of O_3 and CO decreased to as low as 22 and 69 ppbv, respectively, in the subtropical marine boundary layer air on June 24-26.

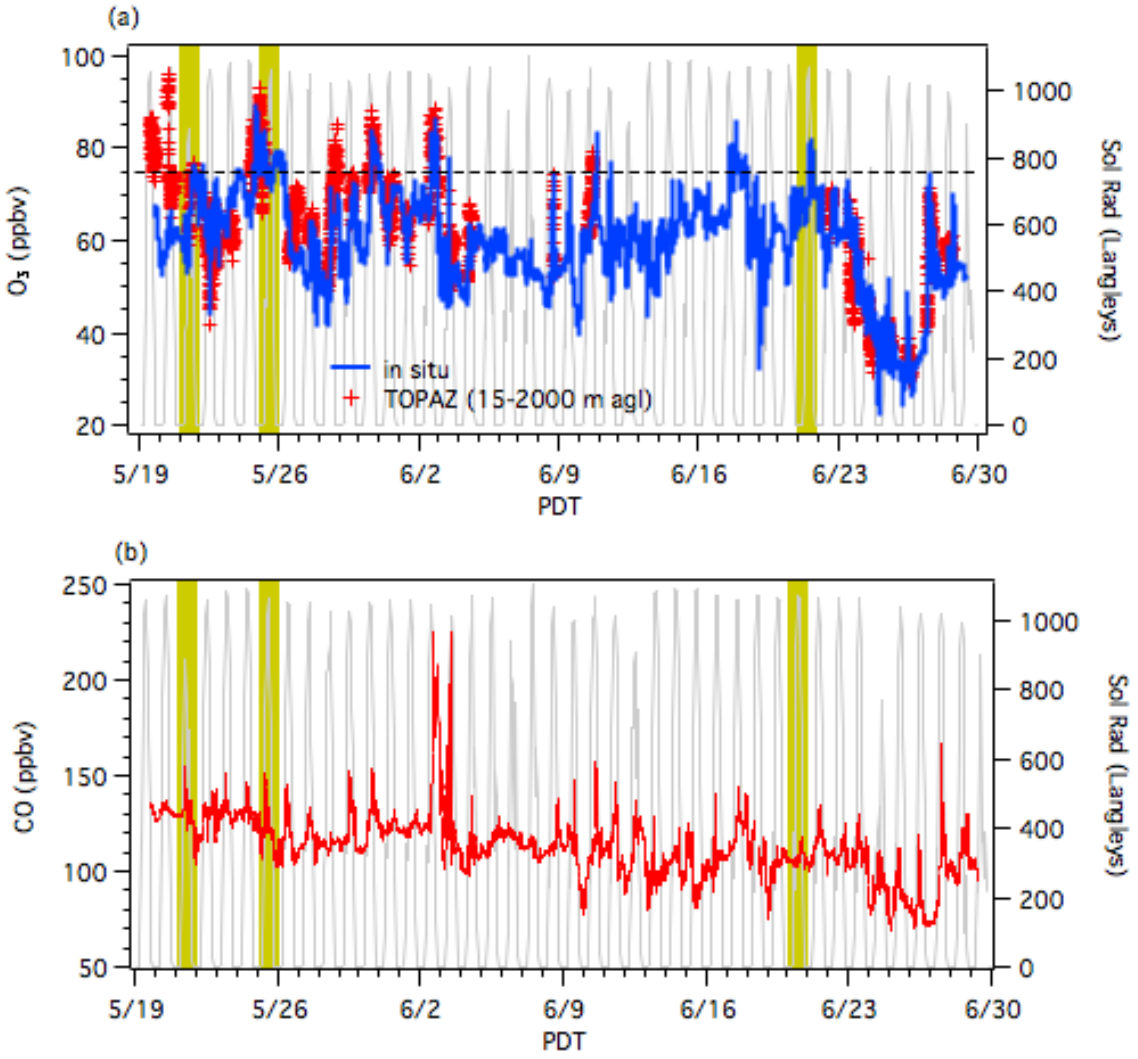

***Figure** 12. Time series of 1-min: (a) O_3 (blue) and (b) CO from Angel Peak. The red symbols in (a) show the average 15 to 2000 m agl O_3 from TOPAZ and the horizontal dashed line marks the 75 ppbv 8-h NAAQS. The gray lines in both plots show the solar radiation measured at the SMYC, and the gray bands mark the O_3 exceedance days in Clark County.*

Surface O_3 and CO averaged 62±8 and 116±15 ppbv over the first 5 weeks of the campaign (May 19 to June 23). These values are similar to the free tropospheric concentrations measured by the CalNex WP-3D flights above the Los Angeles Basin during May of 2010 [*Neuman et al.*, 2011]. The overall average concentrations from those flights were 66 and 120 ppbv for O_3 and CO, respectively, with mean values of 71±8 and 108±6 ppbv for air of upper tropospheric origin, 53±10 and 106±10 ppbv for air from the marine boundary layer, 69±6 and 136±10 ppbv for Asian transport plumes, and 65±4 and 134±7 ppbv for aged regional emissions based on FLEXPART back trajectories. The MDA8 O_3 at Angel Peak on the three Clark County exceedance days was 70±3, 78±1, and 77±3 ppbv, respectively, with corresponding CO concentrations of 115±6, 111±6, and 121±6 ppbv. The low CO concentrations and aerosol backscatter on the first two exceedance days indicate a strong upper troposphere/lower stratosphere (UT/LS) influence; the higher concentrations during the third episode are consistent with an additional contribution from Asian pollution.

The O_3 concentrations measured aloft by TOPAZ were generally higher than those measured at the summit of Angel Peak in late May when there were frequent upper level cyclones, but lower in mid and late June when the strong high-pressure ridges developed. This shows that the surface concentrations at Angel Peak were influenced primarily by descending air in the first instances, and by upslope flow from the valley during the stagnation episodes. The simultaneous operation of TOPAZ with its horizontal viewing capabilities and the in situ O_3 monitor allowed regular comparisons between the two measurement techniques. **Figure** 13 plots the TOPAZ O_3 measurements made at several altitudes against the in situ measurements from Angel Peak. The red crosses represent all of the coincident measurements and the filled black circles those measurements acquired between 1400 and 1600 PDT on days (18 out of 25) when the afternoon (0000 UT or 1700 PDT) soundings at McCarran Airport

showed the top of the mixed layer to be at least 2000 m higher than the summit of Angel Peak (i.e. > 4.7 km asl). The black and red solid lines show the corresponding linear regression fits. The air above Angel Peak was generally too clean to allow direct determination of the local mixed layer height from aerosol gradients [*White et al.*, 1999]. **Figure** 13a shows excellent agreement between the in situ measurements and the lowest TOPAZ measurements despite the spatial differences; the first TOPAZ bin averages the concentrations over a 2° slant path ranging from 400 to 1400 m distant from the inlets horizontally, and from ~15 to 50 m above the summit, or 200 to 400 m above the southeastern flank of Angel Peak. The measurements agree to within 3% with a high degree of correlation (R^2 = 0.930). The correlation is improved (R^2 = 0.967), but the agreement slightly degraded (5%) when only data acquired when the McCarran soundings showed the boundary layer to be deep and well mixed is used. Not surprisingly, the agreement becomes worse when the TOPAZ concentrations from (b) 500 m, (c) 1000 m, or (d) 15 to 2000 m agl are compared to the in situ measurements. The measurement precision should be very similar in **Figures** 13a and 13c since both sets of data were acquired at a range of ~1000 m from the lidar (at beam elevations of 2° and 90°, respectively) and the increased scatter at higher altitudes is almost entirely due to atmospheric variability and the frequent presence of high O_3 layers aloft. The differences between the two measurements under well-mixed conditions are well within the combined uncertainties and much smaller than the observed altitude dependences.

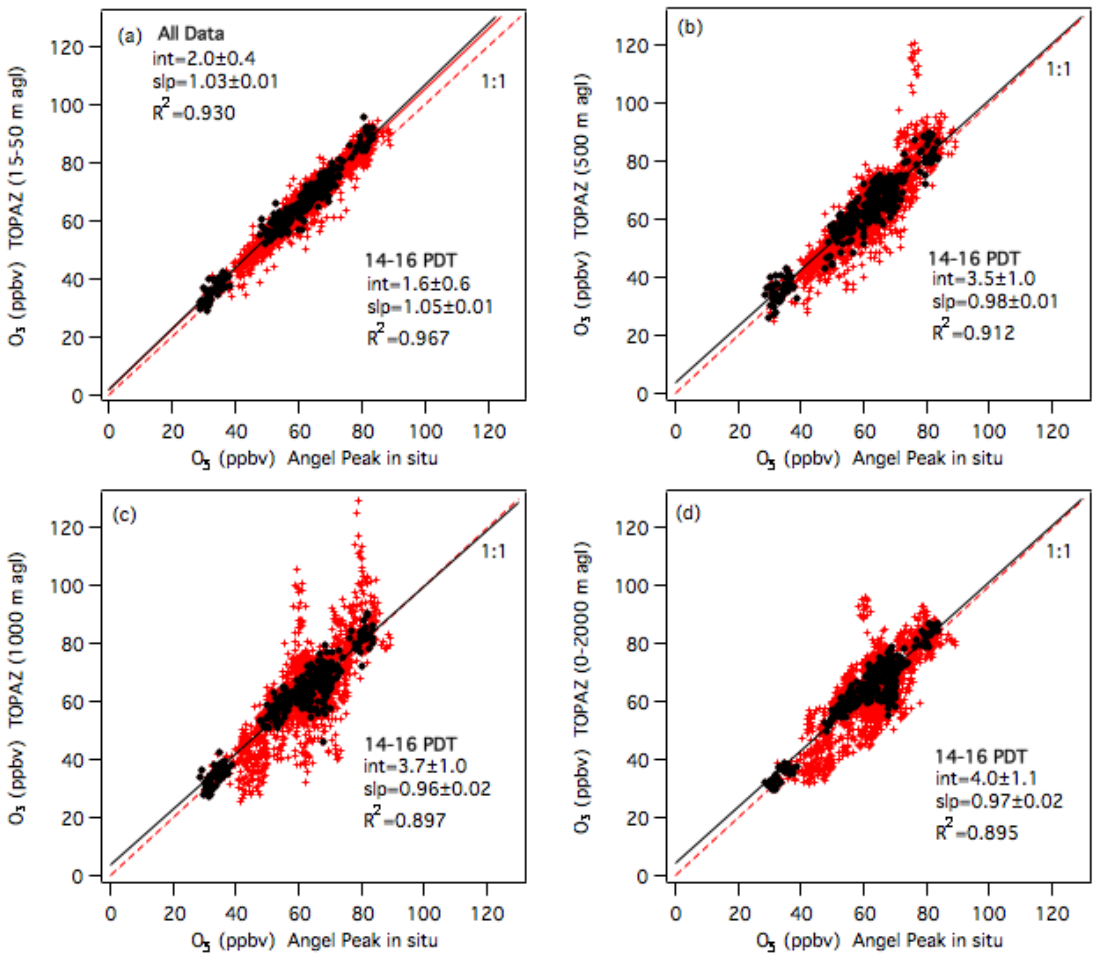

***Figure** 13. Scatter plots showing the correlation between the Angel Peak in situ O_3 measurements and the concentrations measured by TOPAZ at (a) 15-50 m agl, (b) 500 m agl, (c) 1000 m agl, and (d) 15-2000 m agl. The filled black circles show the measurements made when the VEF afternoon soundings show the top of the mixed layer to be at least 2000 m above the summit of Angel Peak (cf. Figure 11). The 1:1 line is dashed.*

3.5 Additional measurements

The routine measurements from the Clark County DAQ network of continuous ambient monitoring sites (CAMS) provide additional points of comparison for the

Angel Peak ozone measurements. **Figure** 4a shows the 7 CAMS that were operational in the Las Vegas Valley (Joe Neal, Palo Verde, J.D. Smith, Walter Johnson, Jerome Mack, Paul Meyer, and Winterwood) during LVOS, with the 4 sites located in outlying areas (Jean, Boulder City, Apex, and Mesquite) shown in **Figure** 2b. Clark County provided 5-min average O_3 data for the duration of the LVOS campaign in addition to the standard hourly and MDA8 data available online (www.ccaqapps5m.co.clark.nv.us). Many of the CAMS also measured meteorological parameters, particulates, or other chemical species in addition to ozone. The U.S. National Park Service also provided O_3 measurements with 1-min integration times from Great Basin and Death Valley, (cf. **Figure** 2a), and 1-h measurements from other locations were obtained from the U.S. EPA AirNow (www.airnowtech.org) or California Air Resources Board (www.arb.ca.gov) online databases. The vertical structure of the atmosphere was profiled hourly by an upper-air monitoring station comprised of a radar wind profiler, sodar, and profiling radiometer maintained by the DAQ at the North Las Vegas Airport (VGT), and by the twice daily (0500 and 1700 PDT) radiosondes launched by the National Weather Service (NWS) from the McCarran International Airport (VEF) (cf. **Figure** 4a). The horizontal distribution of clouds, smoke plumes, and mid-tropospheric water vapor was obtained from hourly GOES-WEST 1 km visible, 4 km infrared, and 8 km water vapor imagery and from the NASA MODIS products.

Figure 14 plots the continuous 1-min in situ surface O_3 measurements from Angel Peak (black) together with the 5-min measurements from the Clark County monitoring stations at Joe Neal (blue), Jean (green), and Apex (purple) (cf. **Figure** 4). The 15 to 2000 m agl TOPAZ measurements are plotted in red. Joe Neal lies to the north of Las Vegas and about 30 km ESE of Angel Peak near the mouth of the Kyle Canyon drainage, which links Angel Peak to the Las Vegas Valley. This site typically measures some of the highest O_3 concentrations in the LVV. Apex is situated in a rural area north of Las Vegas and on the far side of the valley about 61 km ENE of Angel Peak and Jean is located in the Mojave Desert about 65 km to the SSW. Whereas surface O_3 exhibits little diurnal

variation at Angel Peak, the concentrations at all of these lower-lying sites often decrease during the late night and early morning as O_3 is destroyed by surface deposition or titration beneath the shallow inversions that form when the winds are calm. The five data series converge at other times, however, including the afternoons and evenings of May 21, May 25, and June 21 when the Clark County exceedances occurred. The correlation coefficients from scatter plots similar to those in **Figure** 13, but comparing the afternoon (1400 to 1600 PDT) Angel Peak ozone measurements to those made by the CC/DAQ monitors in the valley range from R^2=0.645 for Palo Verde, which lies on the western side of the valley and is the nearest monitor to Angel Peak, to R^2=0.541 at Jerome Mack, which is located near the eastern side of the valley and downtown Las Vegas. The correlation coefficients for Joe Neal and Jean are R^2=0.645 and R^2=0.565, respectively. As noted above, the O_3 concentrations measured on or above Angel Peak were generally higher than those in the valley following cold fronts (e.g. May 20-21 and 24-25), but were usually lower than or comparable to the concentrations in the northern valley during strong ridging (e.g. June 4-8 and June 27-28).

§§§

***Figure** 14. Time series plots of ozone measurements made during LVOS. 1-min in situ measurements from Angel Peak (black), 15-2000 m agl mean from TOPAZ (red), and 5-min measurements from the Clark County monitors at Jean (green), Joe Neal (blue), and Apex (purple). The horizontal dashed line marks the current O_3 NAAQS and the dotted curves show the solar radiation measured at the SMYC.*

§§§

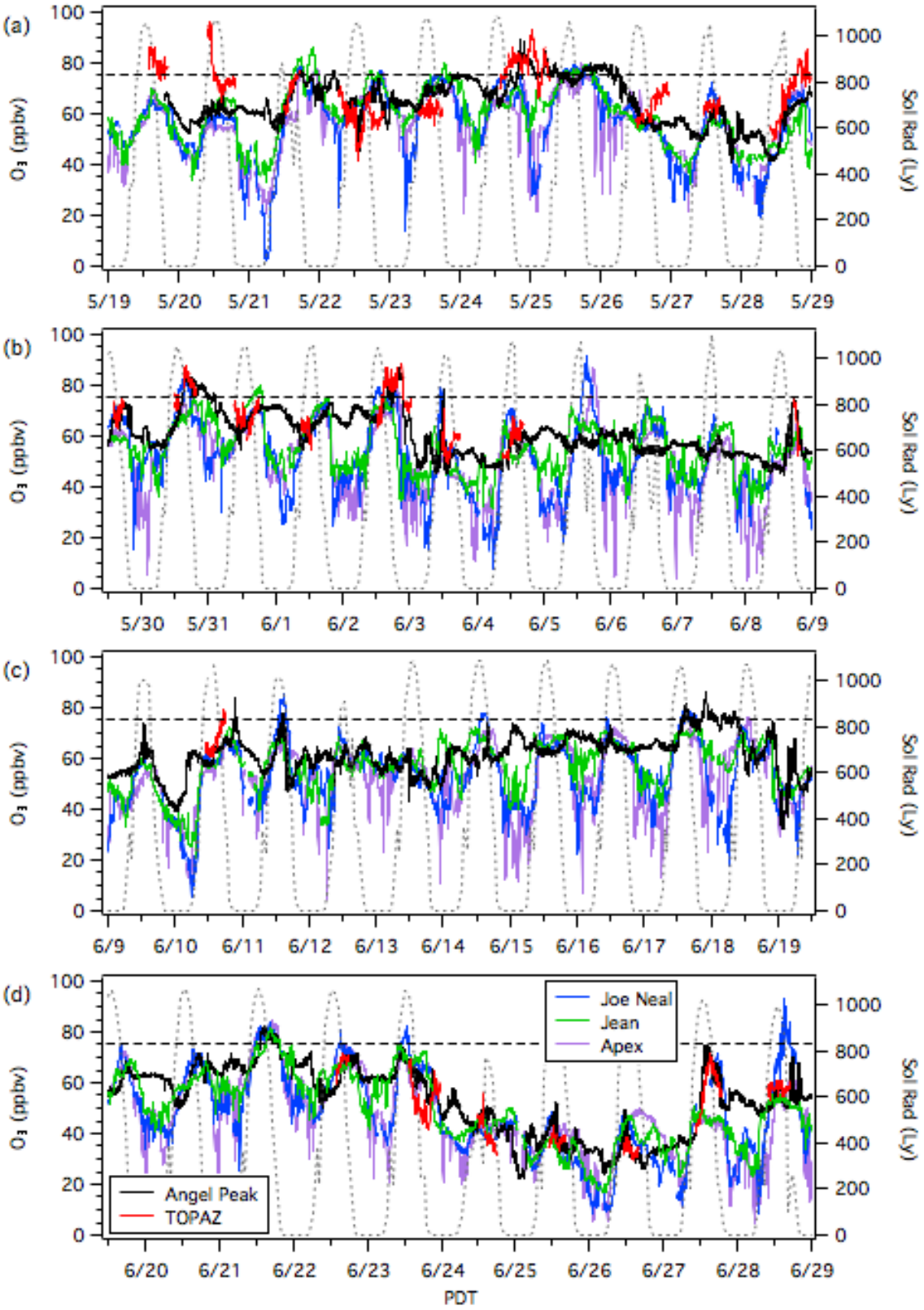
(a)
(b)
(c)
(d)
O3 (ppbv)
Sol Rad (Ly)
0
20
40
60
80
100
0
200
400
600
800
1000
5/19
5/20
5/21
5/22
5/23
5/24
5/25
5/26
5/27
5/28
5/29
5/30
5/31
6/1
6/2
6/3
6/4
6/5
6/6
6/7
6/8
6/9
6/10
6/11
6/12
6/13
6/14
6/15
6/16
6/17
6/18
6/19
6/20
6/21
6/22
6/23
6/24
6/25
6/26
6/27
6/28
6/29
PDT
Joe Neal
Jean
Apex
Angel Peak
TOPAZ

Figure 14

The regional nature of the high O_3 episodes in Clark County during LVOS is apparent from **Figure** 15, which compares the surface measurements from Jean and Angel Peak plotted in **Figure** 14 to the 5-min O_3 measurements from the U.S. National Parks Service monitors at Death Valley and Great Basin National Parks (cf. **Figure** 2a). Ozone was relatively high in Death Valley NP on the evening of May 21 and was also elevated at Great Basin NP later that night. Ozone was also elevated on the night of May 24 at Death Valley NP and at all four sites on May 25. There was another short-lived ozone peak on the afternoon of June 2 at Death Valley NP associated with the Powerhouse Fire followed by an increase later in the evening at Great Basin NP. Great Basin National Park reported only three exceedances of the NAAQS in all of 2013 with the MDA8 reaching 76 ppbv on May 5 (see below), May 25, and June 18. Although there were no exceedances of the NAAQS in Death Valley National Park during 2013, the two highest ozone days of the year were May 24 and 25 where the MDA8 O_3 reached 74 and 73 ppbv, respectively.

§§§

***Figure** 15. Time series plots of ozone measurements made during LVOS. 1-min in situ measurements from Angel Peak (black), and 5-min measurements from the Clark County monitor at Jean (green), and the U.S. National Park Service monitors at Great Basin NP (blue) and Death Valley NP (red). The horizontal dashed line marks the 2008 O_3 NAAQS and the dotted curves show the solar radiation measured at the SMYC.*

§§§

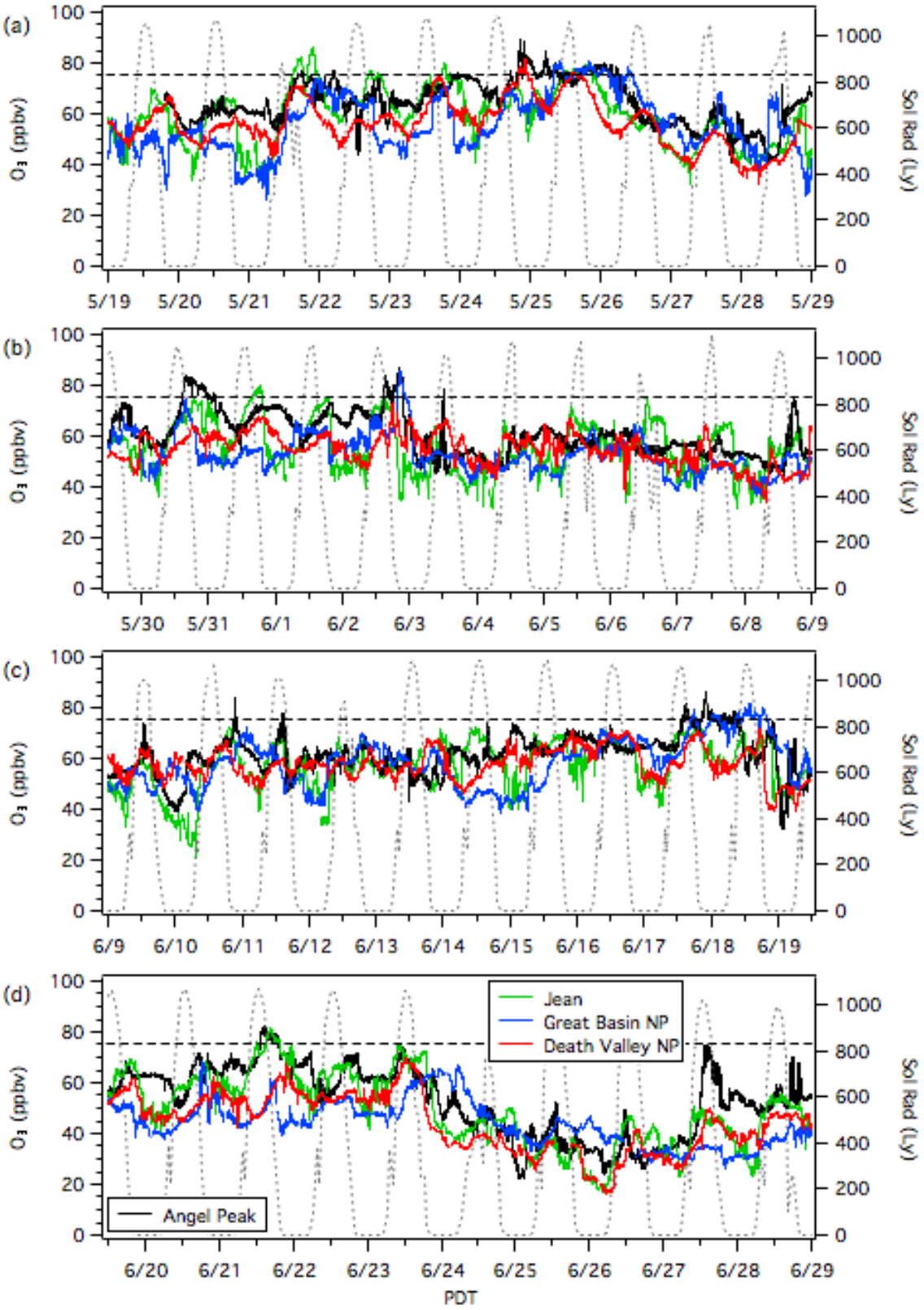
(a)
(b)
(c)
(d)
O3 (ppbv)
Sol Rad (Ly)
0
20
40
60
80
100
0
200
400
600
800
1000
5/19 5/20 5/21 5/22 5/23 5/24 5/25 5/26 5/27 5/28 5/29
5/30 5/31 6/1 6/2 6/3 6/4 6/5 6/6 6/7 6/8 6/9
6/9 6/10 6/11 6/12 6/13 6/14 6/15 6/16 6/17 6/18 6/19
6/20 6/21 6/22 6/23 6/24 6/25 6/26 6/27 6/28 6/29
PDT
Jean
Great Basin NP
Death Valley NP
Angel Peak

Figure 15

4. Model Analyses

The NOAA/NESDIS RAQMS and NOAA/ESRL/CSD FLEXPART models were used to forecast STT and long-range transport events during the LVOS measurement campaign with supplemental analyses from the NOAA/ESRL/GSD Rapid Refresh Air Quality Model (http://ruc.noaa.gov/wrf/WG11_RT/Welcome.cgi) that uses RAQMS lateral boundary conditions. The NOAA GFDL AM3 and FLEXPART models were then used to estimate the contribution of STT and long range transport to surface ozone in the western U.S. and to Clark County following the field campaign.

4.1 RAQMS

RAQMS (Realtime Air Quality Modeling System) is a unified (stratosphere-troposphere) online global chemical and aerosol assimilation/forecasting system that has been used to support several airborne field missions [*Pierce et al.*, 2003; *Pierce et al.*, 2007]. Forecasts were initialized daily at 1200 UT with real-time assimilation of OMI cloud-cleared total column ozone and MLS ozone profiles from the NASA Aura satellite, and MODIS aerosol optical depth from the NASA Terra and Aqua satellites. The O_3 and CO distributions over the North Pacific (10 to 72°N, -110 to -50°E) were predicted at 6-hour intervals for the next 4 days. RAQMS has been run routinely since 2010 with 2° x 2° resolution analyses and forecasts prior to 2012, and 1°x1° resolution after 2012. RAQMS plots are archived online (http://raqms-ops.ssec.wisc.edu).

4.2 FLEXPART

Transport of stratospheric, Asian, and biomass burning tracers to the western U.S. was also followed using the FLEXPART Lagrangian particle dispersion model (version 8.1) [*Stohl et al.*, 2005]. FLEXPART does not map the trajectory of an individual parcel as performed by standard trajectory models such as HYSPLIT (Hybrid Single-Particle Lagrangian Integrated Trajectory) [*Draxler and Rolph*, 2003], but instead calculates the evolving distribution of a multitude of

"particles" transported forward in time from a specified source region or backward in time from a specific receptor location. The particles are transported both by the resolved winds and by parameterized subgrid motions including turbulence and convection. For the present study, FLEXPART was driven by the National Centers for Environmental Prediction (NCEP) Global Forecast System (GFS) model (analyses at 0000, 0600, 1200, and 1800 UT; 3-h forecasts at 0300, 0900, 1500, and 2100 UT) and run at a spatial resolution of 0.5° x 0.5° with 26 vertical levels. FLEXPART parameterizes turbulence in the boundary layer using the Hanna turbulence scheme [*Hanna*, 1982] and uses the convection parameterization scheme of *Emanuel and Zivkovic-Rothman* [1999], which is implemented at each 15-minute model time step, and is intended to describe all types of convection. This scheme includes entrainment and mixing, cloud microphysical processes, and large-scale control of ensemble convective activity, including the interaction between convective downdrafts and surface fluxes.

FLEXPART was run routinely in the source (forward) mode for forecasting during LVOS and the coincident SENEX (Southeast Nexus) field campaigns. The distributions of stratospheric O_3, Asian pollution CO, and biomass burning CO tracers were calculated hourly for an output domain extending from 140 to 90°W and from 25 to 70°N. Horizontal distributions were plotted and archived online for both the boundary layer (below 1.5 km asl) and for the lower free troposphere (3 to 6 km asl). The stratospheric O_3 tracer was carried by particles released into the stratosphere (>2 potential vorticity units or PVU) and the mixing ratios of O_3 calculated using a linear relationship between O_3 and potential vorticity (60 ppbv/PVU) at the particle origin in the stratosphere. The O_3 mixing ratio is conserved and the particle distribution recalculated for up to 20 days with no chemistry. The Asian CO tracer is based on the amount of CO released into the boundary layer from anthropogenic sources in East Asia using the EDGAR 3.2 fast track inventory [*Olivier et al.*, 2005], and is followed for 20 days. Biomass burning CO emissions were calculated using the algorithm of *Stohl et al.* [2007], which incorporates MODIS fire detection data, information on land use, and

published emission factors. Both CO tracers are assumed to be inert. Instead of prescribing a fixed injection height for the fire plume, a probability density function relative to the local PBL height was used [*Brioude et al.*, 2009]. The online tracer distribution plots were updated twice daily as newer GFS input data became available.

FLEXPART was also run in the receptor (backward) mode to trace the origins of air transported to Clark County. In this mode, 20,000 particles were launched every hour from a 1° x 1° domain centered over Angel Peak that includes most of the Las Vegas Valley. The particle distribution was followed backwards in time for up to 10 days and the fraction originating from the boundary layer, free troposphere, and stratosphere calculated, together with the concentrations of O_3 originating from the stratosphere and concentrations of CO transported from Asia or originating from biomass burning. The results from these analyses are plotted as time series (see below).

4.3 GFDL AM3

The contribution of stratospheric ozone to surface concentrations in the western U.S. during the spring of 2013 was also simulated using the NOAA/GFDL AM3 chemistry-climate model, which includes interactive stratospheric and tropospheric chemistry, nudged to NCEP GFS winds [*Lin et al.*, 2012a; *Lin et al.*, 2012b]. The AM3 simulation of STT O_3 is entirely driven by winds, with no dependency on the tropopause definition. We implement a stratospheric ozone tracer, defined relative to the dynamically varying e90 tropopause [*Prather et al.*, 2011], to quantify ozone originating from the stratosphere and account for loss processes in the troposphere. The present study applies a new version of GFDL AM3 at C90 cubed-sphere grid resolution of ~100 x 100 km^2 with daily resolving fire emissions and anthropogenic emissions. Lin et al. [2014, this issue] describe the current version of AM3 in more detail.

Figure 16 displays the AM3 median stratospheric contribution to MDA8 surface

ozone during May and June of 2013. The spatial distribution appears very similar to the mean 2010 concentrations shown in **Figure** 1a, but with lower spatial resolution. As in 2010 (cf. Figure 1), the calculated stratospheric contribution to surface ozone is much larger in the Intermountain West than in the Eastern U.S. and along the Gulf Coast, with median concentrations of 20 ppbv or more in many areas. The Asian pollution contribution was not explicitly calculated, but the FLEXPART analyses suggest that it was similar to that shown in **Figure** 1b.

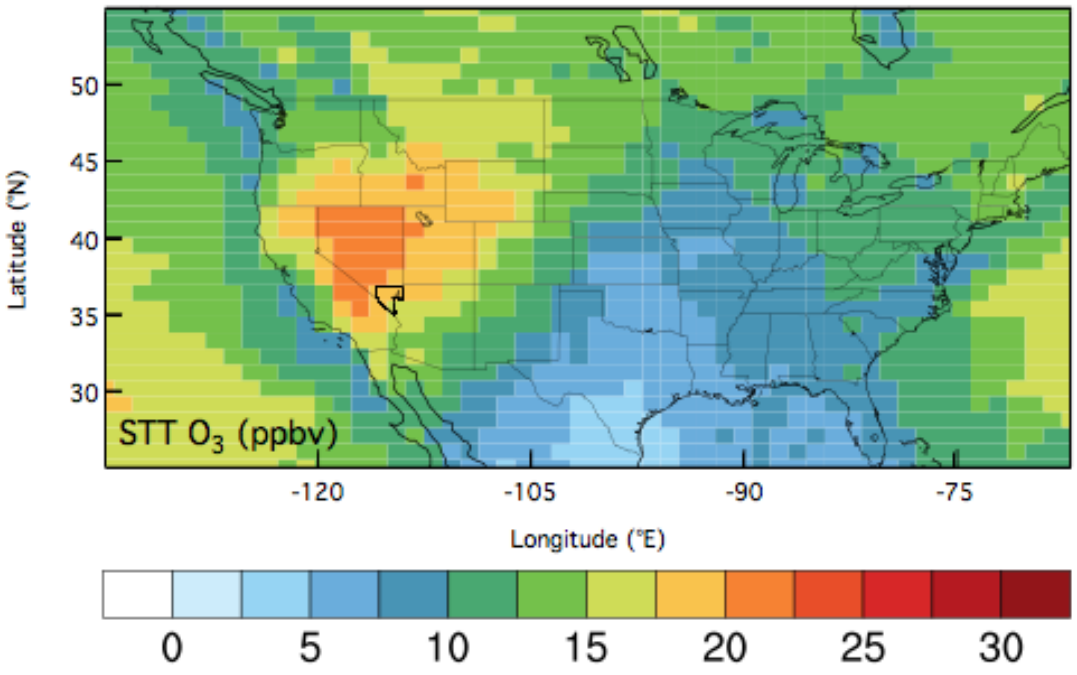

***Figure** 16. NOAA GFDL AM3 model median contribution of STT to MDA8 surface O_3 during May and June of 2013. The resolution is 100 km x 100 km. Clark County, NV is outlined in black.*

5. O_3 – CO – H_2O correlations

Both CO and O_3 have relatively long lifetimes in the free troposphere compared to the timescales of vertical and horizontal transport, and the relationship between the two trace gases has been used to investigate the contribution of photochemistry to tropospheric ozone [*Crutzen*, 1974; *Fishman and Seiler*, 1983], mixing between the upper troposphere and lower stratosphere [*Herman et al.*, 1999], long-range transport of ozone [*Parrish et al.*, 1993; *Parrish et al.*, 1998], and to estimate the ozone production efficiency from biomass burning [*Jaffe and Wigder*, 2012; *Wofsy et al.*, 1992]. Most atmospheric CO originates from the Earth's surface, either directly from natural and anthropogenic combustion processes or indirectly through oxidation of CH_4 and other volatile organic compounds (VOCs) emitted at the surface [*Warneck*, 1988]. Atmospheric concentrations thus generally decrease with altitude and with distance from the continents. The large contribution of anthropogenic sources to the atmospheric burden means that the atmospheric concentrations have a pronounced latitudinal gradient with a maximum at northern midlatitudes [*Seiler and Fishman*, 1981]. The concentrations in the lower troposphere above the North Pacific tend to be highest in springtime [*Kim et al.*, 2008]

Since O_3 is much more abundant in the stratosphere than in the troposphere, the concentrations are usually uncorrelated or negatively correlated with CO in air originating from the upper troposphere or lower stratosphere. Conversely, CO and O_3 tend to be positively correlated in the lower troposphere where much of the O_3 is formed through oxidation of CO and CH_4, or through the reactions of NO_x and VOCs co-emitted with CO from combustion sources. Although simple linear relationships are sometimes observed when homogeneous air parcels with different origins mix, the relationship is usually much more complex, particularly in the lower free troposphere and boundary layer. For example, since O_3 is a secondary product and not directly emitted from combustion sources like CO, there may be little or no correlation in urban or polluted areas where there are

distributed combustion sources, and negative correlations can arise when O_3 is destroyed through titration by NO in fresh combustion plumes or by surface deposition, as is often the case in the nocturnal boundary layer.

The utility of the O_3-CO correlation plots for investigating air parcel origins can be improved by including simultaneous H_2O measurements. Water vapor is not a conserved quantity in the troposphere on timescales longer than a few days, but the concentrations are usually much lower in the free troposphere than in the boundary layer and lower still in the lowermost stratosphere. Thus, stratospheric intrusions are usually drier than long-range transport layers, which are in turn drier than polluted boundary layer air or biomass burning plumes that usually contain large amounts of water vapor.

Figure 17a displays a scatter plot of all the 1-min in situ O_3 and CO data acquired during LVOS at Angel Peak between May 19 and June 29. The points are color-coded by specific humidity with the highest O_3 generally associated with drier air; the inset plot shows the mean specific humidity as a function of altitude from the May-June 2013 VEF soundings. Green and warmer colors reflect boundary layer air from below 2 km asl with red and yellow points being unusually moist. Blue and purple colors reflect air from the middle and upper troposphere, respectively. The highest CO concentrations were associated with the plume from the Powerhouse Fire (see below) that engulfed Angel Peak on June 2. Although the measurements show an overall positive correlation, the data represent many different air parcels and are highly scattered. However, **Figure** 17b shows that simple relationships consistent with the mixing of two homogeneous air parcels can be identified, in some cases, when the measurements from much shorter intervals are isolated. This plot isolates several examples of mixing lines observed over 3 h intervals that are believed to be indicative of the mixing between free tropospheric background air and air parcels influenced by the stratosphere (ST: high O_3, very low H_2O, negative O_3-CO correlation), transport from Asia (AS: high O_3, low H_2O, positive O_3-CO correlation), wildland fire/urban plume (LA/BB: high CO, moderate H_2O, positive

O_3-CO correlation), the subtropical marine boundary layer air (MB: low O_3 and CO, relatively high H_2O, positive O_3-CO correlation) and finally, regional photochemical production and transport from the valley mixed with the subtropical air (MB/LV: moderate O_3, CO, high H_2O, positive O_3-CO correlation). A wide range of slopes can result when air parcels of different origin are combined, but the mingling of air from the UT/LS with air from the free troposphere or boundary layer will create mixing lines with negative or zero slopes and an gradient in H_2O (**Figure** 17c) [*Brioude et al.*, 2007].

§§§

Figure *17. Scatter plots of the 1-min in situ O_3 and CO measurements from Angel Peak during LVOS color-coded by specific humidity. (a) All data from the campaign. (b) Isolated measurements from five different 3-hour intervals showing mixing lines attributed to the influence od stratospheric air (ST), biomass burning and urban pollution from the LA Basin, (LA/BB), transport from Asia (AS), subtropical marine boundary layer air (MB), and local pollution from the Las Vegas Valley (LVV). (c) Characteristic mixing lines associated with the mixing of boundary layer and UT/LS air.*

§§§

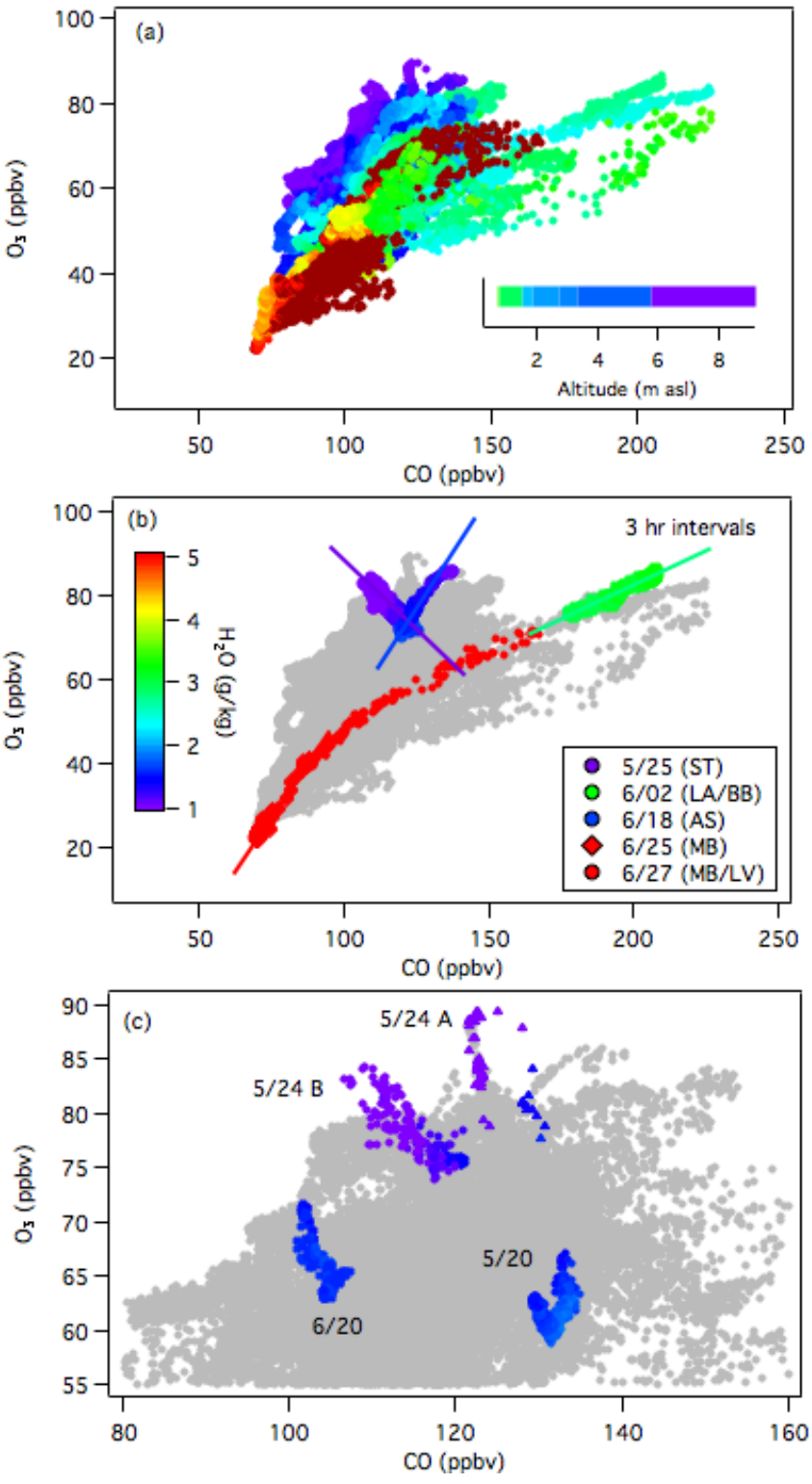
(a)
100
80
60
40
20
O3 (ppbv)
50
100
150
200
250
CO (ppbv)
2
4
6
8
Altitude (m asl)
(b)
3 hr intervals
5
4
3
2
1
(δ17O/δ18O)
5/25 (ST)
6/02 (LA/BB)
6/18 (AS)
6/25 (MB)
6/27 (MB/LV)
(c)
5/24 A
5/24 B
5/20
6/20
90
85
80
75
70
65
60
55
80
100
120
140
160

Figure 17

The simple analysis applied to the examples in **Figure** 17b was extended to the entire time series with the linear regression calculated at 15 minutes intervals for overlapping 3 h periods. **Figure** 18a plots the Angel Peak in situ O_3 mixing ratios color-coded by the resulting slopes with negative values in red. Only data acquired between 1300 and 2200 PDT are included in the analysis to reduce the influence of surface deposition, and symbols are plotted only when the coefficient of determination (i.e. R^2) is greater than 0.5. **Figures** 18b and 18c are similar, but show the O_3 concentrations color-coded by the H_2O and CO concentrations. This analysis shows that there were statistically significant negative correlations before each of the exceedance days, as well as on May 28 when TOPAZ detected a high O_3 layer aloft (**Figure** 11), but the concentrations remained relatively low in the valley (MDA8 ≤ 64 ppbv). All three exceedance days were associated with dry air and relatively low CO concentrations consistent with descending air of UT/LS origin.

§§§

Figure *18. Time series of the in situ O_3 at Angel Peak color-coded by (a) the slope of the regression with CO (R^2>0.5 only), (b) specific humidity, and (c) CO concentrations. The horizontal dashed line indicates the 75 ppbv 8-h NAAQS. The yellow bands mark the three exceedance days in Clark County.*

§§§

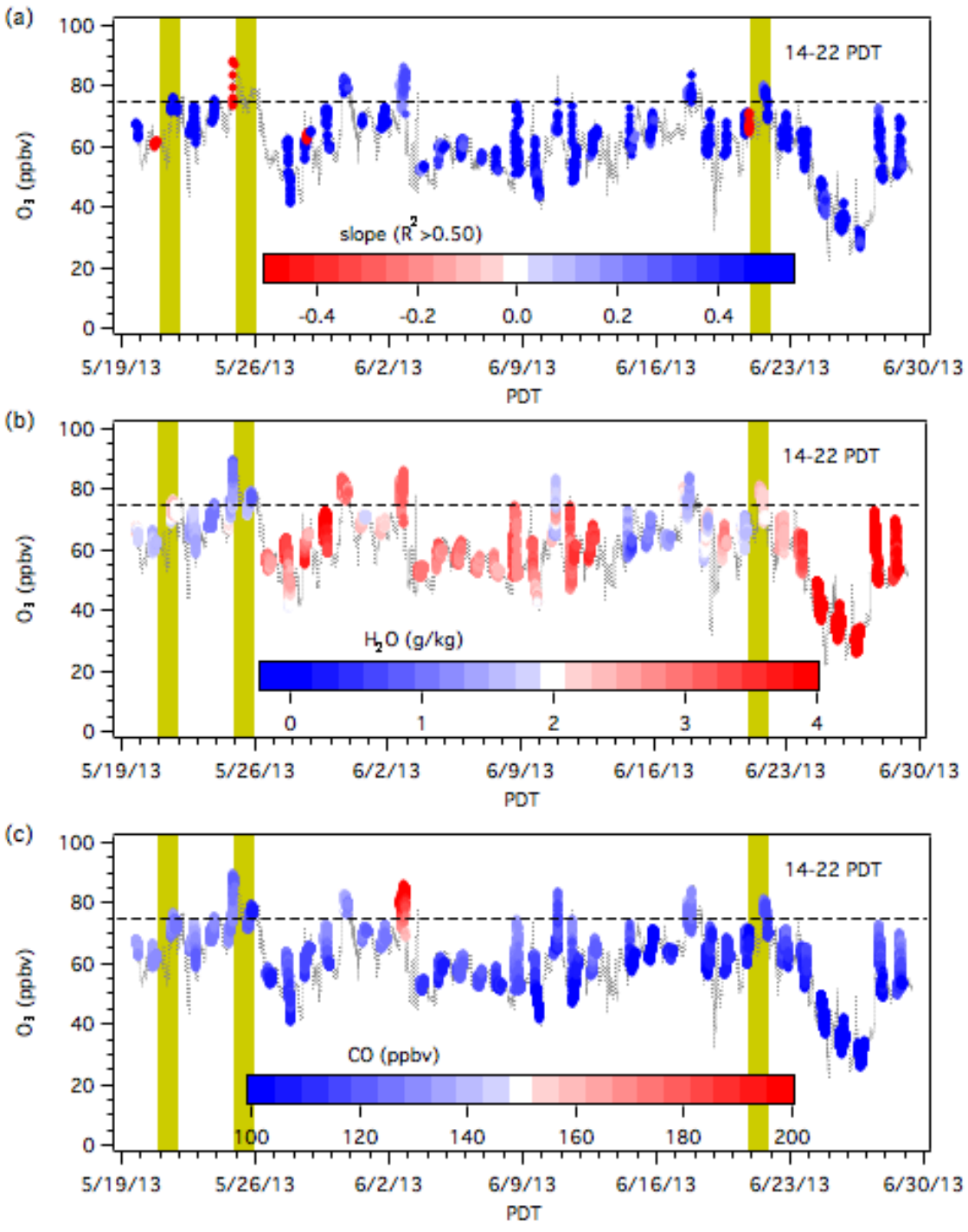
(a)
14-22 PDT
slope (R^2>0.50)
-0.4
-0.2
0.0
0.2
0.4
O_3 (ppbv)
100
80
60
40
20
0
5/19/13
5/26/13
6/2/13
6/9/13
6/16/13
6/23/13
6/30/13
PDT
(b)
14-22 PDT
H_2O (g/kg)
0
1
2
3
4
O_3 (ppbv)
PDT
(c)
14-22 PDT
CO (ppbv)
100
120
140
160
180
200
O_3 (ppbv)
PDT

Figure 18

6. Model estimates of STT contribution to surface ozone during LVOS

The FLEXPART back trajectories and AM3 analyses can be used together with the observations to estimate the contributions of stratospheric intrusions, transport from Asia, and wildland fires to the surface ozone measured at Angel Peak and surrounding areas. **Figure** 19 plots the surface O_3 concentrations from Angel Peak color-coded by the contributions from the FLEXPART (a) stratospheric O_3, (b) Asian CO, and (c) biomass burning CO tracers at 1000 m asl or just above the elevation of the Las Vegas Valley. The vertical yellow bars mark the three Clark County exceedance days as before. The back trajectories show stratospheric contributions of 15 to 30 ppbv to the O_3 at 1000 m asl for extended periods in late May and immediately before or on each of the three exceedance days. The FLEXPART Asian CO tracer is generally much smaller, and exceeded 10 ppbv only on June 17-18. The corresponding O_3 influx is likely much smaller, but the 75 ppbv ozone NAAQS was exceeded at Angel Peak on both days and nearly equaled at Joe Neal (74 ppbv) on June 17. The 2008 NAAQS was also approached (73 ppbv) at Great Basin National Park on June 17 and exceeded (76 ppbv) on June 18. The Asian tracer also had significant concentrations (~8 ppbv of CO) on May 21, the first exceedance day, and during the last week of May, but always remained much smaller than the corresponding stratospheric contribution.

§§§

Figure *19. In situ O_3 and CO measurements from Angel Peak color-coded by (a) stratospheric O_3, (b) Asian transport CO, and (c) biomass burning CO tracers from the FLEXPART back trajectories originating from 1000 m asl. The horizontal dashed line indicates the 75 ppbv 8-h NAAQS. The yellow bands mark the three exceedance days in Clark County.*

§§§

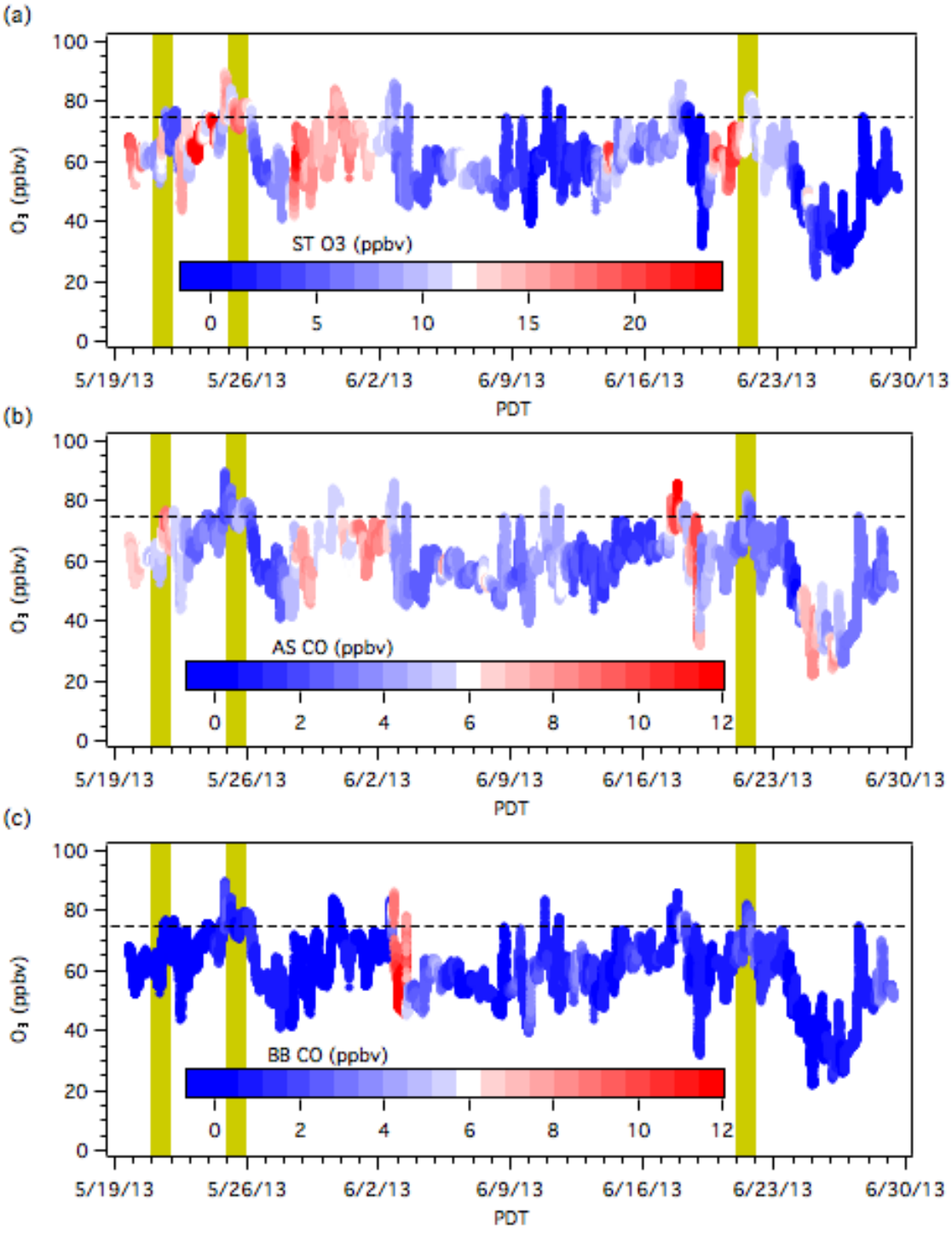
(a)
100
80
60
40
20
0
O3 (ppbv)
ST O3 (ppbv)
0
5
10
15
20
5/19/13
5/26/13
6/2/13
6/9/13
6/16/13
6/23/13
6/30/13
PDT
(b)
100
80
60
40
20
0
O3 (ppbv)
AS CO (ppbv)
0
2
4
6
8
10
12
5/19/13
5/26/13
6/2/13
6/9/13
6/16/13
6/23/13
6/30/13
PDT
(c)
100
80
60
40
20
0
O3 (ppbv)
BB CO (ppbv)
0
2
4
6
8
10
12
5/19/13
5/26/13
6/2/13
6/9/13
6/16/13
6/23/13
6/30/13
PDT

Figure 19

The contributions from the FLEXPART biomass-burning tracer to surface CO in Clark County exceeded 8 ppbv only on June 2, when the plume from the Powerhouse Fire passed through. The CO tracer concentrations reached ~25 ppbv or about 25% of the measured enhancement of 100 ppbv (cf. Figure 7b). The maximum CO and O_3 concentrations measured in this plume were 210 ppb CO and 85 ppb O_3. Assuming the baseline values are 100 ppbv of CO and 50 ppbv of O_3, the plume enhancements are 35 ppbv O_3 and 110 ppbv CO, with a ratio of 0.32. This implies that the Powerhouse fire plume contributed less than 3 ppbv of O_3 to the surface concentrations on June 2, and suggests that the impact of biomass burning on surface ozone during the three exceedance days during LVOS negligible (cf. **Appendix** B).

The stratospheric contribution to surface O_3 at Angel Peak and surrounding areas was calculated by Meiyun Lin of NOAA/ESRL/GFDL using the AM3 model. **Figure** 20 displays time series comparing the calculated May to July MDA8 O_3 concentrations for Death Valley NP, Angel Peak (LVOS only), Jean, and Joe Neal to the observations. Here, the black lines represent the measured MDA8 concentrations and the red traces the modeled concentrations; the blue traces

§§§

Figure *20. Time series comparing the AM3 total MDA8 ozone (red) calculated for (a) Angel Peak, (b) Death Valley, (c) Jean, and (d) Joe Neal to the measured values (black). The blue traces isolate the STT contribution to the calculated totals. The correlation coefficients are derived from linear regression fits using the data from May 19 to June 28 (LVOS) only.*

§§§

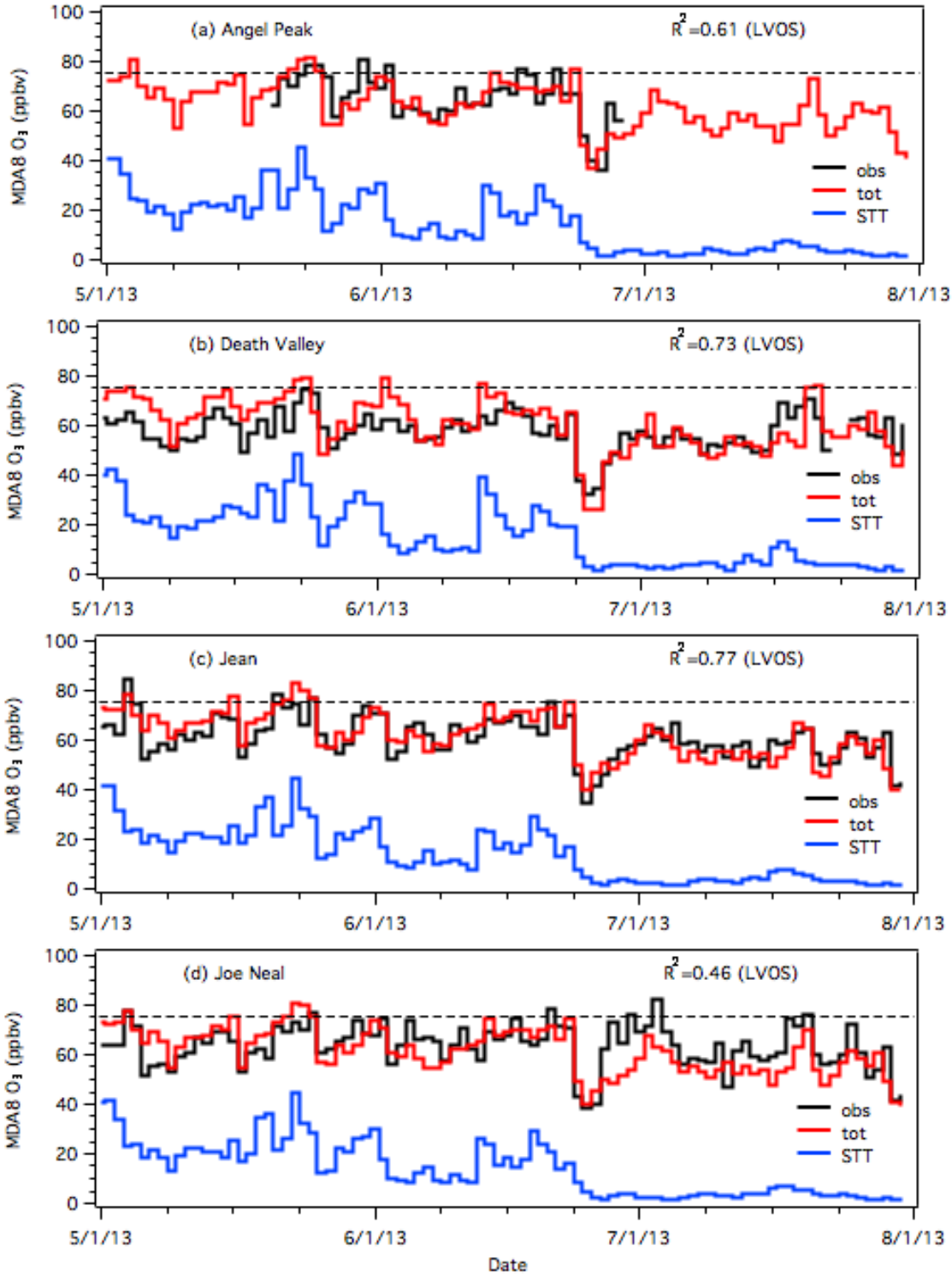
(a) Angel Peak
R2=0.61 (LVOS)
(b) Death Valley
R2=0.73 (LVOS)
(c) Jean
R2=0.77 (LVOS)
(d) Joe Neal
R2=0.46 (LVOS)
obs
tot
STT
MDA8 O3 (ppbv)
0
20
40
60
80
100
5/1/13
6/1/13
7/1/13
8/1/13
Date

Figure 20

isolate the stratospheric contribution to the model total concentrations. The modeled ozone includes contributions from North American pollution and wildland fires in addition to the stratosphere and long-range transport from Asia. As before, the horizontal dashed line represents the 2008 NAAQS of 75 ppbv. The AM3 modeled concentrations are generally in excellent agreement with the observations, capturing most of the day-to-day variability and ozone peaks as well as the unusually low ozone concentrations associated with the large-scale incursion of subtropical air in late June. The model does particularly well at Jean, where linear regression between the calculated and observed MDA8 ozone during LVOS gives AM3 = (0.86±0.08)*OBS+11±5 ppbv with R^2=0.77. The mean ratio is 1.03±0.01. The worst agreement (AM3 = (0.73±0.13)*OBS+16±8 ppbv R^2=0.46 and a mean ratio of 0.98±0.02) is found for Joe Neal, which is the site most impacted by local urban sources. Indeed, the greatest divergence between the model results and the Joe Neal observations was immediately after the subtropical incursion when locally formed ozone was a large fraction of the total (cf. **Figures** 11 and 14); the coefficient of determination increases from R^2=0.46 to R^2=0.57 if the measurements from June 28 are omitted.

The mean MDA8 surface ozone calculated for Angel Peak by AM3 averaged 64±10 ppbv over the course of LVOS, nearly identical to the measured value of 65±10 ppbv. The stratospheric component averaged 18±10 ppbv over this period. The corresponding values for the period from May 19 to May 31 when TOPAZ detected frequent ozone layers aloft were 69±9 ppbv (AM3) and 71±7 ppbv (observed), with an AM3 stratospheric component of 27±9 ppbv. The largest single day AM3 STT contribution was 45 ppbv on May 23 followed by 33 ppbv on May 24, one day before the highest observed concentrations and two days before the second Clark County exceedance event on May 25. The AM3 stratospheric contribution was at least 25 ppbv on each of the three LVOS exceedance days, with contributions in excess of 30 ppbv occurring on May 1, 19, and 30, and on June 13 and 20.

Comparisons between surface concentrations and those calculated using a previous version of AM3 found that the AM3 stratospheric contribution was sometimes biased too high [*Lin et al.*, 2012a]. However, the excellent agreement between AM3 and the observations seen in **Figure** 20 suggests that this is not the case for the present results, which are derived from a significantly improved model [Lin et al., this issue]. **Figure** 21a compares the AM3 results for surface ozone at Angel Peak during LVOS with the concentrations derived from the FLEXPART back trajectories for the 100 x 100 km square centered on Angel peak. The correlation between the two time series is excellent (R^2=0.64), but the stratospheric contributions calculated by FLEXPART are about a factor of two smaller than those derived using AM3. **Figure** 21b shows that the agreement between the AM3 results and the measured concentrations is severely degraded if the AM3 stratospheric contribution is increased by 50%, or decreased by 50% to agree with the FLEXPART results. This implies that the AM3 concentrations are the more accurate. One possible explanation for the systematic differences is that the spatial and temporal boundaries assumed for the FLEXPART source domain excludes a significant contribution from aged stratospheric air. Another possibility is that the assumed 2 PVU definition of the tropopause may have been too restrictive. Note that neither of these possibilities will change the biomass burning and Asian tracer results. In any event, the excellent correlation shows that both models capture the important transport processes.

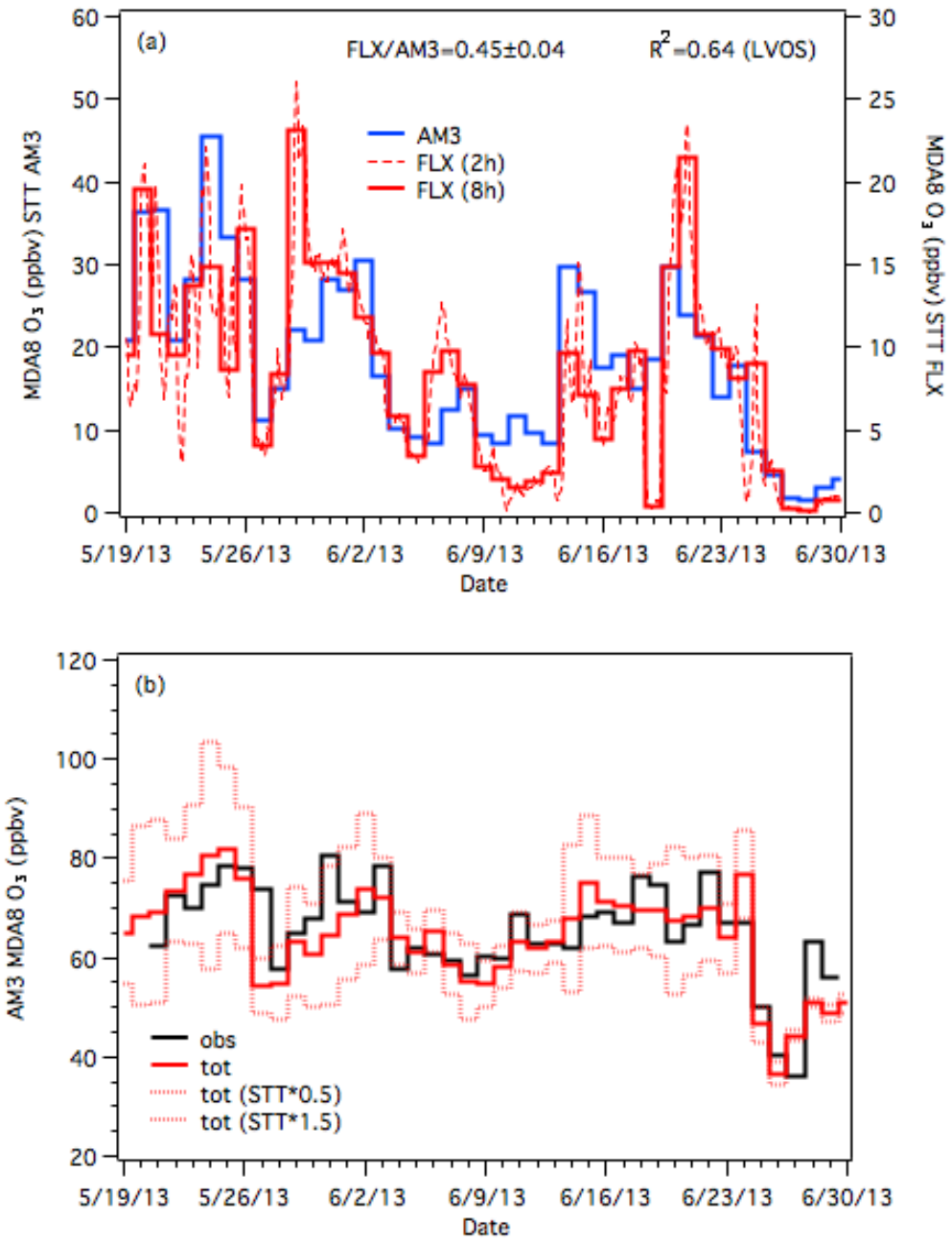

***Figure** 21. (a) Time series comparing the AM3 (blue) and FLEXPART (red) STT ozone calculated for western Clark County during LVOS. The model results are well correlated but differ by about a factor of two (note the different vertical scales). (b) Angel Peak MDA8 observations with the calculated AM3 STT contribution (solid red line) and the AM3 STT contribution scaled by ±50% (dotted red lines).*

7. A closer look at the high ozone days during LVOS

The 2008 NAAQS of 75 ppbv was exceeded by one or more of the CC DAQ regulatory monitors a total of 6 times during 2013 (**Table** 1). The standard was exceeded at Joe Neal on 5 of those days, and at Jean, Paul Meyer, and Palo Verde on 3 days. There were 2 exceedances at Walter Johnson, and one each at Apex, JD Smith, and Winterwood. The May and June exceedances at Jean, which lies upwind of Las Vegas (cf. **Figure** 2), show the influence of transported O_3 and high background concentrations on surface O_3 in Clark County.

***Table** 1: Exceedances of the 2008 NAAQS by Clark County monitors (2013). High ozone events during LVOS are shown in **boldface**.*

Date	MDA8 O_3	Clark County Monitors in Exceedance
May 4	84	Jean, Palo Verde, Paul Meyer, Walter Johnson, Joe Neal, Winterwood
May 21	**78**	**Jean**
May 25	**76**	**Jean, Paul Meyer, Palo Verde, Joe Neal**
June 21	**78**	**Apex, Joe Neal, JD Smith**
July 3	87	Paul Meyer, Walter Johnson, Palo Verde, Joe Neal
July 20	76	Joe Neal

The NAAQS was exceeded in Clark County once before the LVOS campaign (May 4) and twice afterwards (July 3 and 20), but three of the high ozone days (May 21, May 25, and June 21) occurred during the LVOS campaign. The NAAQS was surpassed at Angel Peak on six days (**Table** 2), including two of the exceedance days in the valley (May 25 and June 21). **Table** 2 shows that most of the Angel Peak exceedances occurred in the early morning hours when O_3 was much lower in the valley as a result of nocturnal deposition, and in some cases, titration by NO. The factors contributing to these 3 high ozone events exceedances during LVOS are described in more detail here. The exceedances

on May 4, July 3, and July 20 and the role of wildland fires are discussed in Appendix A.

***Table** 2: Highest ozone days at Angel Peak during LVOS. Exceedances of the 2008 NAAQS are shown in **boldface**.*

Date	AP MDA8	Time (PDT)	Jean MDA8	Joe Neal MDA8	Palo Verde MDA8
May 21	73	(0200-1000)	78	71	72
May 22	71	(0000-0800)	72	68	69
May 23	72	(0400-1200)	73	72	72
May 24	**77**	**(0400-1200)**	**65**	**72**	**69**
May 25	**77**	**(0400-1200)**	**76**	**76**	**76**
May 26	75	(0200-1000)	61	60	61
May 30	**81**	**(0000-0800)**	**69**	**73**	**66**
May 31	71	(0000-0800)	73	67	65
June 2	**79**	**(0200-1000)**	**70**	**73**	**73**
June 17	**76**	(0400-1200)	**69**	**74**	**71**
June 18	75	(0000-0800)	64	65	64
June 21	**77**	**(0000-0800)**	**75**	**77**	**74**

7.1 May 21: Stratospheric ozone and Asian pollution

The first official high ozone day during the LVOS campaign was May 21 when the MDA8 O_3 at Jean reached 78 ppbv. Nine of the 11 regulatory monitors in Clark County measured MDA8 O_3 concentrations greater than 70 ppbv, but none of the other monitors exceeded the standard. The 5-min ozone concentrations measured by several of these monitors on May 21 are plotted in **Figure** 22a. The O_3 concentrations at Jean reached a maximum of 86 ppbv at about 2200 PDT with the highest 8-h average (78.4 ppbv) between 1500 and 2300 PDT. The time series shows two distinct peaks separated by about 4 hours, which were also seen at several of the more northerly monitors on the eastern side of the Las Vegas Valley including Apex (72 ppbv) and Frenchman Mountain (76 ppbv), which is non-regulatory. The second peak was much less pronounced at

the more westerly sites (e.g. Joe Neal). The time lags between the peaks at the different monitors suggest that the high ozone was advected up the Las Vegas Valley from the south.

§§§

Figure *22. (a) Time series of the 5-min O_3 concentrations measured at Jean, Frenchman Mountain, Joe Neal, and Apex between May 20 and May 22. The yellow band brackets the highest 8-h average concentrations. The dashed curve shows the solar radiation measurements from the Spring Mountain Youth Camp and the solid black staircase the AM3 stratospheric O_3. (b) Time series from Jean plotted with the 1-min measurements from the Death Valley, Great Basin, and Zion National Parks, and the 1-h measurements from the Mojave National Preserve.*

§§§

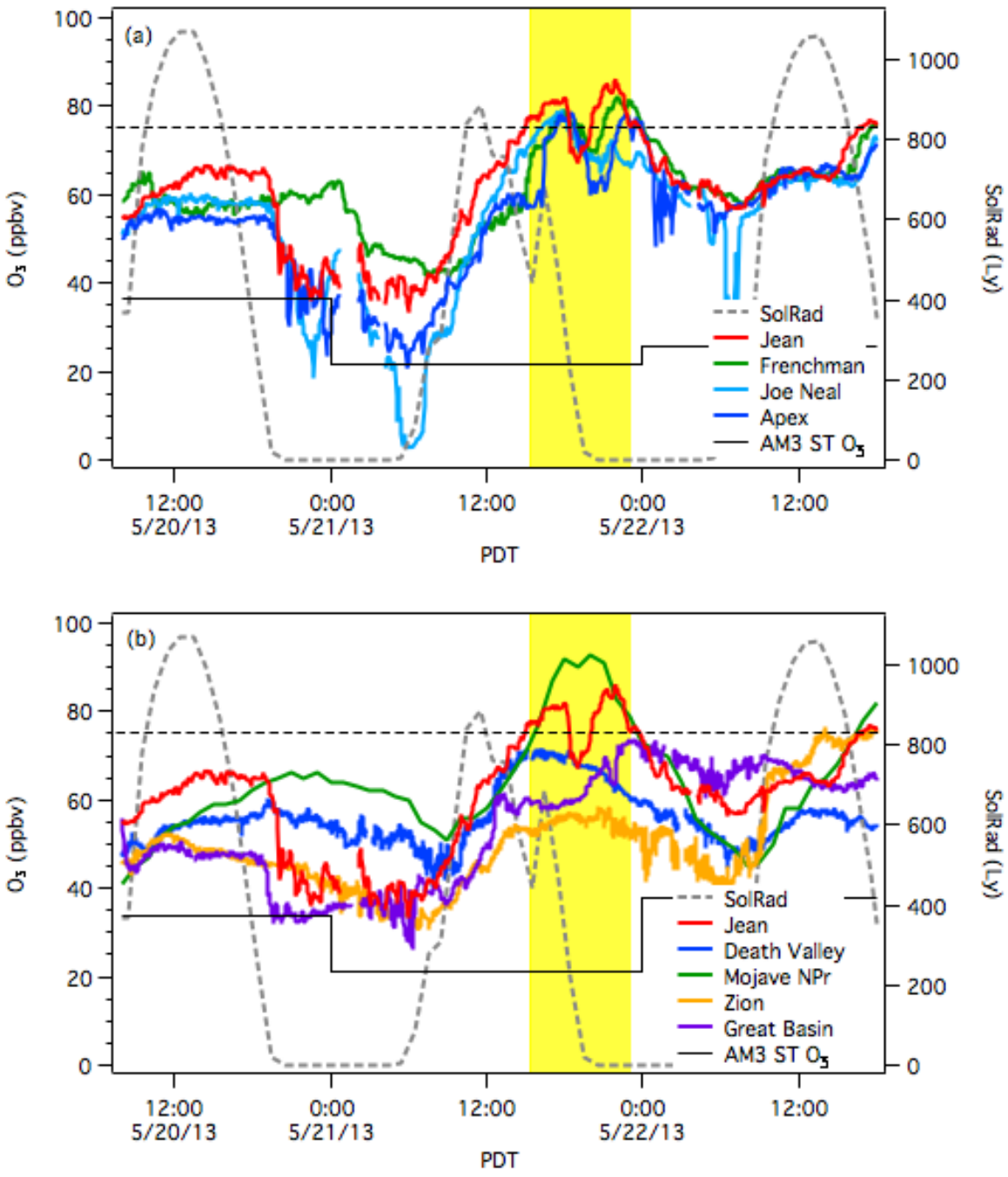
(a)
O3 (ppbv)
SolRad (Ly)
SolRad
Jean
Frenchman
Joe Neal
Apex
AM3 ST O3
12:00 5/20/13
0:00 5/21/13
12:00
0:00 5/22/13
12:00
PDT
(b)
O3 (ppbv)
SolRad (Ly)
SolRad
Jean
Death Valley
Mojave NPr
Zion
Great Basin
AM3 ST O3
12:00 5/20/13
0:00 5/21/13
12:00
0:00 5/22/13
12:00
PDT

Figure 22

Concurrent measurements from regional monitors operated by the National Park Service (**Figure** 22b) also show a spatial gradient, with ozone decreasing from the southwest (Mojave NPr) to the northeast (Zion NP). This gradient is consistent with STT or long-range transport from Asia, but could also be explained by regional transport from the Los Angeles Basin. However, the similar timing of the peak concentrations at the Mojave National Preserve, Jean, and Zion National Park suggests that the elevated ozone was not the result of regional transport.

The AM3 model calculated a stratospheric contribution of about 35 ppbv to the surface concentrations at Jean on May 20 and about 20 ppbv on May 21, and **Figure** 22a shows that the O_3 concentrations were also relatively high (55-65 ppbv) at several of the Clark County monitors on May 20. The O_3 distribution on the 310K isentropic surface (~2-4 km asl) from the 1800 UT (1100 PDT) RAQMS forecast on May 20 (**Figure** 23, upper panel) shows a red orange band of high O_3 (≥100 ppbv) with the characteristic appearance of a tropopause fold on the western flank of an upper level trough centered over the upper Midwest. This band curves above the western U.S. and above southern Nevada. The corresponding CO map (**Figure** 23, lower panel) shows a coincident pale blue band of lower CO (110-120 ppbv) that can just be discerned from the greenish colors (120-130 ppbv) above most of the western United States.

The RAQMS distributions analyzed near the time of the high O_3 in Clark County at 0600 UT on May 22 (2300 PDT on May 21) are displayed in **Figure** 24. The first trough has weakened considerably and now lies above Minnesota and Iowa, and a second, deeper trough that is visible off the west coast in **Figure** 23 has moved ashore above Washington and Oregon. A filament of elevated O_3 trailing behind the second trough stretches across central California and northwestern Nevada. The lower panel shows that this filament is associated with higher CO consistent with transported Asian pollution.

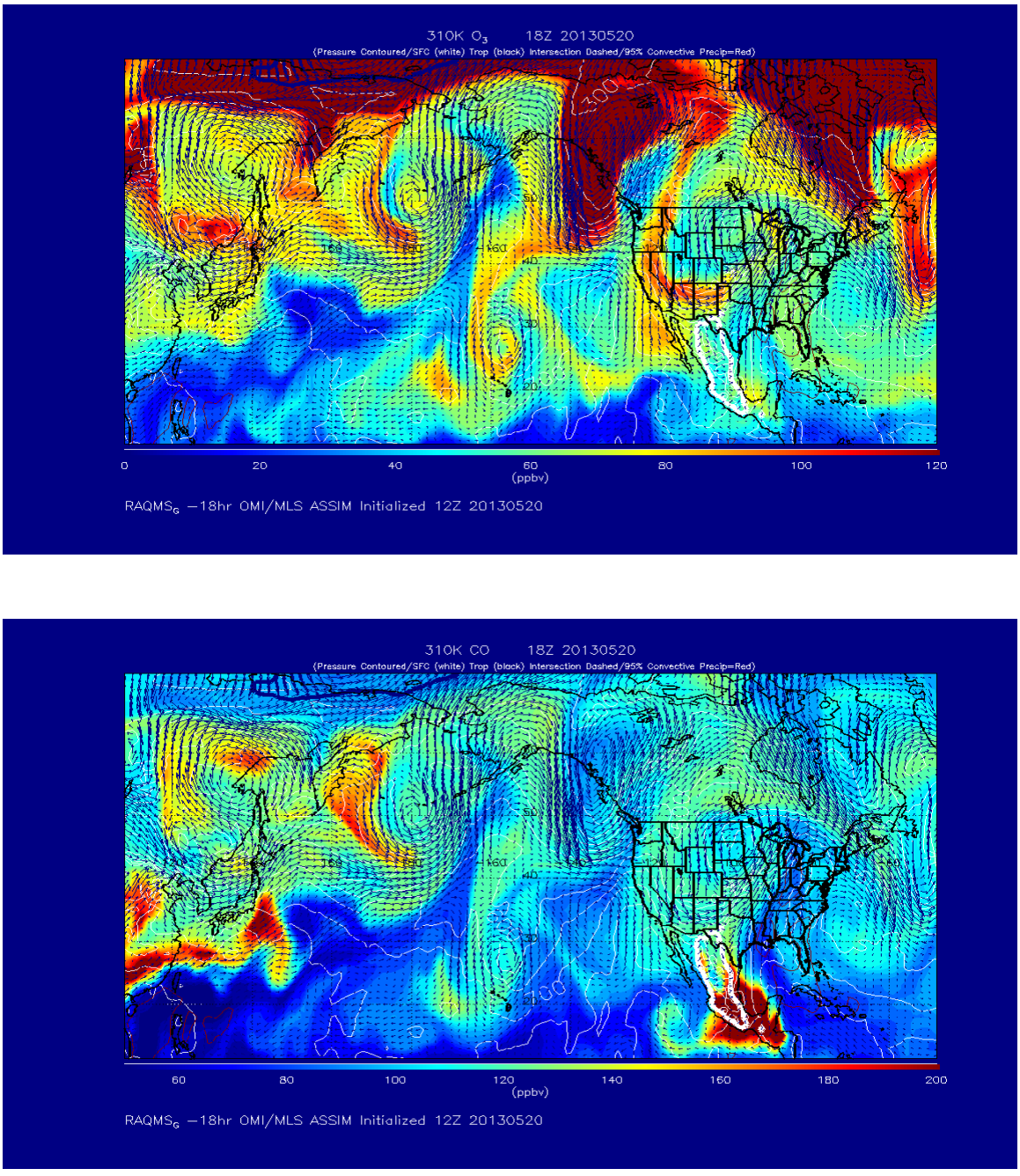

***Figure** 23. RAQMS distributions of O_3 (upper panel) and CO (lower panel) on the 310K potential temperature surface at 1800 UT (1100 PDT) on May 20, 2013.*

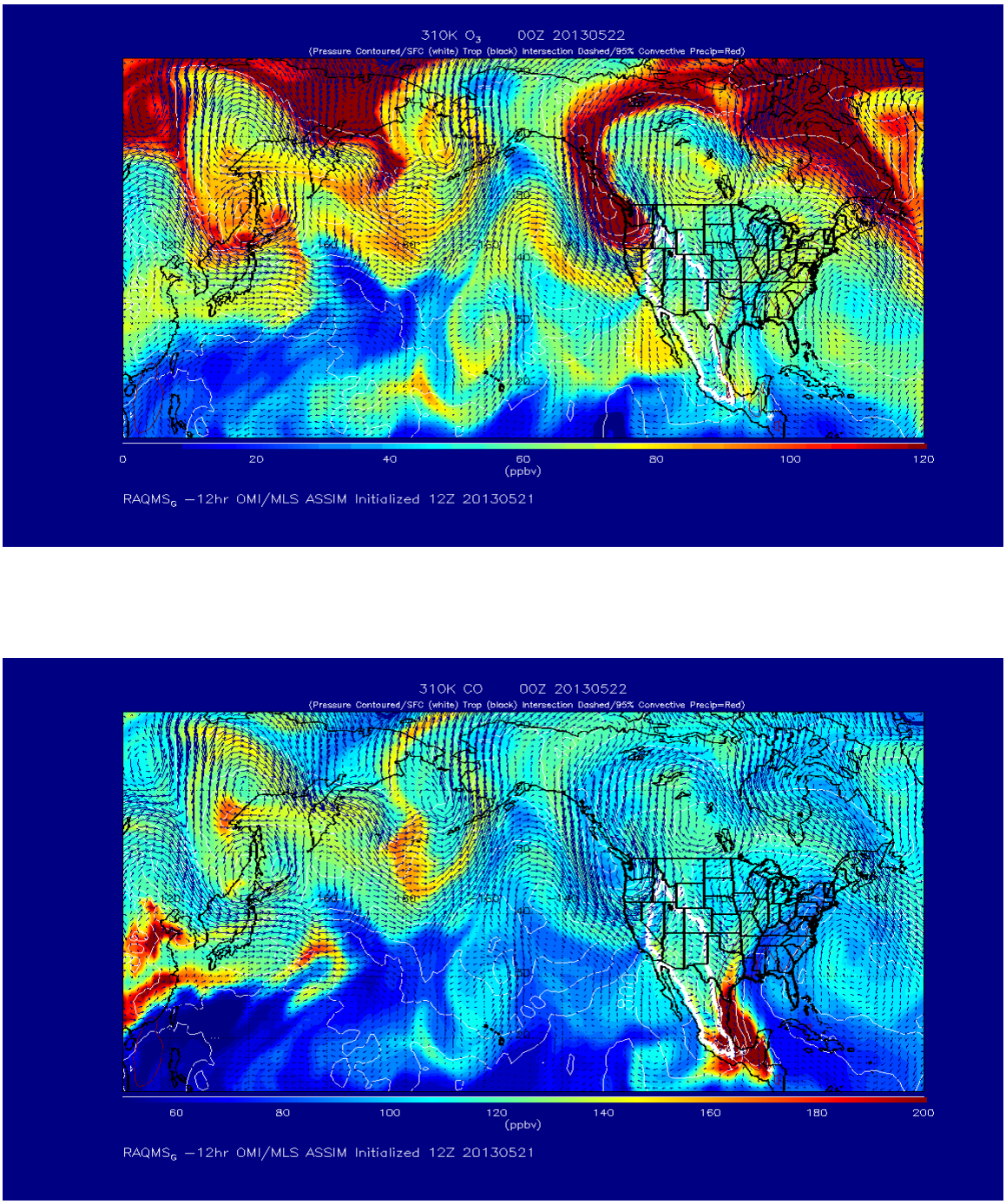

Figure 24. RAQMS distribution of O_3 (upper panel) and CO (lower panel) on the 310K potential temperature surface at 0000 UT on May 22, 2013 (1700 PDT on May 21).

The FLEXPART tracer distributions in the lower free troposphere (3 to 6 km asl) and boundary layer (0 to 1.5 km agl) from the forward model for the same two periods are shown in **Figures** 25 and 26. **Figure** 25 clearly shows the stratospheric intrusion above Nevada prominent in the RAQMS analysis in **Figure** 23, with mean O_3 concentrations in excess of 50 ppbv between 3 and 6 km agl and from 20 to 30 ppbv in the boundary layer above western Clark County in agreement with the AM3 results. There is also an enhancement (10-15 ppbv) in the Asian CO tracer that suggests another 3 to 5 ppbv of transported O_3, but negligible CO (and hence O_3) from biomass burning. The corresponding distributions from 0000 UT on May 22 in **Figure** 26 show that most of the stratospheric O_3 tracer has moved southeast from Nevada into southern Arizona and northern Mexico, with a much larger influx of the Asian pollution CO tracer into southern California and Nevada in the lower free troposphere. The biomass burning CO tracer is still insignificant. The RAQMS and FLEXPART plots are included here to qualitatively illustrate the horizontal distribution and to a lesser degree, the vertical extents, of these transport events. **Figures** 19 and 21 show a more quantitative estimate of the impact of these STT events on MDA8 O_3 in Clark County from the AM3 and FLEXPART models.

The TOPAZ lidar and Angel Peak in situ measurements made during the same time period are displayed in **Figure** 27. Panel (a) shows time-height curtain plots of the colorized ozone concentrations together with the integrated aerosol backscatter (ß in units of 10^{-4} sr^{-1}) from 0 to 2000 m agl and the SMYC solar irradiance. The red “X”s marks the approximate top of the mixed layer derived from the 0000 UT (1700 PDT) VEF soundings on May 22 and 23 (the May 21 sounding failed). Panel (b) plots the corresponding 0 to 2000 m agl average O_3 from the lidar in red with the in situ measurements plotted in blue; the gray dotted line shows the in situ CO concentrations. The Jean O_3 measurements from **Figure** 22 (green) are included for comparison with the 8-h high O_3 period highlighted in yellow as before. The two bottom panels (c) and (d), show the winds, temperature, and specific humidity measured at Angel Peak.

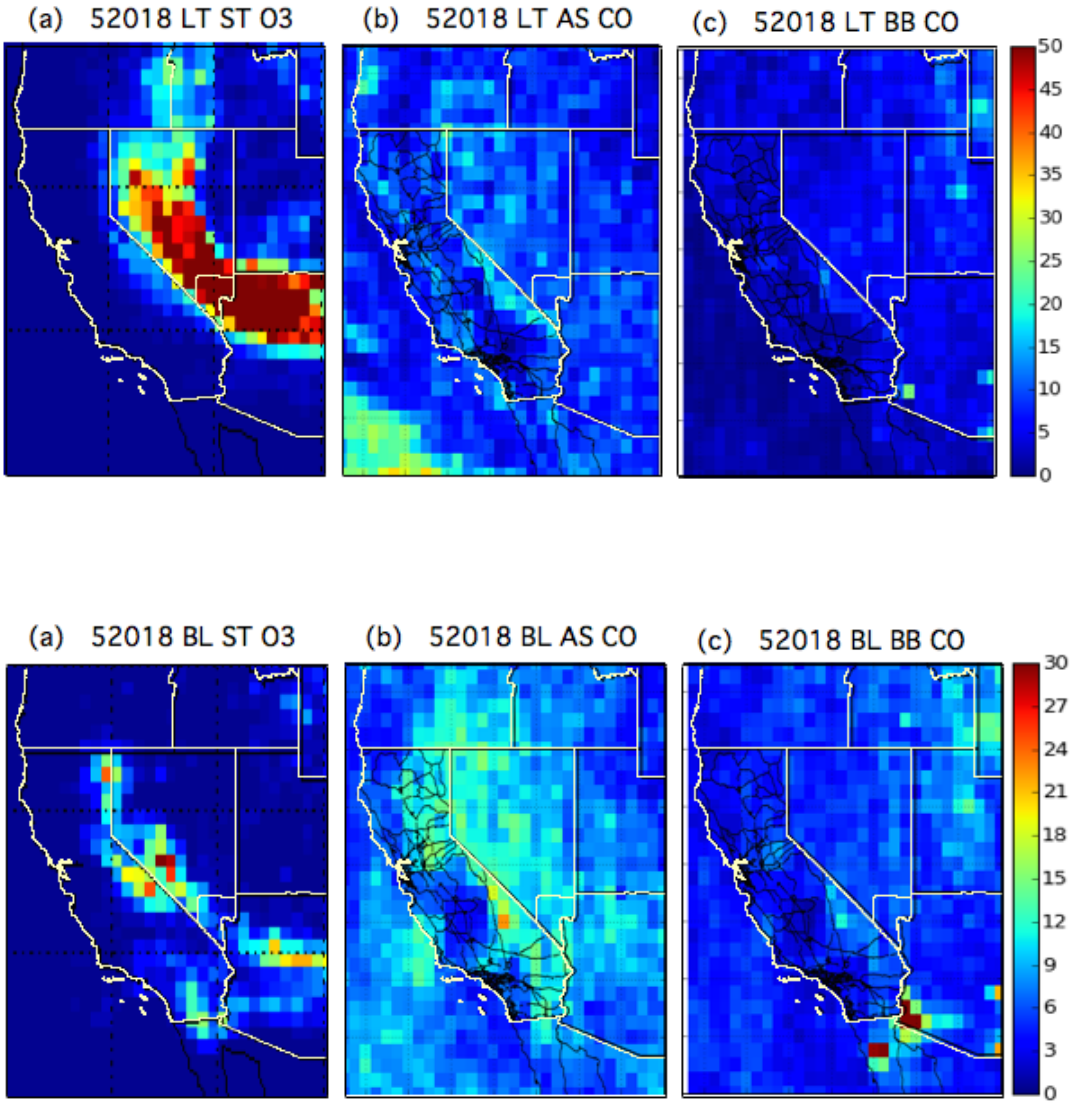

***Figure** 25. Mean (a) stratospheric (ST) O_3, (b) Asian pollution (AS) CO, and (c) biomass burning (BB) CO FLEXPART tracers at 1800 UT (1100 PDT) on May 20. The upper and lower panels show the mean concentrations in the lower free troposphere (3-6 km asl) and boundary layer (0 to 1.5 km agl), respectively. Note the different color scales. **Figures** 19 and 21 show a more quantitative estimate of the STT contribution to MDA8 O_3 in Clark County from the AM3 and FLEXPART models.*

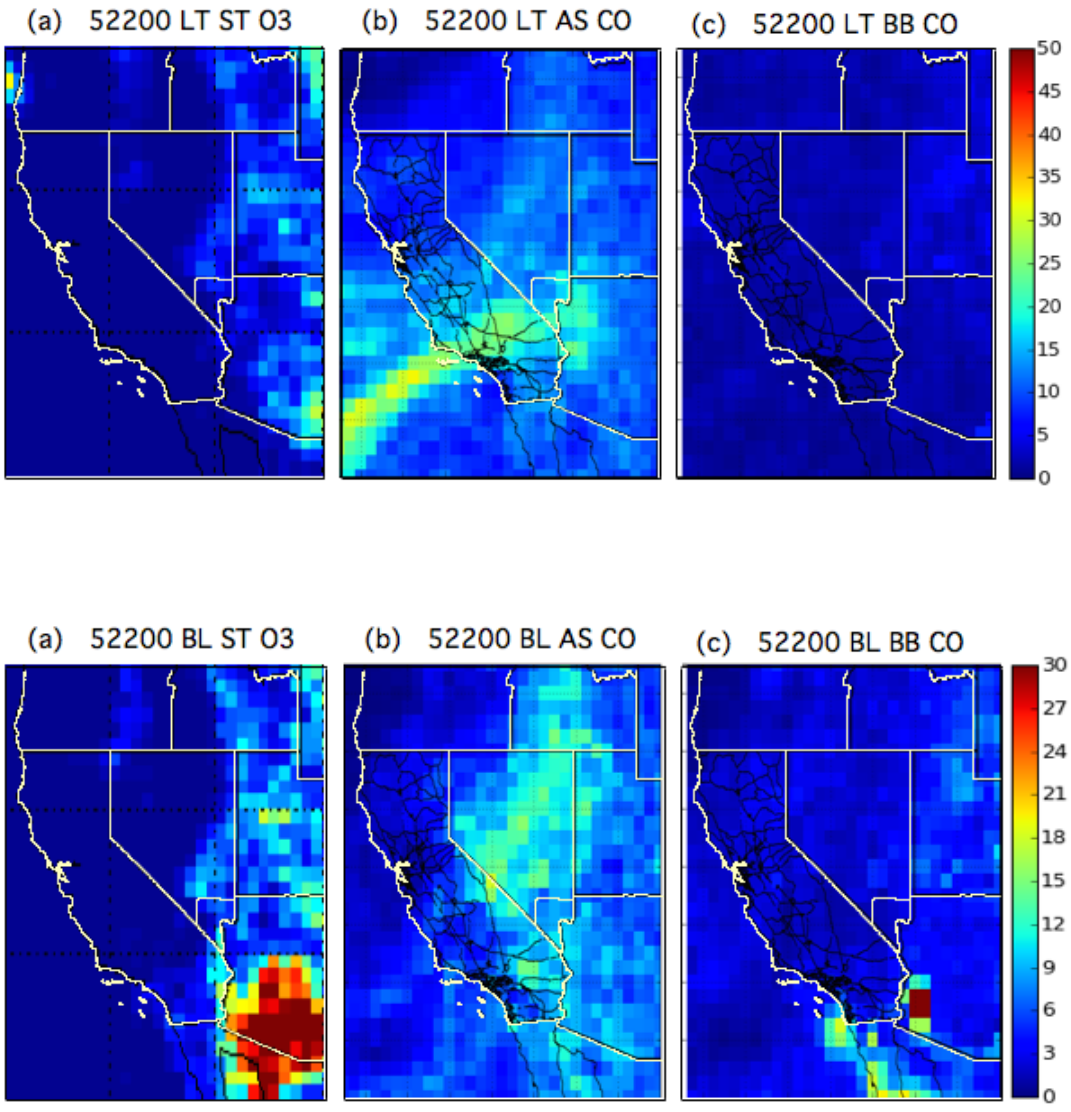

***Figure** 26. Same as Figure 25, but for 0000 UT on May 22 (1700 PDT on May 21). **Figures** 19 and 21 show a more quantitative estimate of the STT contribution to MDA8 O_3 in Clark County from the AM3 and FLEXPART models.*

The TOPAZ measurements from May 20 show a layer of high O_3 between 4 and 5 km asl with peak concentrations in excess of 100 ppbv and low integrated aerosol backscatter consistent with the stratospheric intrusion seen in the RAQMS and FLEXPART analyses. The surface winds were weak and the in situ O_3 and CO concentrations at Angel Peak on the order of 60 and 130 ppbv, respectively. The surface O_3 and CO concentrations slowly increased and decreased, respectively, by about 5 ppbv during the late afternoon and evening as the high O_3 layer slowly descended. Both O_3 and CO remained relatively constant at Angel Peak through the late night and early morning as the winds increased and became southerly, while surface deposition depleted the O_3 at Jean. The winds at Angel peak became stronger and more southwesterly in the early afternoon of May 21 and the O_3 concentrations increased from about 60 to 75 ppbv from the surface to at least 2000 m above Angel Peak. The aerosol backscatter remained very low indicating that this O_3-enriched air did not originate in the boundary layer (e.g. from the Los Angeles Basin).

§§§

***Figure** 27. Time series of Angel Peak measurements from May 20 to 22. (a) TOPAZ O_3 time-height curtain plots with aerosol backscatter (ß = black) and SMYC solar flux (black dashed) superimposed. The red X's shows the mixed layer depth from the afternoon (0000 UT May 22 and 23) VEF soundings. (b) In situ O_3 from Jean (green) and Angel Peak (blue) and the 0 to 2000 m agl integrated TOPAZ O_3 concentrations (red). The dashed black line represents the in situ CO concentrations. (c) Wind speed (blue) and direction (dashed red). (d) Temperature (red) and specific humidity (red).*

§§§

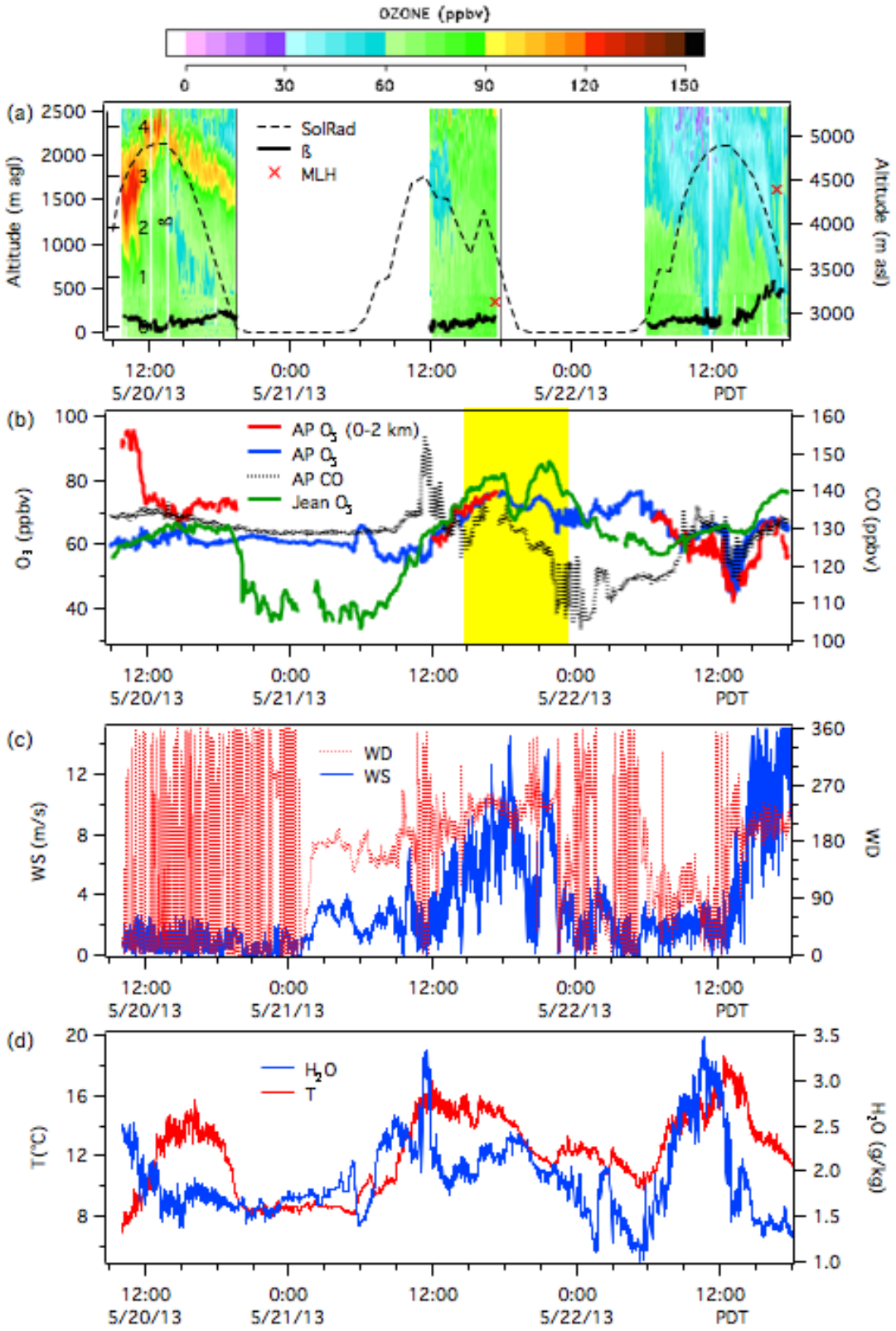
OZONE (ppbv)
0
30
60
90
120
150
(a)
Altitude (m agl)
Altitude (m asl)
SolRad
ß
MLH
12:00
5/20/13
0:00
5/21/13
12:00
0:00
5/22/13
12:00
PDT
(b)
O_3 (ppbv)
CO (ppbv)
AP O_3 (0-2 km)
AP O_3
AP CO
Jean O_3
(c)
WS (m/s)
WD
WD
WS
(d)
T (°C)
H_2O (g/kg)
H_2O
T

Figure 27.

The Angel Peak measurements confirm the sequential influx of stratospheric and Asian pollution seen in the RAQMS and FLEXPART analyses. **Figure** 28 shows a scatter plot of the in situ O_3 and CO concentrations measured at Angel Peak over the 24 hour period beginning at 0930 PDT on May 20 (filled triangles, lower cluster) and the 8-h period from 1500 to 2300 PDT on May 21 (filled circles, upper cluster) when the MDA8 O_3 was measured at Jean. The uncorrelated measurements in the lower cluster show the mixing of lower tropospheric air with drier, O_3-enriched air from the UT/LS as the latter subsided over Clark County. The modest O_3 concentrations and water vapor content of the subsiding air show that there had been substantial mixing with upper tropospheric air as the intrusion descended from the lower stratosphere. In contrast to the measurements from May 20, the mixing lines from the afternoon and evening of May 21 show a strong positive correlation. However, the relatively low water vapor content of this air shows a free tropospheric origin consistent with long-range transport from Asia and not from the Los Angeles Basin (cf. **Figure** A3). The net increase in O_3 associated with these transport processes appears to be on the order of 20 ppbv.

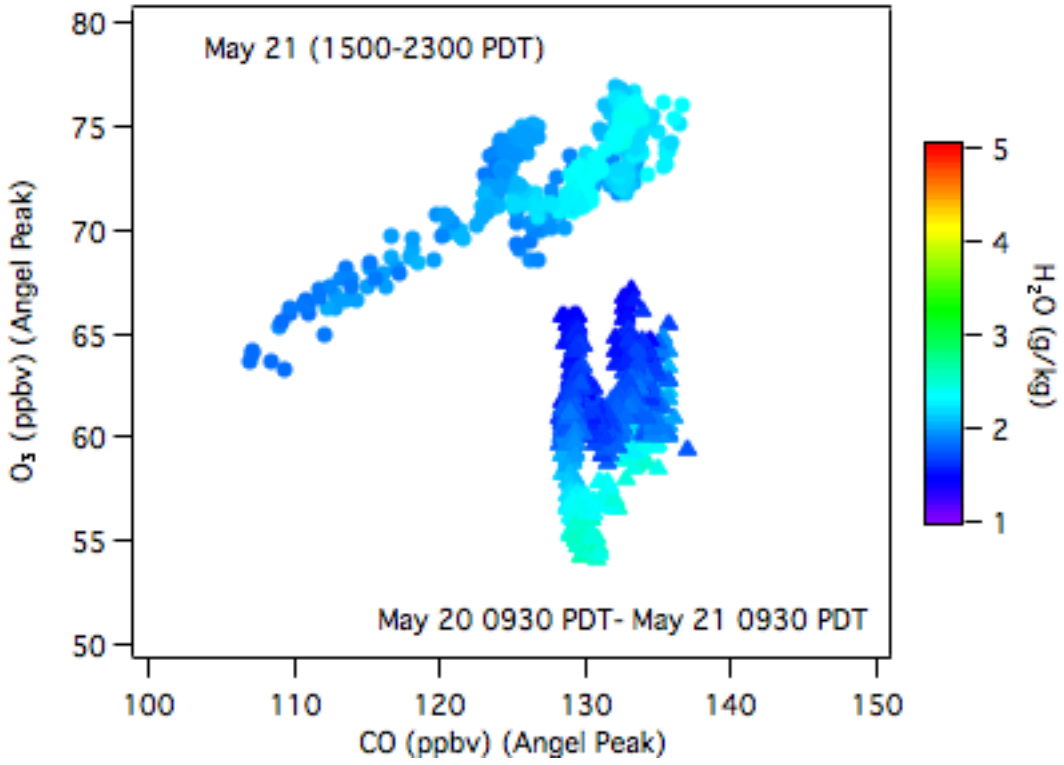

Figure 28. *Scatter plot comparing the in situ Angel Peak O_3 and CO measurements during the 24 hour period beginning at 0930 PDT on May 20 (filled triangles, lower cluster) and the 8-h period from 1500 to 2300 PDT on May 21 (filled circles, upper cluster). The points are colorized by specific humidity.*

7.2 May 25: Stratospheric ozone

The second high ozone event during LVOS occurred on May 25 when all but one of the 11 Clark County monitors recorded an MDA8 of at least 70 ppbv and 4 of the monitors exceeded the 2008 standard with MDA8 concentrations of 76 ppbv. Three of the four highest 24-hour average O_3 concentrations measured in Clark County during 2013 were recorded on that day with values of 72 ppbv at Paul Meyer, 71 ppbv at Jean, and 70 ppbv at Palo Verde. The NAAQS was also exceeded (76 ppbv) at Great Basin National Park and nearly equaled at Death Valley National Park (73 ppbv) to the north and west of Clark County, respectively. **Figure** 29a shows time series of the 5-min O_3 concentrations measured at several of the Clark County and NPS sites with the SMYC solar radiation and AM3 STT O_3 plotted as before. The highest 8-h average O_3 at most of the Clark County monitors was measured between 1400 and 2200 PDT on May 25, but O_3 remained high for several days with an average concentration at Jean of 68 ppbv over the 60 h period from noon on May 23 to midnight on May 25. **Figure** 29a shows the high O_3 to be quite homogeneous across a large area with the highest concentrations between sunset and midnight on all three days.

§§§

Figure *29. (a) Time series of 5-min ozone concentrations at Jean, Joe Neal, Palo Verde, and Paul Meyer between May 23 and May 26. The yellow band brackets the highest 8-h average concentrations on May 25. The dashed curve shows the solar radiation measurements from the Spring Mountain Youth Camp and the solid black staircase the AM3 stratospheric O_3. (b) Same as (a), but with the 1-min. measurements from the Death Valley, Great Basin, and Zion National Parks, and 1-h measurements from the Mojave National Preserve.*

§§§

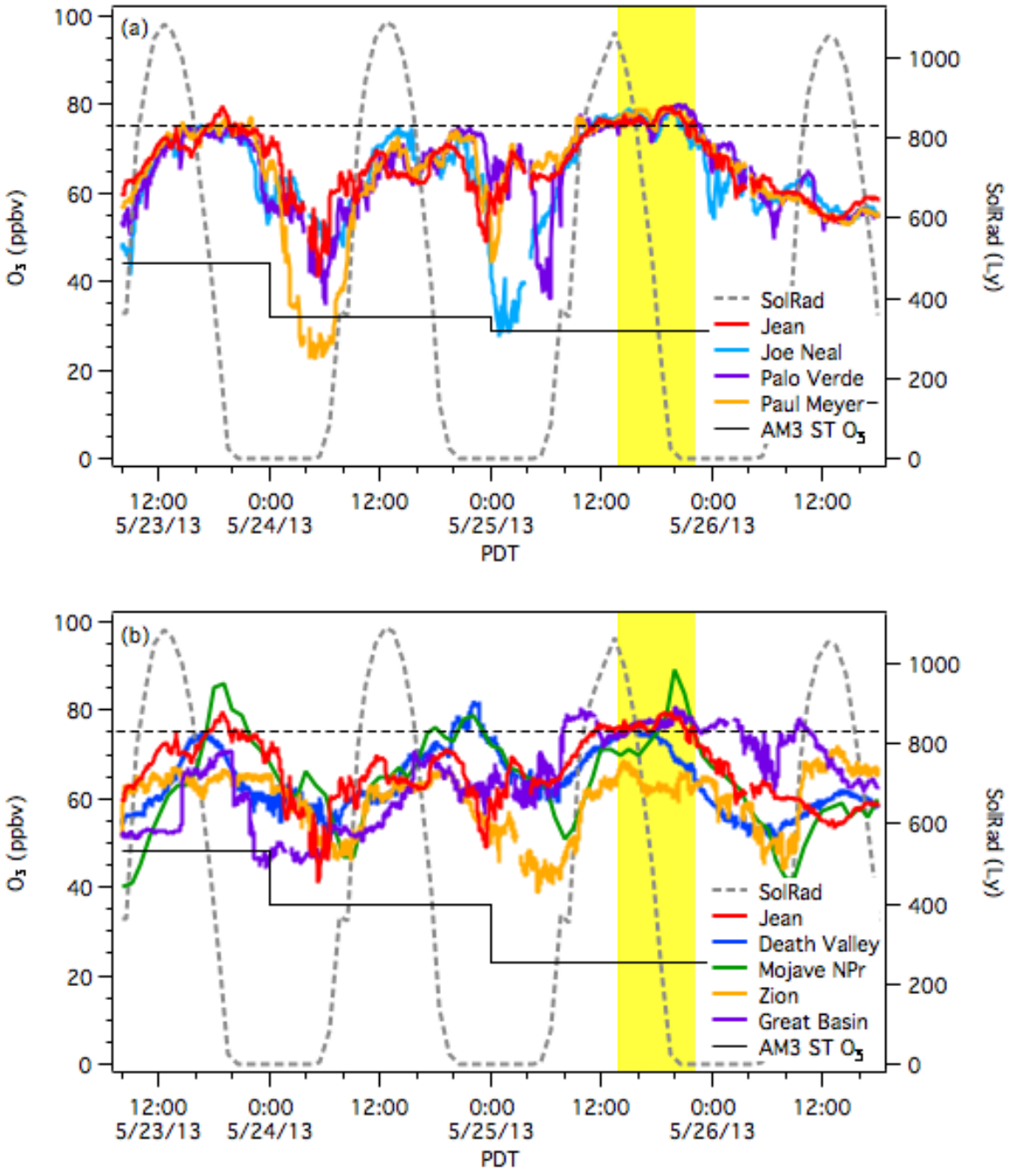
(a)
O3 (ppbv)
SolRad (Ly)
SolRad
Jean
Joe Neal
Palo Verde
Paul Meyer
AM3 ST O3
12:00 5/23/13
0:00 5/24/13
12:00
0:00 5/25/13
12:00
0:00 5/26/13
12:00
PDT
(b)
O3 (ppbv)
SolRad (Ly)
SolRad
Jean
Death Valley
Mojave NPr
Zion
Great Basin
AM3 ST O3
12:00 5/23/13
0:00 5/24/13
12:00
0:00 5/25/13
12:00
0:00 5/26/13
12:00
PDT

Figure 29

The AM3 analyses indicate that a very large fraction (35 to 45 ppbv) of the high surface O_3 measured in Clark County between May 23 and 25 was of stratospheric origin. This influx was associated with the deep trough seen over the Pacific Northwest in **Figure** 24, which became cutoff from the main flow at 500 hPa and trailed a broad plume of O_3 rich/CO poor air across the western U.S. over the next few days (**Figures** 30-32).

The FLEXPART tracer distributions in the lower free troposphere (3-6 km asl) at 1800 UT (1100 PDT) on May 23 (**Figure** 33**)** show 20-30 ppbv of stratospheric O_3 in the lower free troposphere and boundary layer above central Nevada and in the boundary layer the Mojave Desert. A similar amount of Asian CO can be seen in the lower free troposphere (cf. **Figure** 26b, upper). The influence of biomass burning is completely negligible. The stratospheric tracer descended and spread out over most of Nevada over the next 24 hours as the Asian pollution layer moved southeastward. The distributions in the boundary layer (0 to 1.5 km agl) show 20 to 30 ppbv of stratospheric O_3 just to the west of Clark County with 5-10 ppbv of Asian CO and negligible concentrations of the biomass burning CO tracer. The stratospheric contribution is diminished, but still significant 24 hours later at 1800 UT (1100 PDT) on May 25 (**Figure** 35). As before, the RAQMS and FLEXPART plots are included here to qualitatively illustrate the horizontal distribution and to a lesser degree, the vertical extents, of these transport events. **Figures** 19 and 21 provide a more quantitative estimate of the impact of these STT events on MDA8 O_3 in Clark County from the AM3 and FLEXPART models.

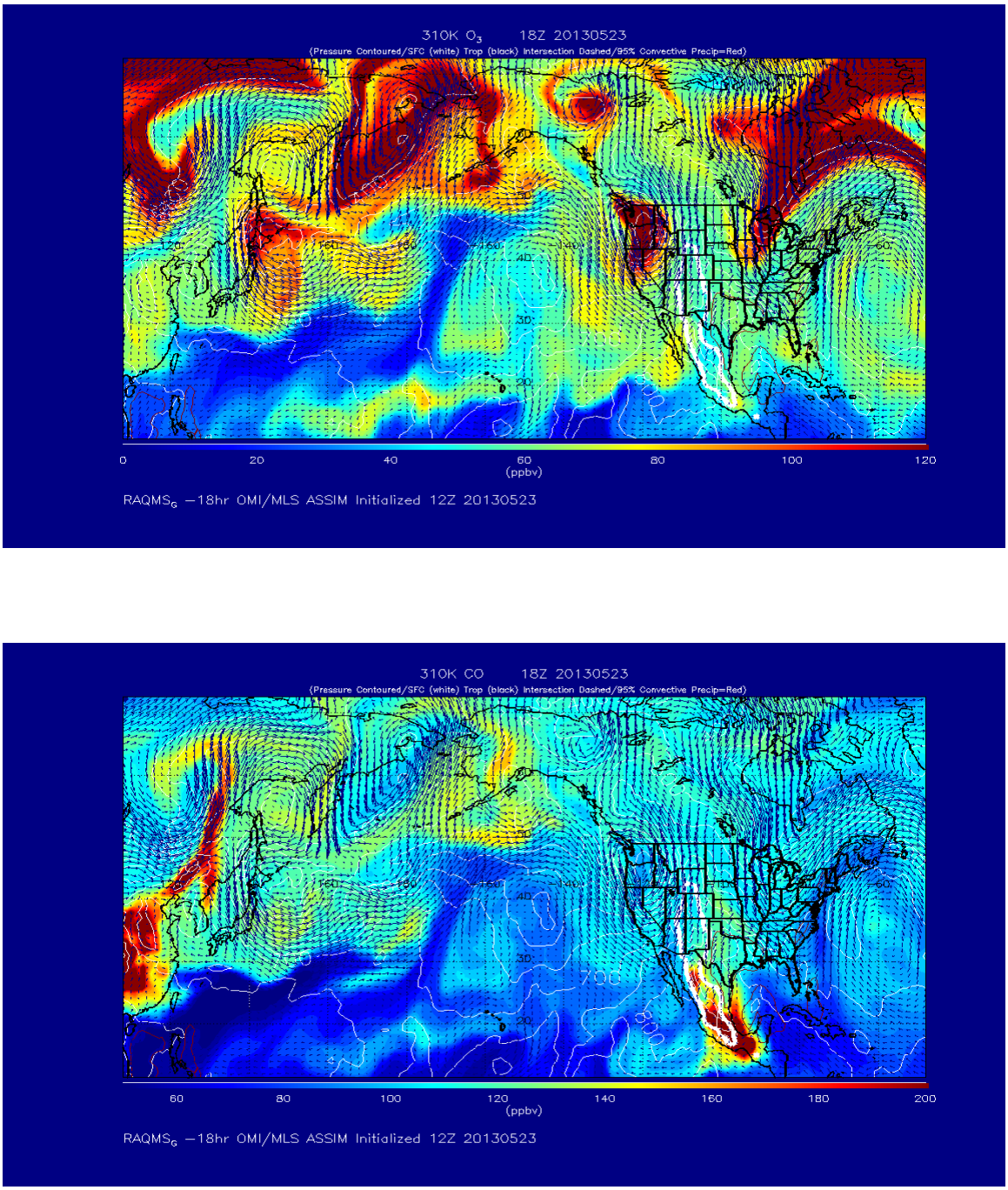

***Figure** 30. RAQMS distributions of O_3 (upper panel) and CO (lower panel) on the 310K potential temperature surface at 1800 UT (1100 PDT) on May 23, 2013.*

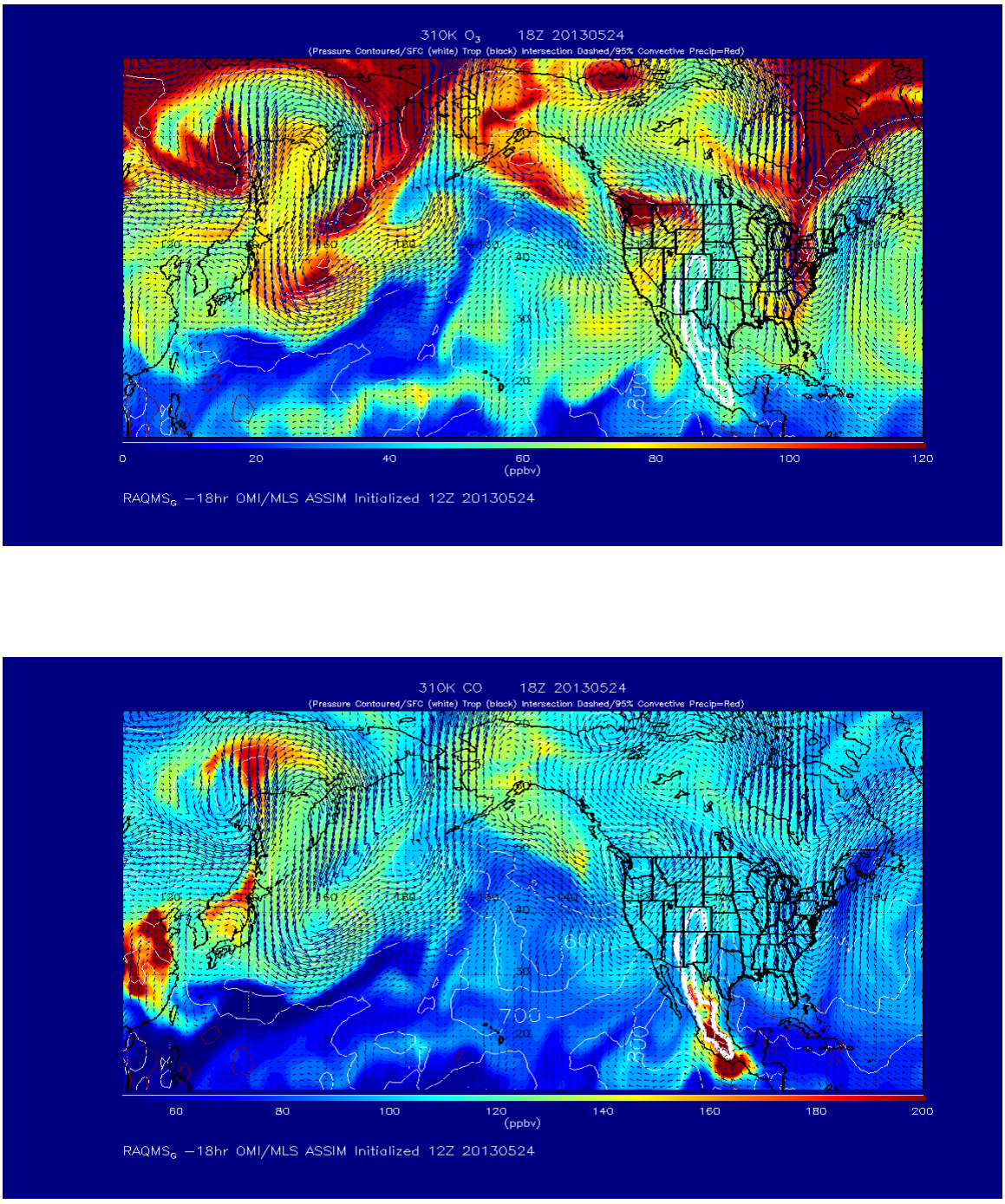

***Figure** 31. RAQMS distributions of O_3 (upper panel) and CO (lower panel) on the 310K potential temperature surface at 1800 UT (1100 PDT) on May 24, 2013.*

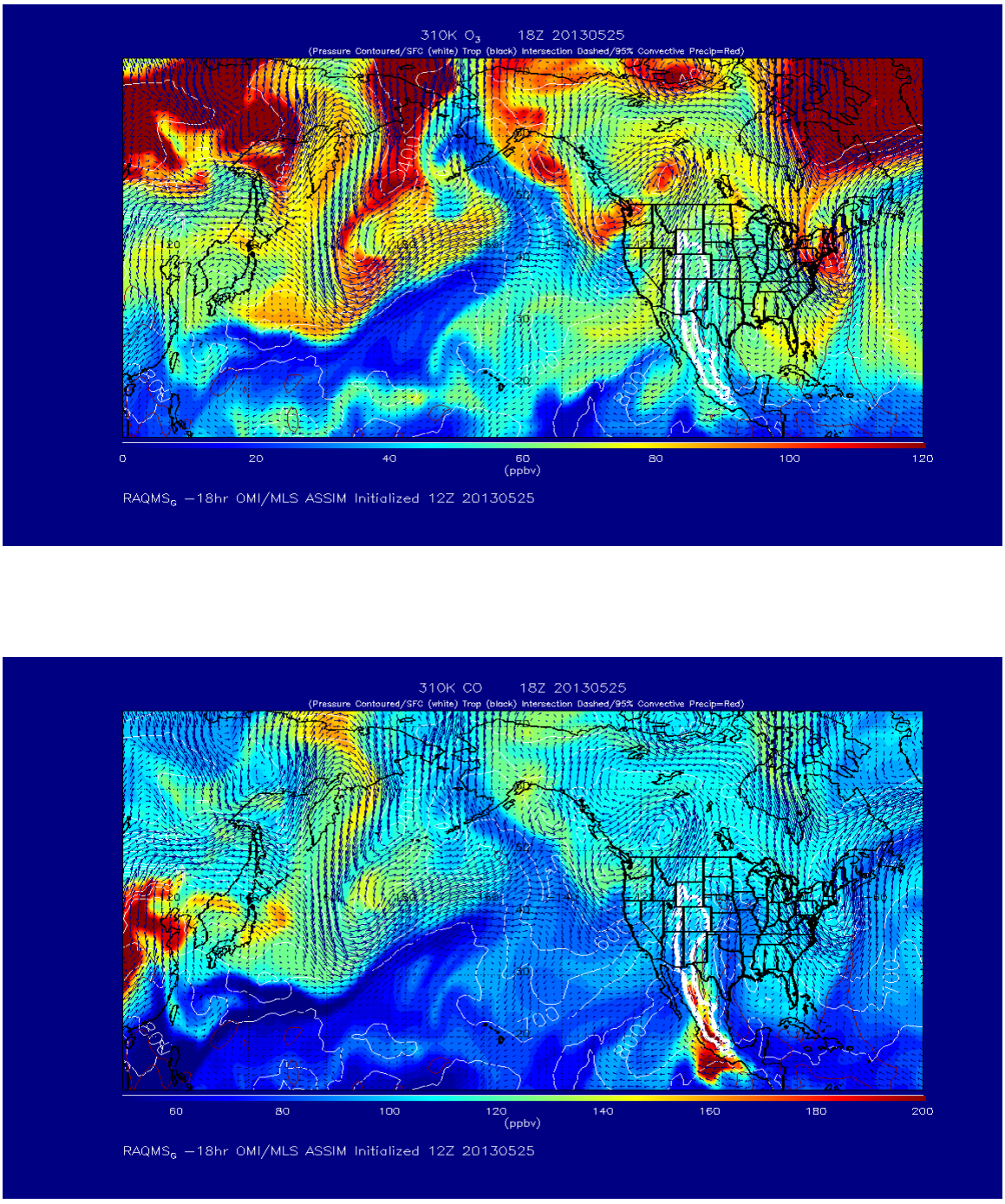

***Figure** 32. RAQMS distributions of O_3 (upper panel) and CO (lower panel) on the 310K potential temperature surface at 1800 UT (1100 PDT) on May 25, 2013.*

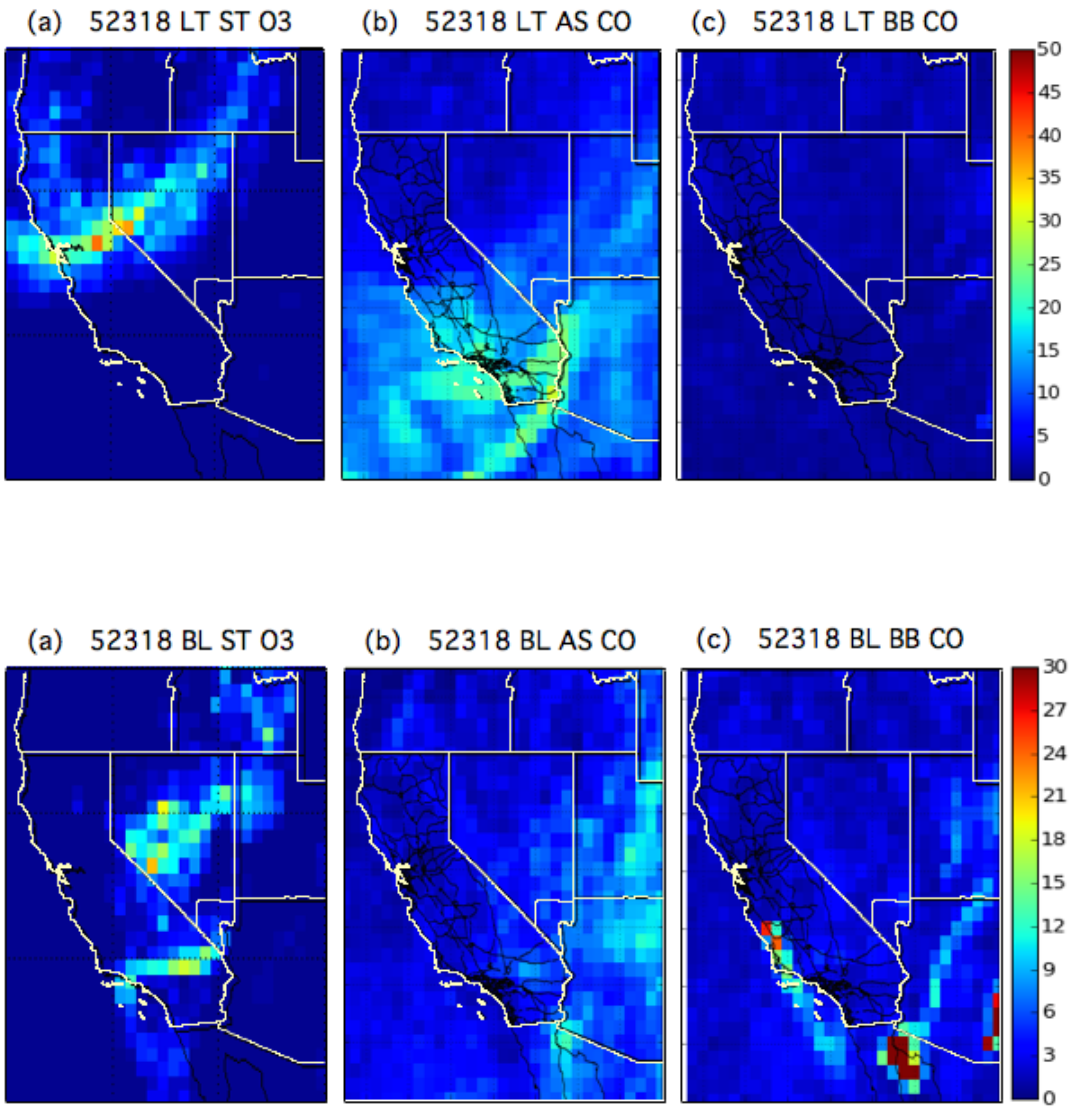

***Figure** 33. Same as Figure 25, but for 1800 UT (1100 PDT) on May 23. **Figures** 19 and 21 show a more quantitative estimate of the STT contribution to MDA8 O_3 in Clark County from the AM3 and FLEXPART models.*

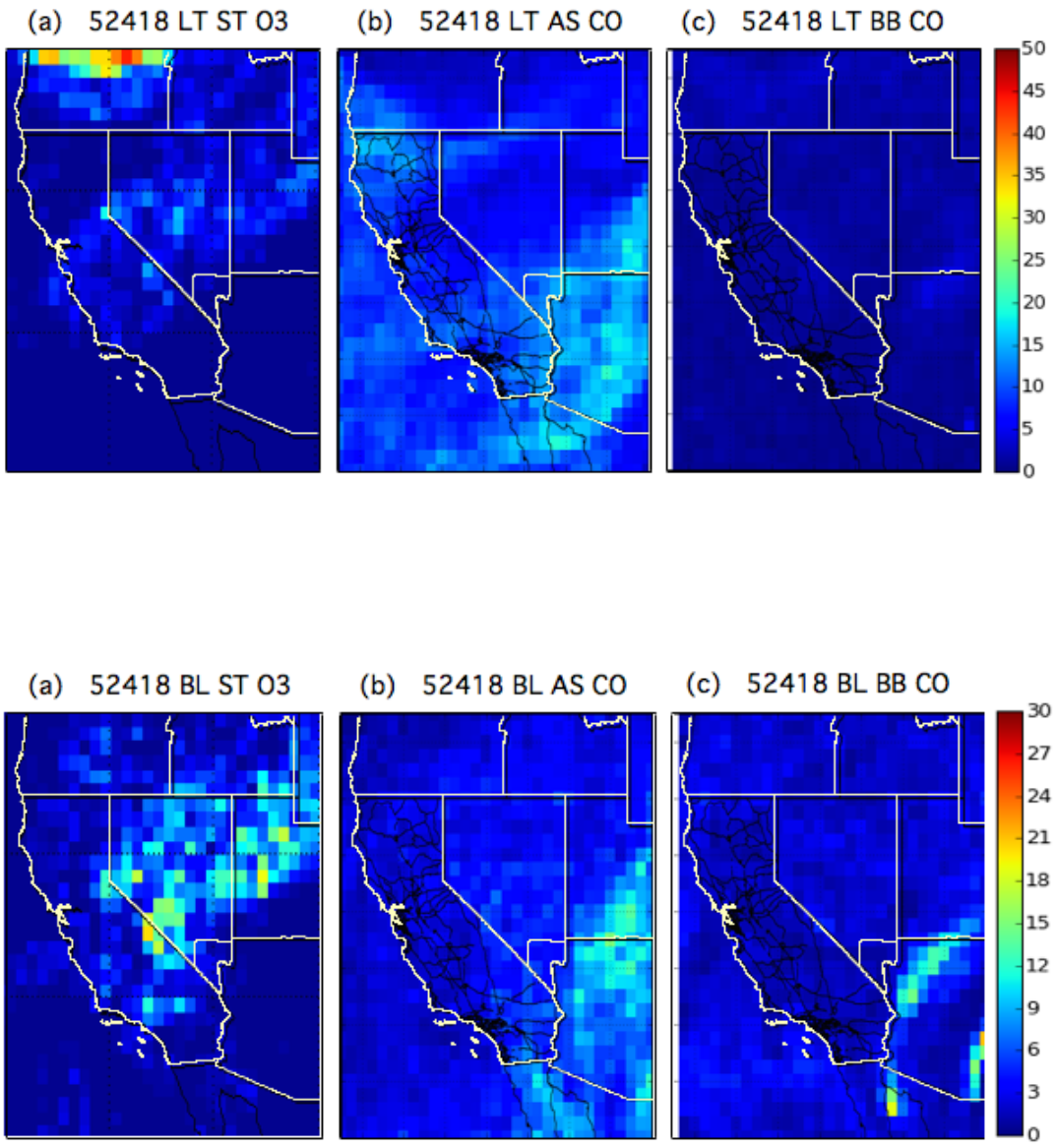

***Figure** 34. Same as Figure 25, but for 1800 UT (1100 PDT) on May 24. **Figures** 19 and 21 show a more quantitative estimate of the STT contribution to MDA8 O_3 in Clark County from the AM3 and FLEXPART models.*

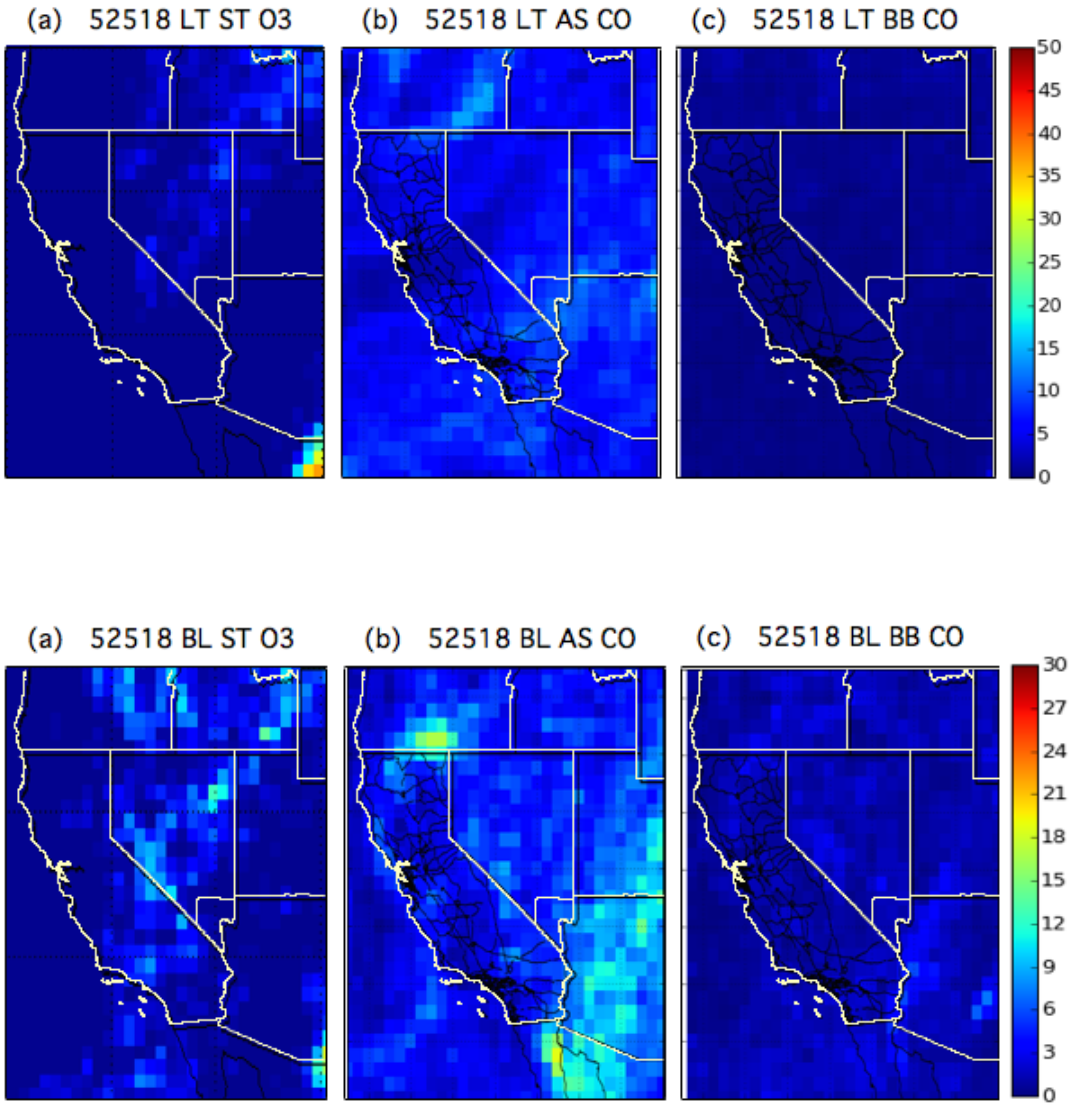

***Figure** 35. Same as Figure 25, but for 1800 UT (1100 PDT) on May 25. **Figures** 19 and 21 show a more quantitative estimate of the STT contribution to MDA8 O_3 in Clark County from the AM3 and FLEXPART models.*

The in situ measurements from Angel Peak plotted in **Figure** 36-1 also show a surface O_3 maximum at about 2100 PDT on the night of May 24 when the TOPAZ lidar showed several filaments of high O_3 sloping downward toward the surface. These filaments were associated with low column aerosol loadings and the high surface O_3 was associated with low CO and very dry air, indicative of a lower stratospheric origin. The lidar tracked one of these filaments all the way down to the surface where there was a simultaneous increase in the surface O_3 and decrease in CO and water vapor. Low CO and water vapor were also measured at Angel Peak on the afternoon of May 25 when the O_3 concentrations were highest. Note the brisk southwesterly winds associated with the circulation around the upper level trough during the night. The monitor at Angel Peak exceeded the NAAQS on May 24, 25, and 26. Figure 36-2 is an expanded view of the measurements from the night of May 24 and morning of May 25 showing the direct correspondence between the descending O_3 layers seen by the lidar and changes in the surface O_3, CO, and H_2O (RH) at Angel Peak.

§§§

Figure *36. Angel Peak measurements from May 23-26 (36-1) with an expanded view of May 24-25 (36-2). (a) TOPAZ O_3 time-height curtain plots with aerosol backscatter (ß = black) and SMYC solar flux (black dashed) superimposed. The red X's shows the mixed layer depth from the afternoon (0000 UT) VEF soundings. (b) Surface O_3 from Jean (green) and Angel Peak (blue), and 0 to 2000 m agl integrated TOPAZ O_3 concentrations (red), from Angel Peak along with the in situ CO (dashed black). (c) Wind speed (blue) and direction (dashed red). (d) Temperature (red) and specific humidity (red).*

§§§

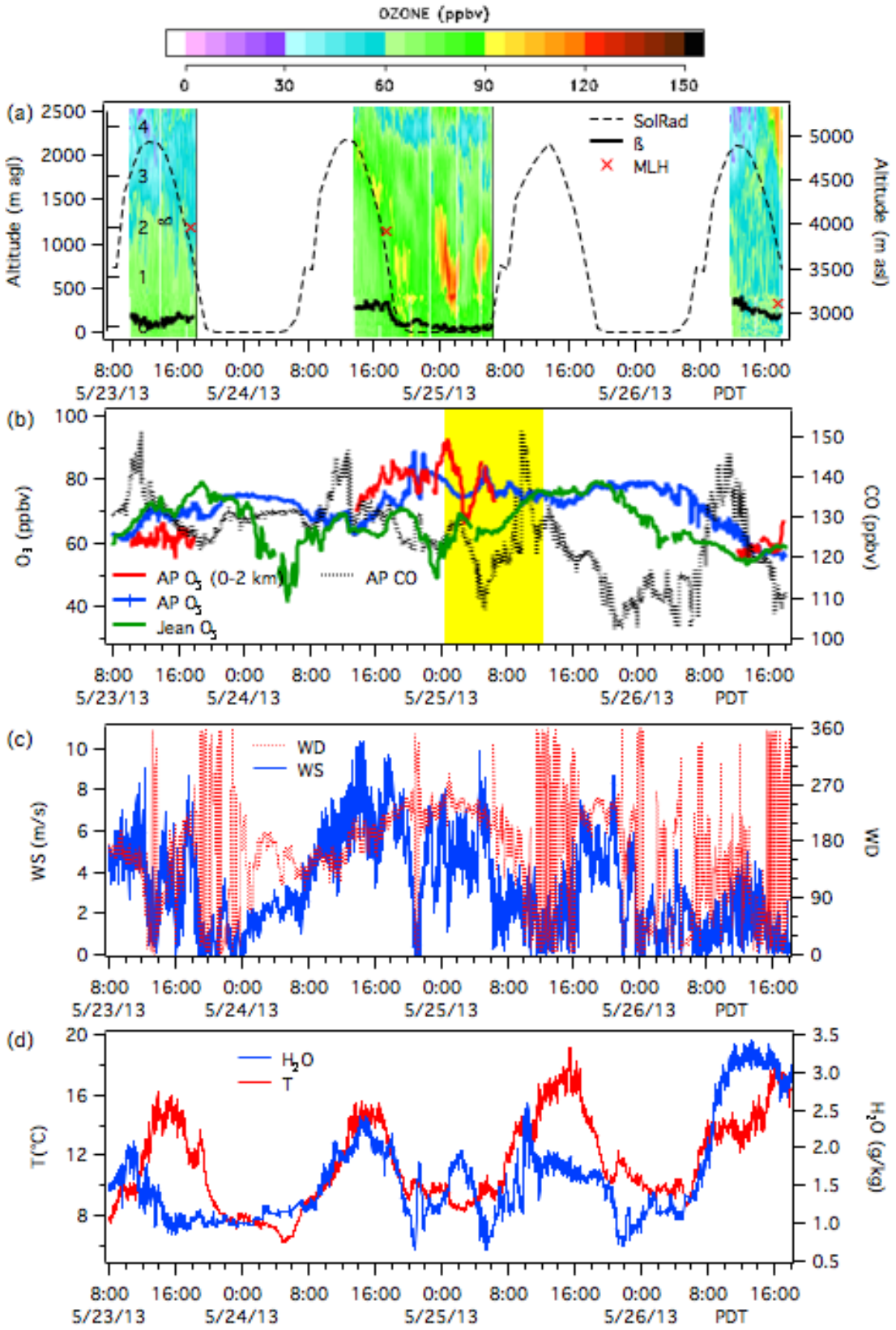
OZONE (ppbv)
0
30
60
90
120
150
(a)
Altitude (m agl)
Altitude (m asl)
SolRad
ß
MLH
(b)
O3 (ppbv)
CO (ppbv)
AP O3 (0-2 km)
AP CO
AP O3
Jean O3
(c)
WS (m/s)
WD
WS
(d)
T(°C)
H2O (g/kg)
H2O
T
8:00
16:00
0:00
8:00
16:00
0:00
8:00
16:00
0:00
8:00
16:00
5/23/13
5/24/13
5/25/13
5/26/13
PDT

Figure 36-1

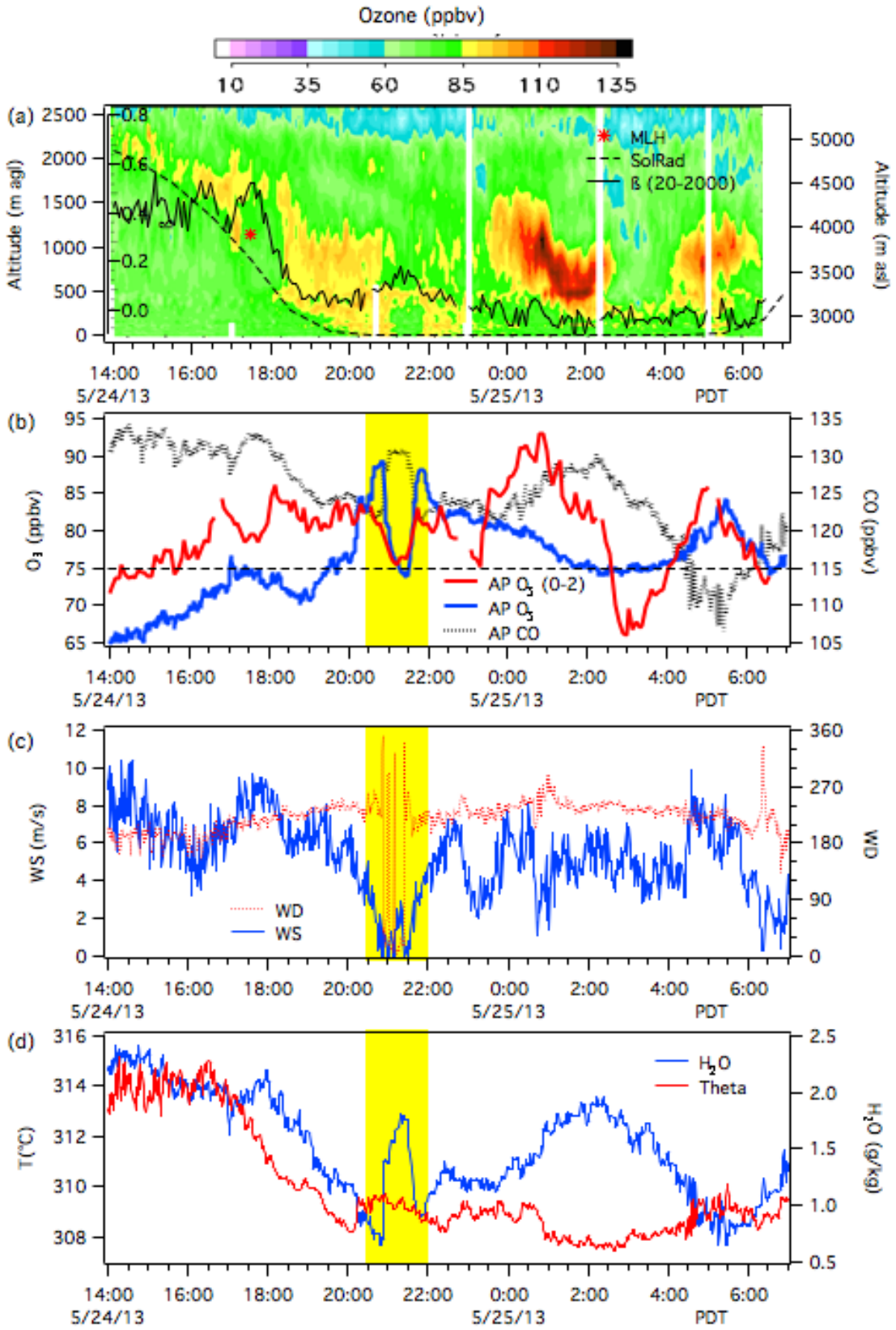
Ozone (ppbv)
10
35
60
85
110
135
(a)
Altitude (m agl)
Altitude (m asl)
MLH
SolRad
ß (20-2000)
(b)
O3 (ppbv)
CO (ppbv)
AP O3 (0-2)
AP O3
AP CO
(c)
WS (m/s)
WD
WD
WS
(d)
T (°C)
H2O (g/kg)
H2O
Theta
14:00
16:00
18:00
20:00
22:00
0:00
2:00
4:00
6:00
5/24/13
5/25/13
PDT

Figure 36-2

Figure 37 shows a scatter plot of the in situ O_3 and CO concentrations measured at Angel Peak over the 12-hour period beginning at 1900 PDT on May 24 when the descending high O_3 filaments were detected by TOPAZ. The uncorrelated or negatively correlated measurements show the mixing of lower tropospheric air with drier, O_3-enriched air from the UT/LS. Note that the air is much drier with higher O_3 than was measured on May 21. The additional increase in O_3 associated with these descending filaments appears to be on the order of 15 ppbv.

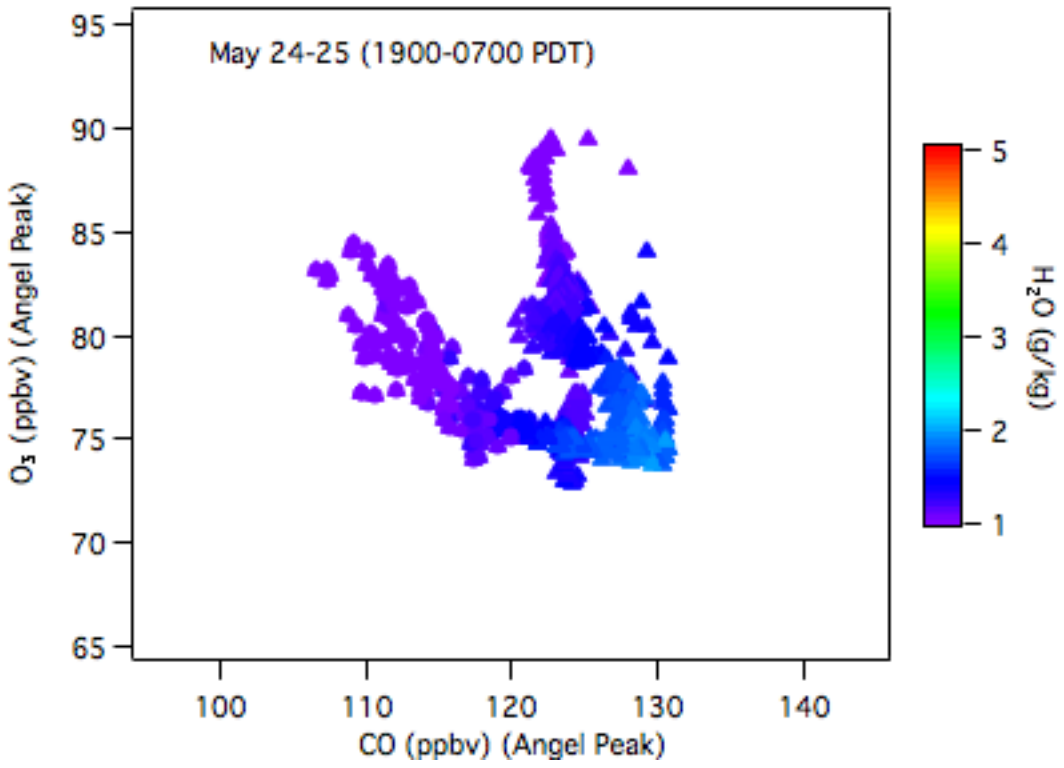

***Figure** 37. Scatter plot comparing the in situ Angel Peak O_3 and CO measurements during the 12 hour period beginning at 1900 PDT on May 24. The points are colorized by specific humidity. The axes span 30 ppbv for O_3 and 50 ppbv for CO as in **Figure** 28.*

7.3 June 21

The last of three high ozone events during the LVOS campaign was on June 21 when 3 of the Clark County CAMS exceeded the 2008 NAAQS with MDA8 concentrations of 78 ppbv at Apex, 77 ppbv at Joe Neal, and 76 ppbv at JD Smith. The NAAQS was equaled at 3 more sites (Jean, Paul Meyer, and Winterwood). The in situ measurements plotted in **Figure** 38 show relatively homogeneous O_3 concentrations in Clark County and high concentrations in the Mojave National Preserve and to a lesser extent Zion National Park. The AM3 analyses show a smaller stratospheric contribution to surface O_3 (20-25 ppbv) than in the two previous events.

The event followed the arrival of a slow moving cutoff low off the coast of Washington and Oregon on June 17, which trailed a plume of Asian pollution similar to that seen in the May 21 RAQMS analysis (cf. **Figure** 24). This plume passed over Nevada during the next 24 hours leading to high surface O_3 at Angel Peak and MDA8 concentrations of up to 74 ppbv at Joe Neal, but no exceedances of the NAAQS in the valley. The trough can be seen in the 310 K O_3 distribution at 1800 UT on June 20 (**Figure** 39) and is still weakly visible in the O_3 distribution at 0000 UT on June 22 (**Figure** 40). The high CO over Colorado in the lower panels is related to a wildland fire in that state.

§§§

***Figure** 38. (a) Time series of 5-min ozone concentrations at Jean, Joe Neal, Palo Verde, and Paul Meyer between May 23 and May 26. The yellow band brackets the highest 8-h average concentrations on May 25. The dashed curve shows the solar radiation measurements from the Spring Mountain Youth Camp and the solid black staircase the AM3 stratospheric O_3. (b) Same as (a), but with the 1-min. measurements from the Death Valley, Great Basin, and Zion National Parks, and 1-h measurements from the Mojave National Preserve.*

§§§

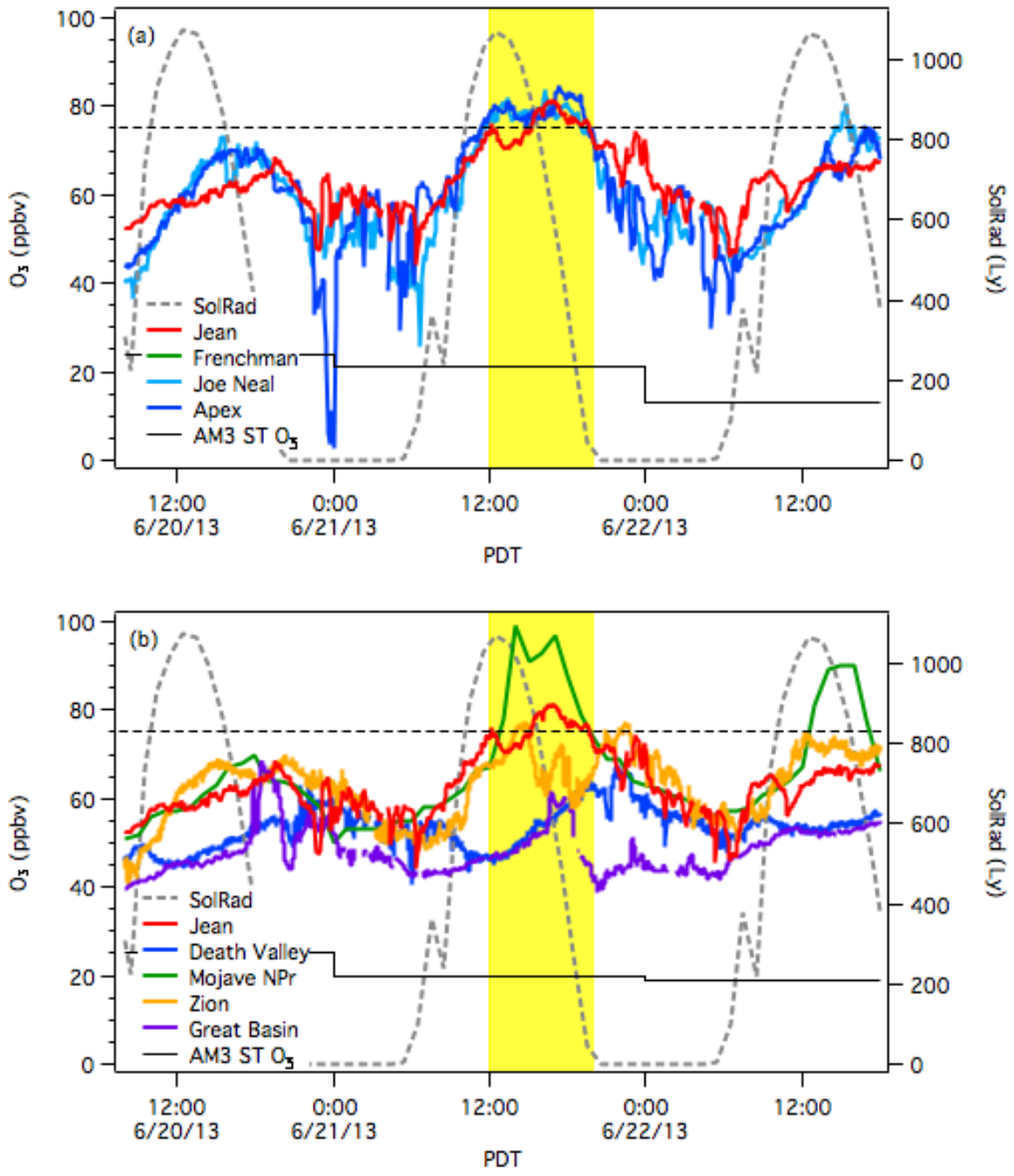
(a)
SolRad
Jean
Frenchman
Joe Neal
Apex
AM3 ST O3
O3 (ppbv)
SolRad (Ly)
12:00 6/20/13
0:00 6/21/13
12:00
0:00 6/22/13
12:00
PDT
(b)
SolRad
Jean
Death Valley
Mojave NPr
Zion
Great Basin
AM3 ST O3
O3 (ppbv)
SolRad (Ly)
12:00 6/20/13
0:00 6/21/13
12:00
0:00 6/22/13
12:00
PDT

Figure 38

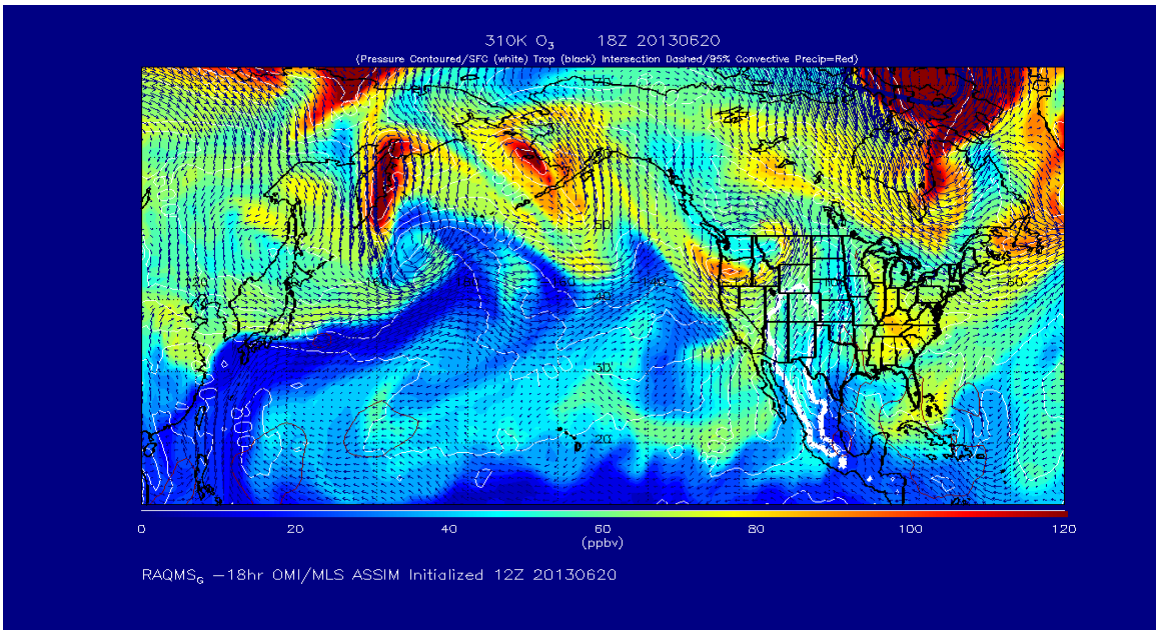

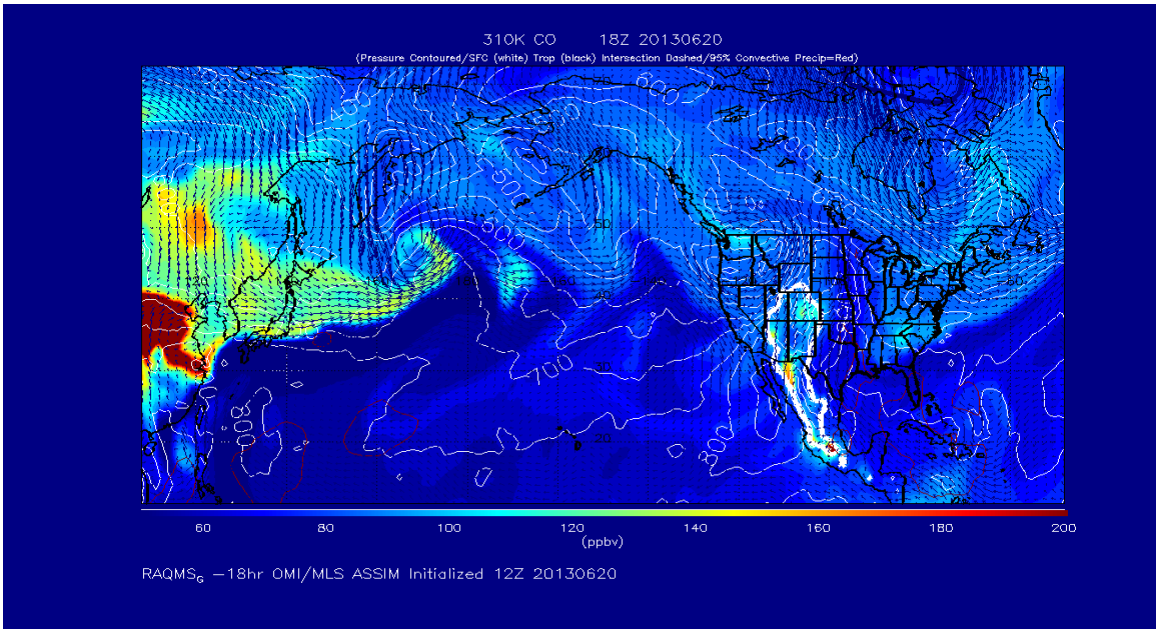

***Figure** 39. RAQMS distributions of O_3 (upper panel) and CO (lower panel) on the 310K potential temperature surface at 1800 UT (1100 PDT) on June 20, 2013.*

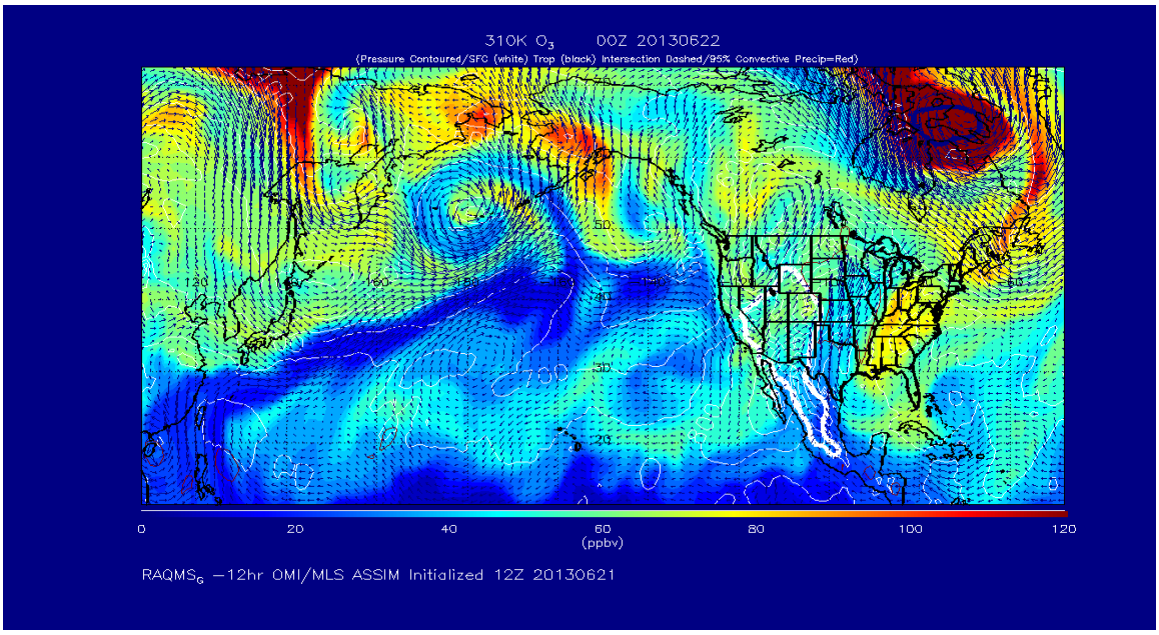

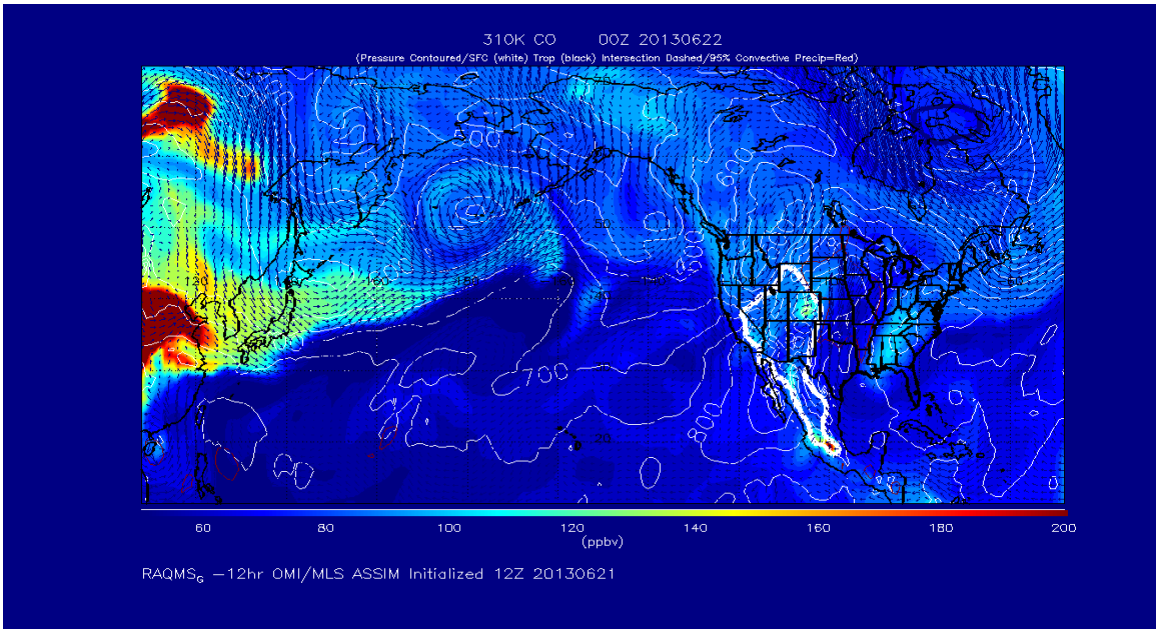

***Figure** 40. RAQMS distributions of O_3 (upper panel) and CO (lower panel) on the 310K potential temperature surface at 0000 UT on June 22, 2013 (1700 PDT on June 21).*

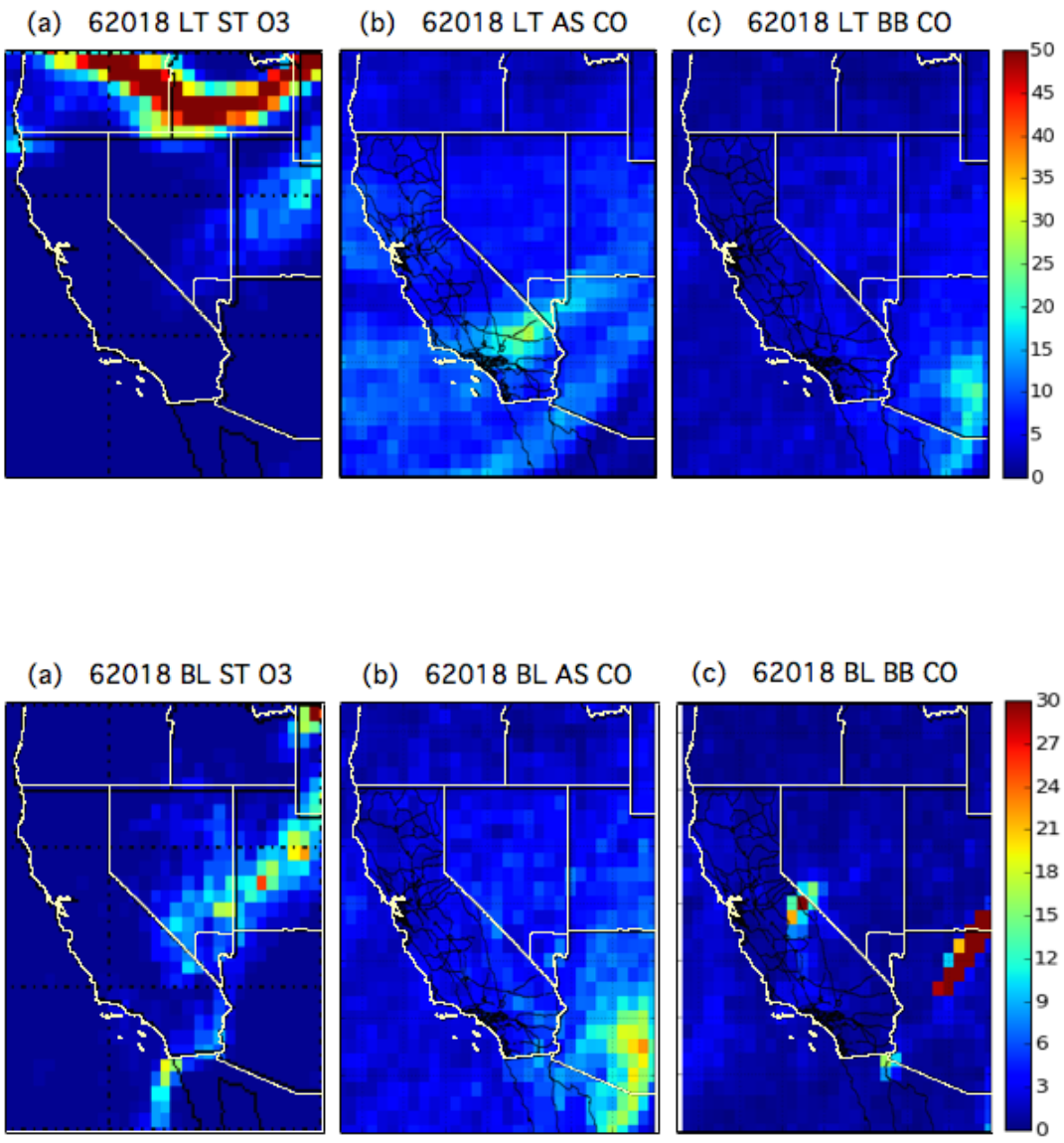

***Figure** 41. Same as Figure 25, but for 1800 UT (1100 PDT) on June 20.*

***Figures** 19 and 21 show a more quantitative estimate of the STT contribution to MDA8 O_3 in Clark County from the AM3 and FLEXPART models.*

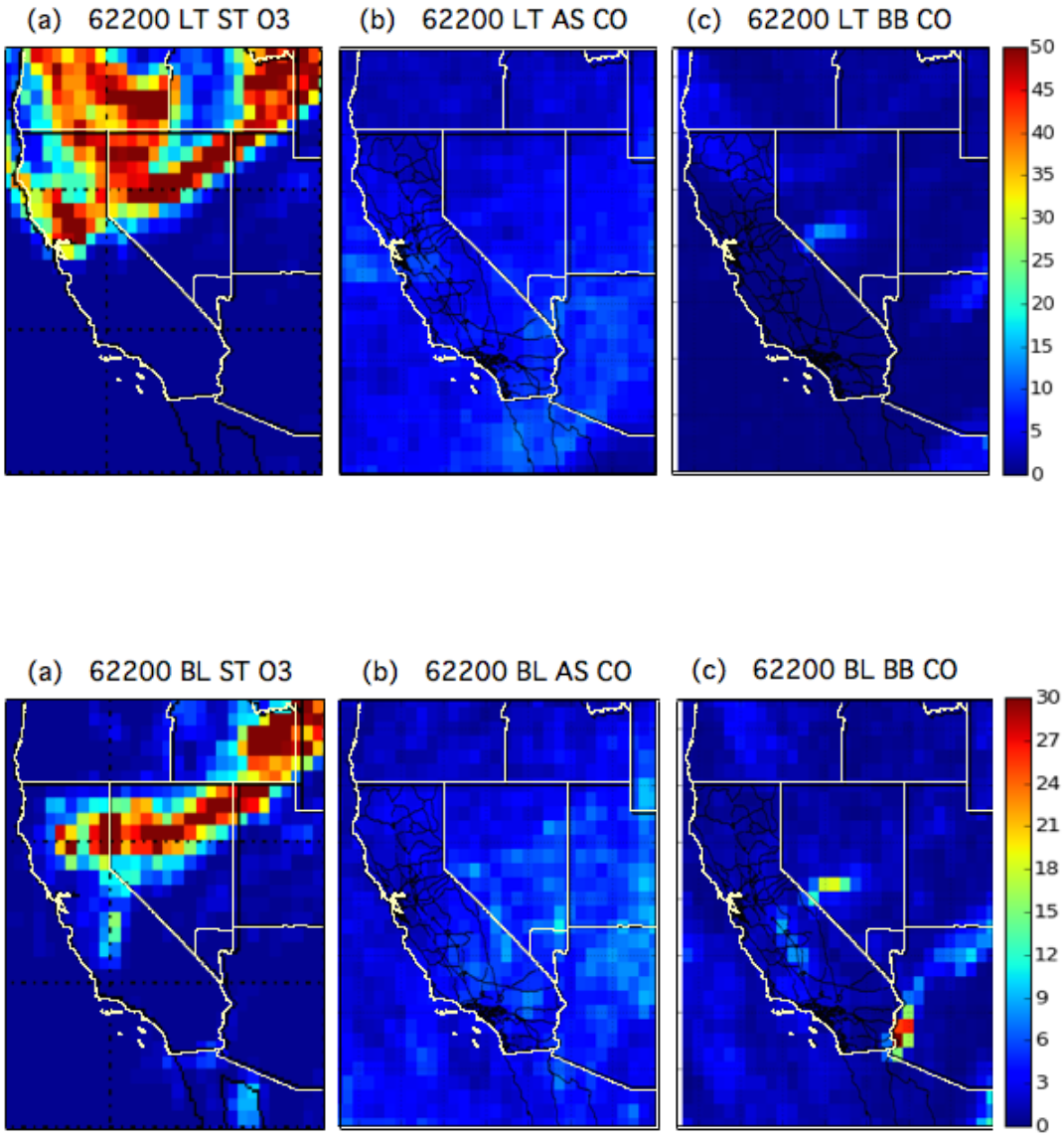

***Figure** 42. Same as Figure 25, but for 0000 UT on June 22 (1700 PDT on June 21. **Figures** 19 and 21 show a more quantitative estimate of the STT contribution to MDA8 O_3 in Clark County from the AM3 and FLEXPART models.*

The FLEXPART tracer distributions for 1800 UT on June 20 (**Figure** 41) show a filament of stratospheric O_3 above Clark County in the boundary layer with a

more diffuse layer of Asian pollution in the lower free troposphere. The biomass burning tracer shows the plume from a fire in western Arizona blowing northeastward in the boundary layer and to the south in the free troposphere. The tracers for 0000 UT on June 22 (1700 PDT on June 21 (**Figure** 42) show significant amounts of stratospheric O_3 in both the lower free troposphere and boundary layer over northern Nevada, but nothing in the vicinity of Clark County. As before, the RAQMS and FLEXPART plots are included here to qualitatively illustrate the horizontal distribution and to a lesser degree, the vertical extents, of these transport events. **Figures** 19 and 21 provide a more quantitative estimate of the impact of these STT events on MDA8 O_3 in Clark County from the AM3 and FLEXPART models.

The measurements from Angel Peak are displayed in **Figure** 43. The TOPAZ system was out of commission due to an equipment failure from June 11-22 and thus was not operational during the last high O_3 event. The system was returned to service on June 23. The winds were light on the afternoon of June 21 with relatively high CO concentrations at Angel Peak.

§§§

Figure*43. Angel Peak measurements from June 20-22. (a) TOPAZ O_3 time-height curtain plots with aerosol backscatter (ß = black) and SMYC solar flux (black dashed) superimposed. The red X's shows the mixed layer depth from the afternoon (0000 UT) VEF soundings. (b) Surface O_3 from Jean (green) and Angel Peak (blue), and 0 to 2000 m agl integrated TOPAZ O_3 concentrations (red), from Angel Peak along with the in situ CO (dashed black). (c) Wind speed (blue) and direction (dashed red). (d) Temperature (red) and specific humidity (red).*

§§§

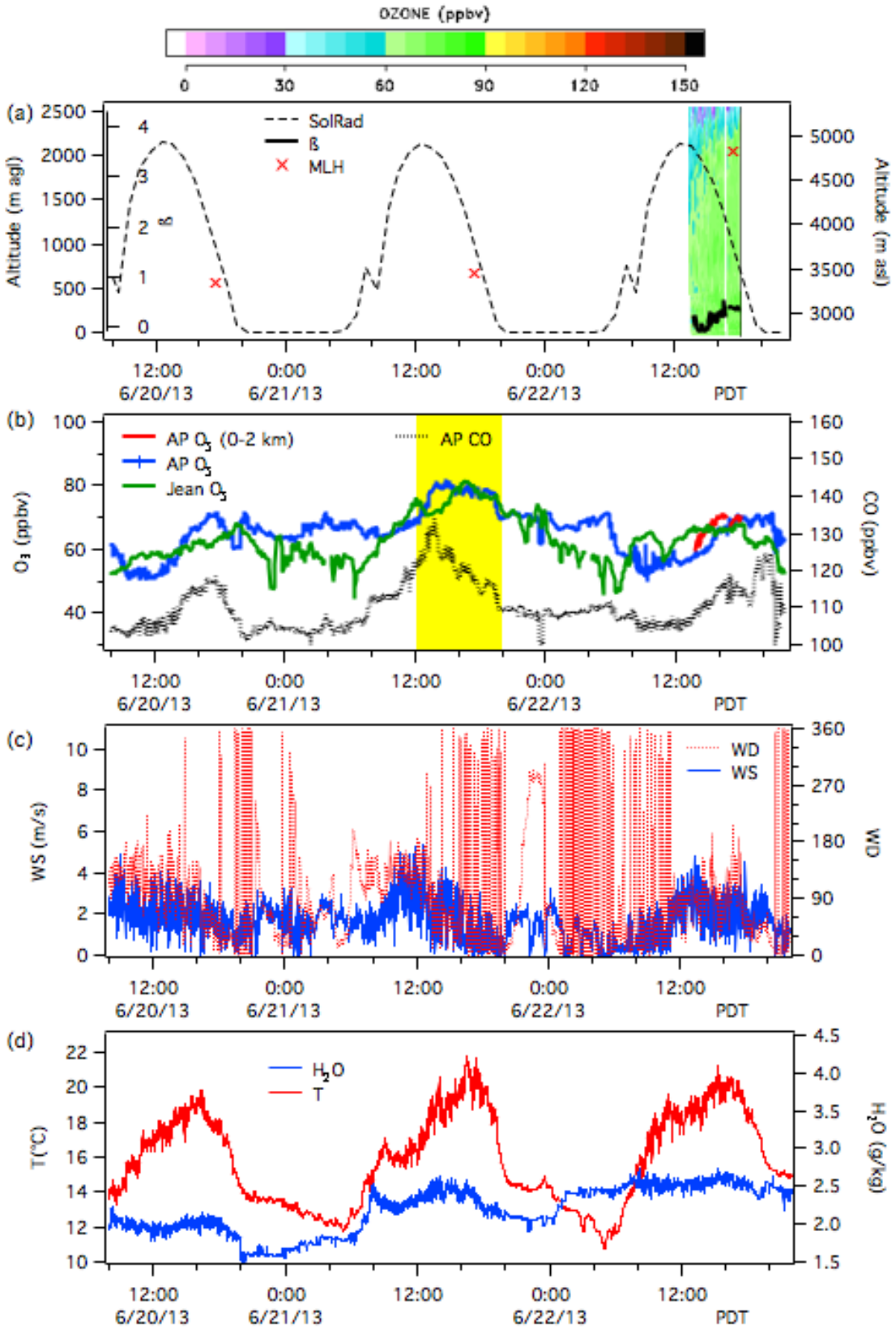
OZONE (ppbv)
0
30
60
90
120
150
(a)
Altitude (m agl)
Altitude (m asl)
SolRad
ß
MLH
12:00
6/20/13
0:00
6/21/13
12:00
0:00
6/22/13
12:00
PDT
(b)
O3 (ppbv)
CO (ppbv)
AP O3 (0-2 km)
AP O3
Jean O3
AP CO
(c)
WS (m/s)
WD
WD
WS
(d)
T(°C)
H2O (g/kg)
H2O
T

Figure 43

The CO-O_3 scatter plot from Angel Peak in **Figure** 44 clearly shows the influence of descending stratospheric air during the night of June 20, but the CO and O_3 in the air sampled during the afternoon of June 21 when the MDA8 was highest have a weak positive correlation. The very similar O_3 concentrations seen at Angel Peak, Jean, and Apex (cf. **Figure** 38) and the coincident peak at the Mojave National Preserve suggest that the sampled airmass covered a large area and the relatively low specific humidity suggests a residual influence from the Asian pollution layer seen in **Figure** 41 and not transport from the LA Basin or the Ls Vegas Valley (cf. **Figure** A3).

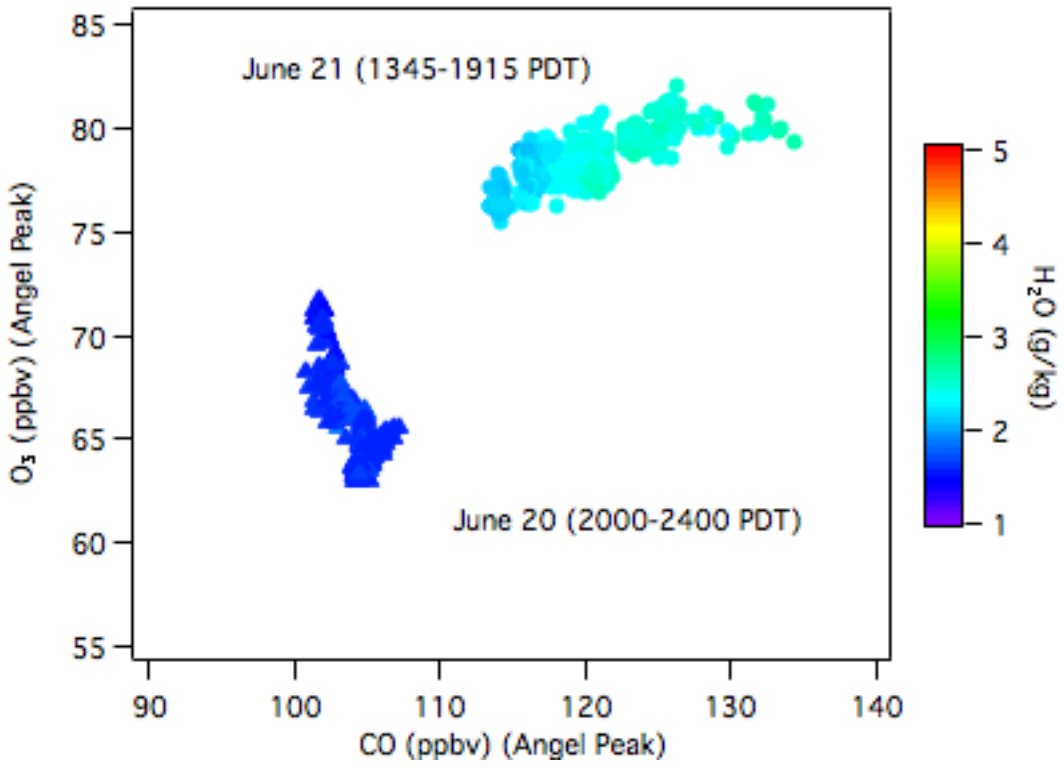

***Figure** 44. Scatter plot comparing the in situ Angel Peak O_3 and CO measurements during the night of June 20 (filled triangles) and the afternoon of June 21 (filled circles). The points are colorized by specific humidity. The axes span 30 ppbv for O_3 and 50 ppbv for CO as in **Figure** 28.*

8. Summary and Conclusions

The LVOS measurement and model results provide compelling evidence that STT, and to a lesser extent, transported Asian pollution significantly increased surface O_3 concentrations in Clark County, NV during the late spring and early summer of 2013. Contributions from wildland fires and pollution plumes from the Los Angeles Basin were of secondary importance during the LVOS campaign. Both measurements and model analyses suggest that these transport processes directly contributed to the exceedances of the 2008 ozone NAAQS of 75 ppbv reported at one or more of the Clark County monitors on May 21, May 25, and June 21. The AM3 model results suggest that the stratospheric contribution to the surface MDA8 O_3 was at least 30 ppbv during each of these events, which were characterized by entrainment of ozone-rich air that had descended from the UT/LS to the lower free troposphere over a large area during the preceding 1-2 days. There were more exceedance days at Angel Peak than in the Las Vegas Valley, consistent with downward transport of O_3 from aloft. These findings are consistent with earlier work, including the 50 km AM3 model results, which showed Clark County to be a major receptor of transported ozone from STT and Asian pollution sources in the spring of 2010.

The Angel Peak measurements and FLEXPART tracer distributions also show that emissions from the Powerhouse Fire in southern California contributed to elevated MDA8 O_3 (73 ppbv) in Clark County on June 2. The FLEXPART tracer distributions also suggest that regional wildland fires contributed to exceedances of the NAAQS before or after the LVOS campaign on May 4, July 3, and July 20, 2013, and that STT also contributed to the May 4 event. These findings imply that all 6 of the O_3 exceedance days in Clark County during 2013 were largely due to outside influences.

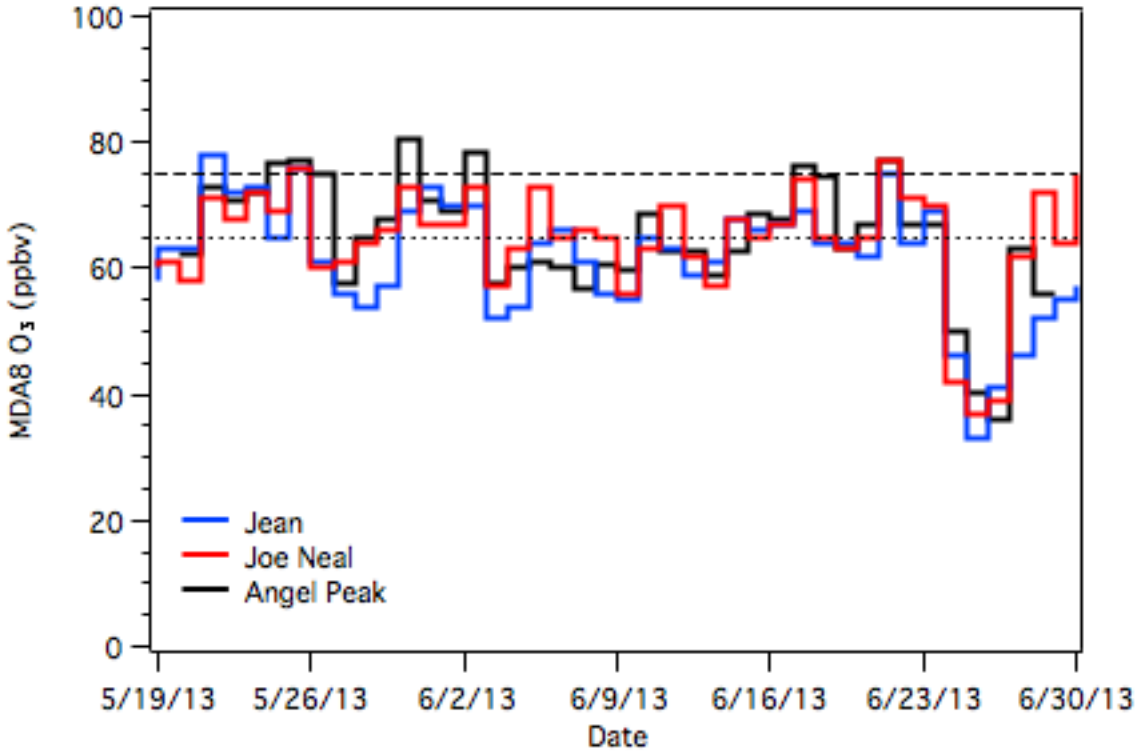

***Figure** 45. MDA8 O_3 at Jean, Joe Neal, and Angel Peak during LVOS. The horizontal dashed and dotted lines mark the 2008 NAAQS of 75 ppbv and the potential 2014 NAAQS of 65 ppbv.*

The mean surface MDA8 ozone at Jean, NV in rural Clark County was 67 ppbv during May and June of 2013, which is only 8 ppbv less than the current 2008 NAAQS and greater than some values that are currently being considered (www.epa.gov/oaqps001/greenbk/hindex.html). The number of exceedance days in Clark County during the 43-day LVOS field campaign would have increased from 3 to 14 if the NAAQS had been 70 ppbv instead of 75 ppbv, and from 3 to 25 if the NAAQS had been 65 ppbv. In other words, exceedances of a (65 ppbv) NAAQS would have occurred on 60% of the days during LVOS, making these events the rule rather than the exception.

APPENDIX A: Transport of ozone from the Los Angeles Basin

The Los Angeles Basin is home to more than 20 million people and the emissions of NOx and VOCs from the transportation and industrial activities associated with this population, coupled with the interactions between the land-sea breeze and the surrounding mountains ranges, produce some of the highest O_3 concentrations measured in the United States. This O_3, as well as other pollutants, can be transported out of the Basin via passes through the San Bernardino, San Gabriel, or San Gorgonio Mountains, or can be lofted over the mountains and into the lower free troposphere by the so-called "Mountain Chimney" effect. The latter process, which becomes more important in July and August, can lead to long-range transport of ozone to surface sites more than 1000 km away [Langford et la. 2010]. These transport processes were a major focus of the Pre-CalNex and CalNex field campaigns in 2009 and 2010.

Low-level transport through the Cajon or San Gorgonio Passes and across the Mojave Desert are the primary pathways by which pollution can be exported from the Los Angeles Basin into the Las Vegas Valley in the late spring and early summer. This transport should create a concentrations gradient across the Mojave Desert with higher O_3 concentrations at measurement sites located near the Basin than at Jean some 300 km to the northeast, and should influence the O_3 and CO concentrations at Angel Peak only after being transported through the Valley first. **Figure** A1 compares the MDA8 O_3 measured at Jean and Angel Peak during LVOS with the corresponding time series from Barstow, which is located about two-thirds of the way along the I-15 corridor from the Cajon Pass. The concentrations are generally similar with all three sites influenced by the larger-scale processes that control background O_3 and the stratospheric intrusions of May 21 and May 25. The isolated NAAQS exceedances at Angel Peak on May 30, June 2, and June 17-18 stand out, but the most persistent divergence between the O_3 concentrations in Barstow and in Clark County occurs during the first high-pressure episode between June 3 and 9 when the

MDA8 O_3 at Barstow was 7 to 16 ppbv higher. These conditions also favored local photochemical production and **Figure** A2 shows the day-by-day evolution of the afternoon (1600 PDT) ozone concentrations in Clark County and southern California from June 3 to June 6, 2013. The superimposed 24-hour HYSPLIT back trajectories are consistent with transport of ozone from southern California to Clark County on the first 2-3 days, followed by stagnation and local production on the fourth days. The highest MDA8 O3 in Clark County during this period was 73 ppbv measured at Joe Neal on June 5, which is less than the 2008 NAAQS, but higher than the lower values currently being proposed.

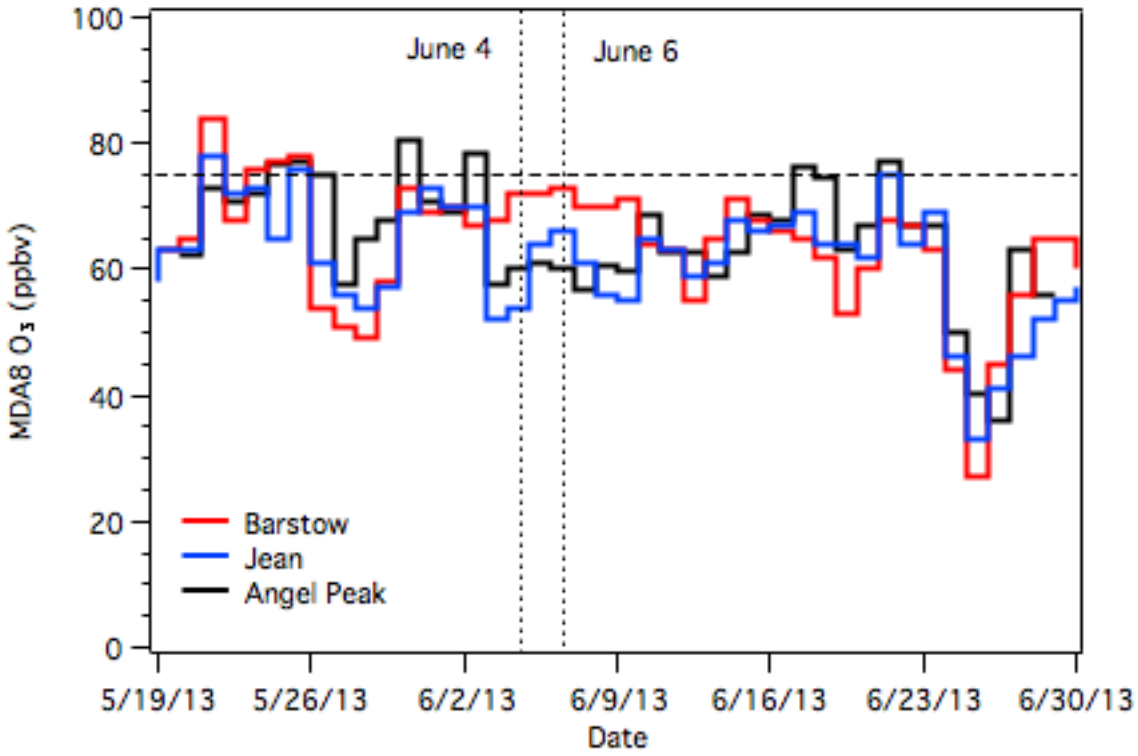

***Figure** A1. MDA8 O_3 measured at Barstow, CA (red) and at Jean, NV (blue) during LVOS. The horizontal dashed line marks the 2008 NAAQS of 75 ppbv. The vertical dotted lines mark June 4 and June 6.*

Figure A3 shows a scatter plot of the O_3 and CO concentrations measured at Angel Peak between 1300 and 1900 PDT on June 4 and 6, bracketing the times shown in Figures A2 (b) and (d). The axes have the same spans as in **Figure** 28. The data from the afternoon of June 4 are (weakly) positively correlated, showing mixing between different airmasses that might reflect the influence of the LA Basin (cf. **Figure** A2(b)). In contrast, the close grouping of the data on June 6 reflects the sampling of a homogeneous air mass consistent with the stagnation within the Las Vegas Valley shown by **Figure** A2(d). In both cases, the high specific humidity compared to **Figures** 28, 37, and 44 shows a strong boundary layer influence.

§§§

***Figure** A2. Hourly ozone distributions from the AirNOW network at 1600 PDT on (a) June 3, (b) June 4, (c) June 5, and (d) June 6. The green, red, and blue lines show the 24 hour HYSPLIT back trajectories at 500, 1000, and 1500 m asl originating from Jean.*

§§§

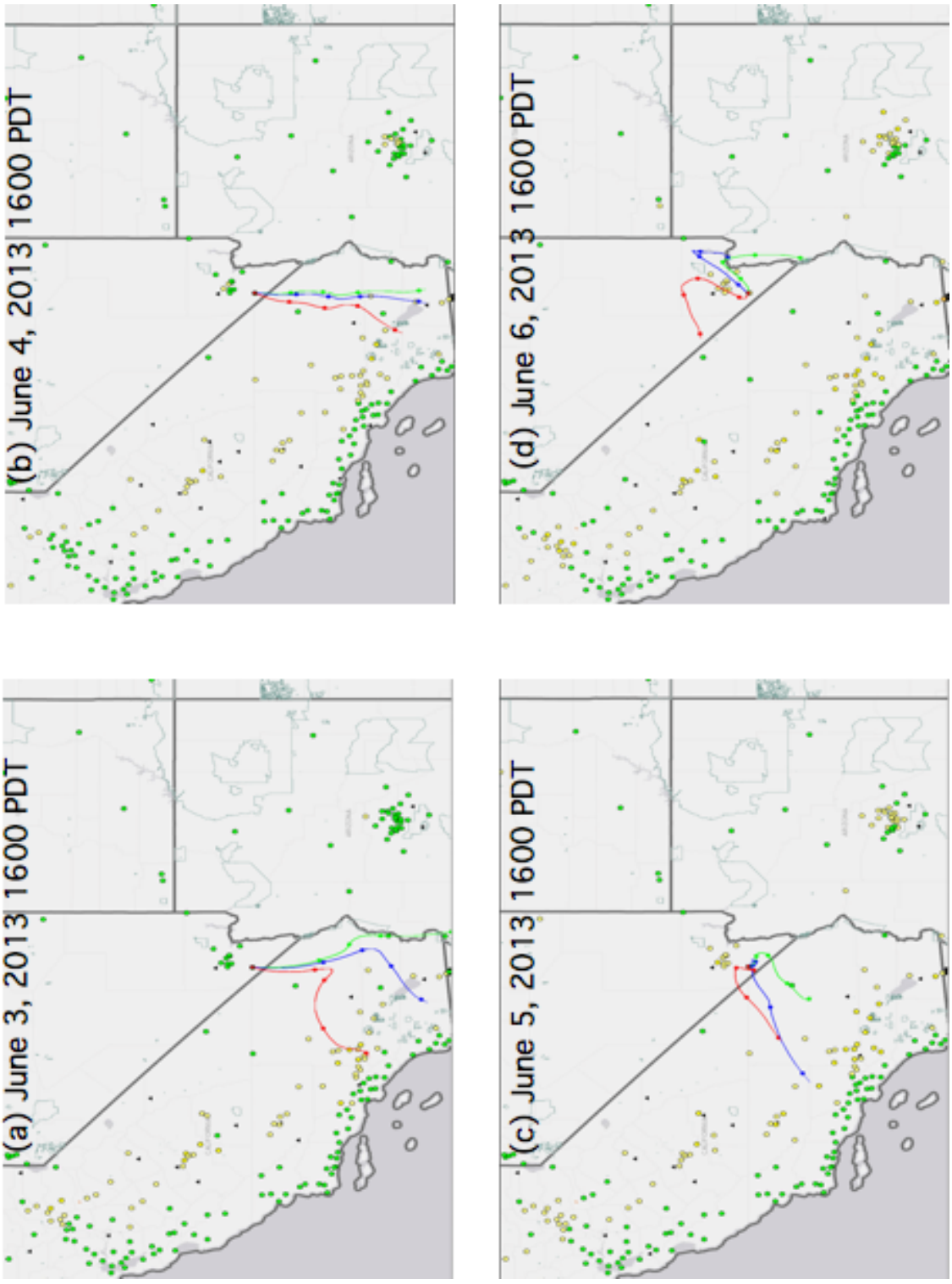
(a) June 3, 2013 1600 PDT
(b) June 4, 2013 1600 PDT
(c) June 5, 2013 1600 PDT
(d) June 6, 2013 1600 PDT

Figure A2

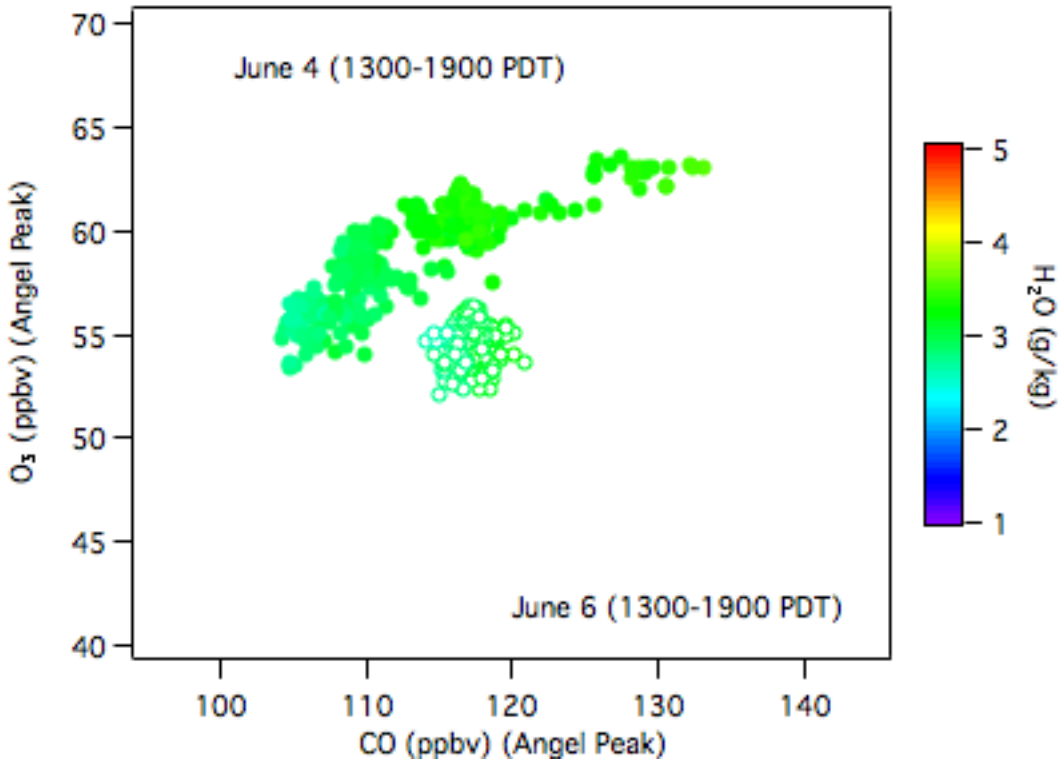

***Figure** A3. Scatter plot comparing the in situ Angel Peak O_3 and CO measurements during the afternoon of June 4 (filled circles) and the afternoon of June 6 (open circles). The points are colorized by specific humidity. The axes span 30 ppbv for O_3 and 50 ppbv for CO as in **Figure** 28.*

APPENDIX B: Wildland fires and ozone in Clark County during 2013

The literature describing the influence of wildland fires on tropospheric ozone has a long and confusing history with many seemingly contradictory results [Jaffe and Wigder, 2012]. Wildland fires can emit copious amounts of NOx, which is usually the limiting reagent in the photochemical formation of O_3, but the amount and rate of O_3 production depends on a wide range of factors including fuel mix, burn rate, injection height, smoke density, relative humidity, and temperature. Reactions with NO can destroy O_3 in fresh fire plumes and the production in older plumes may become limited as the NOx is converted to peroxyacetylnitrate (PAN) and nitric acid (HNO_3). Some O_3 may then be formed many days later and thousands of kilometers downwind when the PAN thermally decomposes back to NOx. Ozone production can also increase when NOx-depleted plumes pass over urban/suburban areas (e.g. the Los Angeles Basin) and receive a fresh infusion of NOx.

Indirect evidence linking wildland fire with high ozone in Clark County comes from the fact that the highest 8-h concentrations recorded during 2013 occurred on July 3, less than one week after the end of the LVOS measurement campaign and two days after lightning ignited the Carpenter 1 Fire about 15 km SW of Angel Peak. This fire, which started the day after the all time high temperature of 47°C (117°F) in Las Vegas was tied, forced evacuation of the area surrounding Angel Peak and eventually burned 27,881 acres vegetated primarily by a mix of chaparral and juniper similar to that consumed in the Powerhouse Fire in Los Angeles County. The plume from the Carpenter 1 Fire spread over a large area, mingling with emissions from the 5,400 acre Dean Peak Fire near Kingman, Arizona, and the 4,000 acre Black Mountain Fire near Cedar City, Utah (cf. **Figure** B1), which were also started by lightning strikes. The NOAA Hazard Mapping System (HMS) shows three other smaller fires burning within 300 km of Las Vegas on July 3.

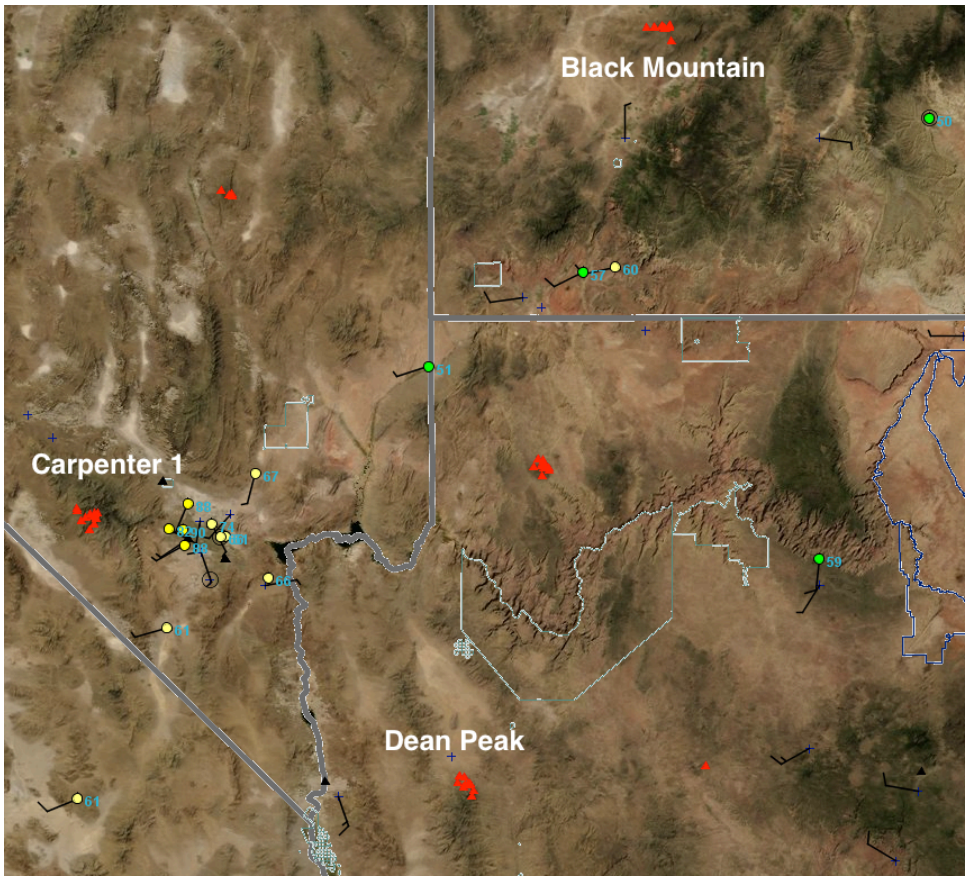

***Figure** B1. Hourly ozone distribution from the AirNow network for 1800 PDT on July 3, 2013 showing high concentrations in Clark County. The red triangles from the NOAA Hazard Mapping System (HMS) show six fires burning within 300 km of Las Vegas.*

B1: Wildland Fires during LVOS

The 2013 fire season began unusually early in the southwestern U.S. with nearly 40 documented wildland fires, ranging in size from less than 15 to more than 30,000 acres burning in southern California (30 fires) and Arizona (9 fires) during the LVOS field campaign (May 19 to June 29). **Table** B1 lists the major (i.e. >1000 acre) Southern California fires that burned during May, June, and July. The three largest fires (Springs, Powerhouse, and Mountain) shown in bold burned more than 20,000 acres each. The prevailing southwesterly flow during April, May, and early June makes it likely that the larger fires could have

adversely impacted the air quality in Clark County. The Powerhouse Fire in Ventura County described in **Section** 6 was the only one of these three fires active during LVOS, and the in situ CO measurements and FLEXPART tracer time series plotted in **Figure** 15 show that this was the only fire to significantly impact air quality at Angel Peak during LVOS. However, as is discussed below, the FLEXPART forward tracer runs suggest that the Springs and Mountain Fires in early May and mid-July, respectively, also contributed to exceedances of the 2008 NAAQS in Clark County on May 4 and July 21.

The Powerhouse Fire burned 30,274 acres of heavy, old growth brush (Chaparral) and light desert scrub on the north side of the San Gabriel Mountains between May 30 and June 6. Strong southwesterly winds associated with a upper level trough transported the plume from Venture County to Clark County and O_3 increased at most of the Clark County monitors (**Figure** B2), but the highest MDA8 was 73 ppbv. The plume reached Angel Peak on the afternoon and evening of June 2, increasing particulate backscatter at 294 nm by more than a factor of 30 and nearly doubling the CO concentrations from (**Figure** B3).

Table B1: Southern California fires burning 1000+ acres in May-July 2013

Fire	Size (acres)	County	Date started	Containment
Summit	3,166	Riverside	May 1	May 4
Springs	**24,251**	**Ventura**	**May 2**	**May 11**
Grand	4,346	Kern/Ventura	May 15	May 21
San Felipe	2,781	San Diego	May 23	May 26
General	1,271	San Diego	May 26	May 31
White	1,984	Santa Barbara	May 27	May 30
Powerhouse	**30,274**	**Los Angeles**	**May 30**	**June 8**
Hathaway	3,825	Riverside	June 9	June 9
Carstens	1,708	Mariposa	June 16	June 26
Chariot	7,055	San Diego	July 6	July 15
Mountain	**27,531**	**Riverside**	**July 15**	**July 30**

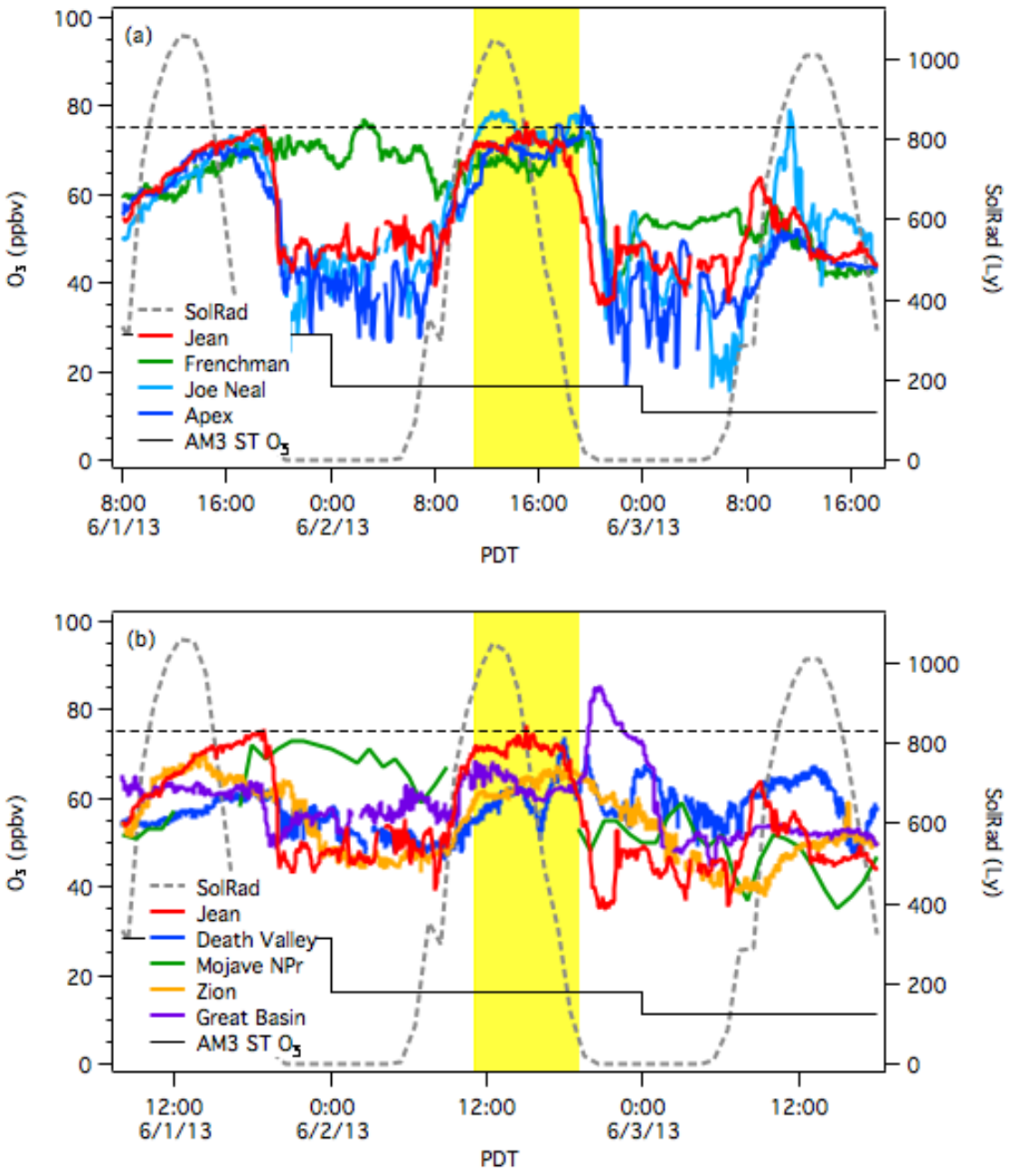

***Figure** B2. (a) 5-min ozone concentrations at Jean, Joe Neal, Palo Verde, and Paul Meyer between June 1 and 3. The yellow band brackets the highest 8-h average concentrations on June 2. The dashed curve shows the solar radiation from the Spring Mountain Youth Camp and the solid black staircase the AM3 stratospheric O_3. (b) Same as (a), but with the 1-min. measurements from the Death Valley, Great Basin, and Zion National Parks, and 1-h measurements from the Mojave National Preserve.*

§§§

Figure *B3. Angel Peak measurements from June 1-3. (a) TOPAZ O_3 time-height curtain plots with aerosol backscatter (ß = black) and SMYC solar flux (black dashed) superimposed. The red X's shows the mixed layer depth from the afternoon (0000 UT) VEF soundings. (b) Surface O_3 from Jean (green) and Angel Peak (blue), and 0 to 2000 m agl integrated TOPAZ O_3 concentrations (red), from Angel Peak along with the in situ CO (dashed black). (c) Wind speed (blue) and direction (dashed red). (d) Temperature (red) and specific humidity (red).*

§§§

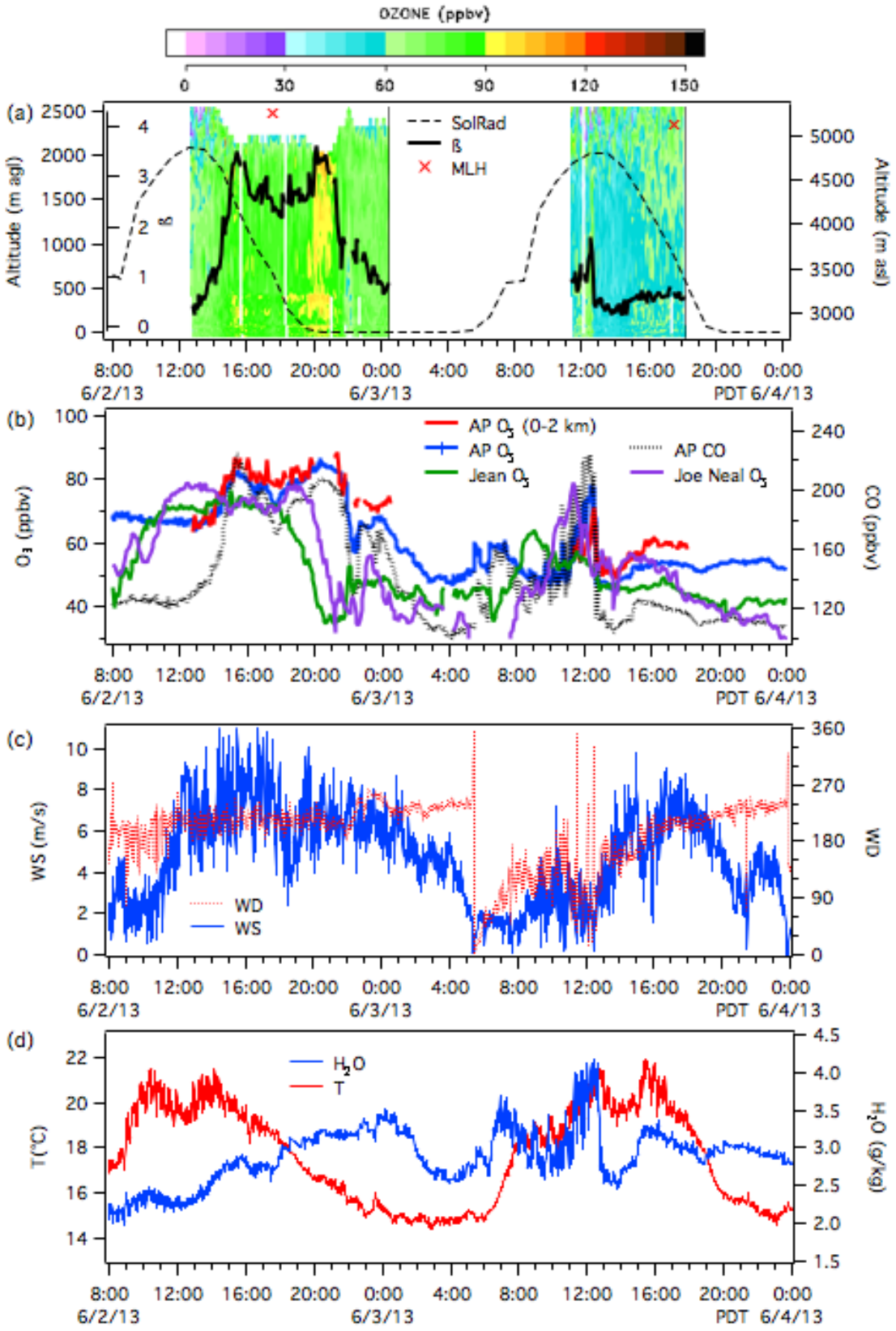
OZONE (ppbv)
0
30
60
90
120
150
(a)
Altitude (m agl)
Altitude (m asl)
SolRad
ß
MLH
(b)
O3 (ppbv)
CO (ppbv)
AP O3 (0-2 km)
AP O3
Jean O3
AP CO
Joe Neal O3
(c)
WS (m/s)
WD
WD
WS
(d)
T(°C)
H2O (g/kg)
H2O
T
8:00
12:00
16:00
20:00
0:00
4:00
6/2/13
6/3/13
PDT 6/4/13

Figure B3

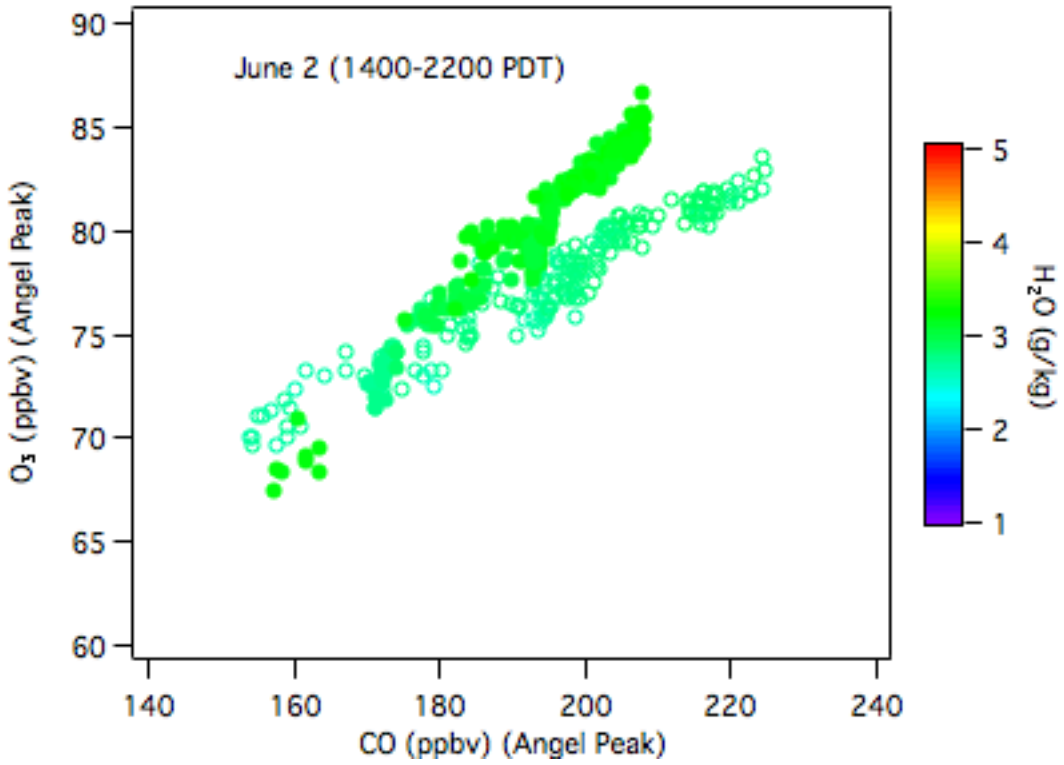

***Figure** B4. Scatter plot comparing the in situ Angel Peak O_3 and CO measurements during the 8 hour period beginning at 1400 PDT on June 2. The points are colorized by specific humidity as before. Note that the span of the CO scale is double (100 ppbv) that shown in previous scatter plots.*

Figure B4 shows that an increase of nearly 20 ppbv in the O_3 of at Angel Peak was positively correlated with CO with at least two slightly different plumes. This episode was also distinguished from the STT events by much higher (~2x) H_2O vapor concentrations consistent with a boundary layer origin. Although the MDA8 O_3 at Angel Peak exceeded 78 ppbv on June 2, the highest 8-h average concentration recorded by one of the regulatory monitors in the Las Vegas Valley was 73 ppbv (both Palo Verde and Joe Neal) so there were no exceedances of the 2008 NAAQS associated with this particular fire. The advection of the Powerhouse fire plume over southern Nevada in June 2-3 is shown in **Figure** B5, which displays the FLEXPART biomass burning CO tracer distributions over the western U.S. between 1200 UT (0500 PDT) on June 2, and 1200 UT on June 3.

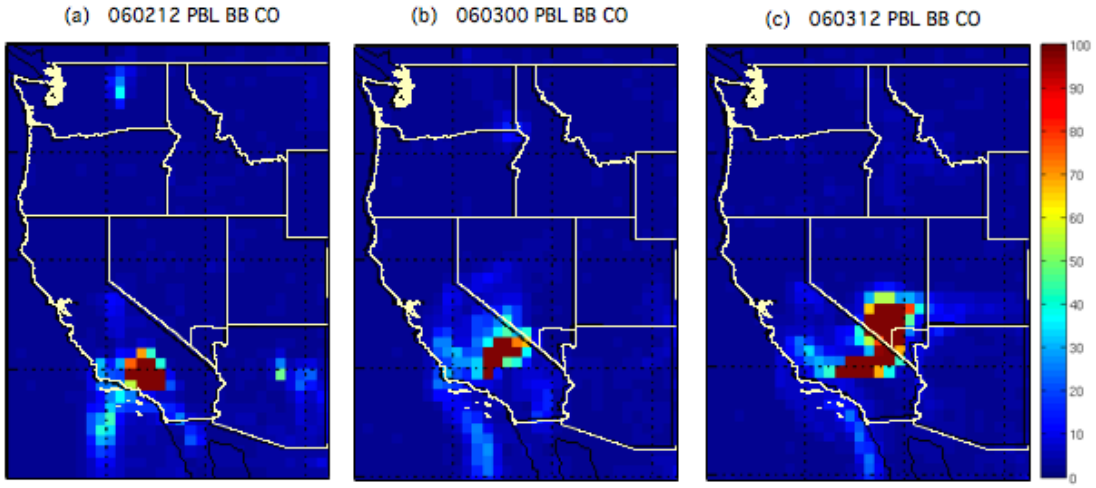

***Figure** B5: FLEXPART biomass burning CO tracer distributions (ppbv) in the boundary layer (<1.5 km) showing the Powerhouse Fire plume at: a) 1200 UT on June 2 (0500 PDT on June 2), (b) 0000 UT on June 3 (1700 PDT on June 2), and (c) 1200 UT on June 3 (0500 PDT on June 3).*

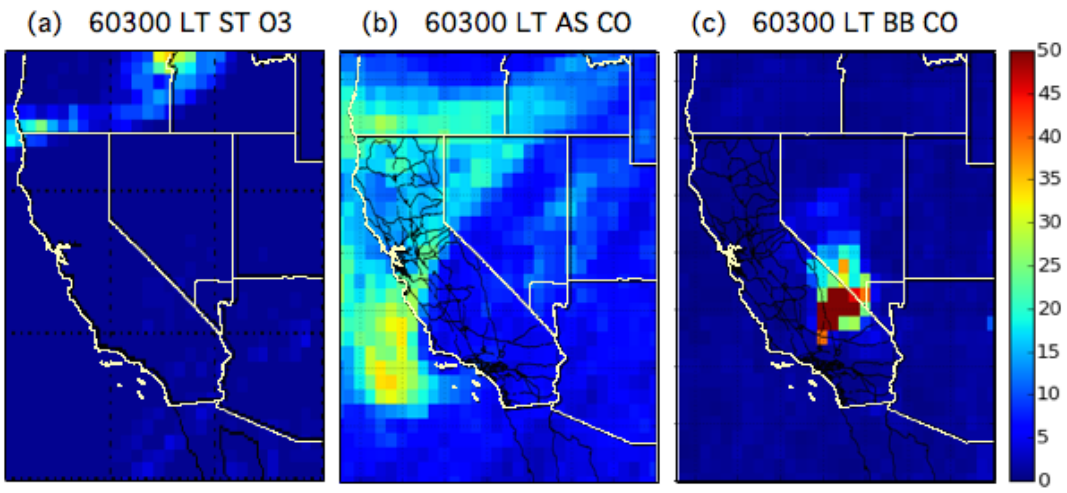

***Figure** B6: FLEXPART ST O_3, AS CO, and BB CO tracer distributions (ppbv) in the lower free troposphere showing that STT and long range transport did not contribute to the high O_3 on June 2. Note that the tracer scale of 50 ppbv is the same as was used earlier in this report.*

The proximity of the Powerhouse Fire to the Los Angeles Basin also means that some NOx-rich urban emissions were likely mixed into the fire plume, increasing the ozone production.

B2. Wildland Fires before and after LVOS

The FLEXPART biomass burning CO tracer distributions also suggest that wildland fires also influenced the high ozone days in Clark County May 4, July 3, and July 20 although there were no measurements of O_3 or CO from Angel Peak to support this hypothesis. Each of these events occurred when large fires were burning in the southwest including the 24,251 acre Springs Fire in Ventura County, CA, the simultaneous 27,881 acre Carpenter 1 Fire in Clark County and 5,400 acre Dean Peak Fire in NW Arizona, and the 27,531 acre Mountain Fire in Riverside County. These fires were most likely responsible for the ozone exceedances that occurred in Clark County on May 4, July 3 and July 20, 2013, respectively. The Carpenter 1 fire, which started the day after the record high

temperature (47°C or 117°F) in Las Vegas was tied, forced evacuation of the area surrounding Angel Peak and burned a chaparral and juniper mix similar to that consumed in the Powerhouse Fire.

The second highest MDA8 ozone concentrations recorded in Clark County during 2013 were measured on May 4 with MDA8 ozone concentrations of 76 ppbv or more at six of the Clark County CAMS. The maximum value of 84 ppbv was recorded at Jean and 82 ppbv was recorded at Palo Verde. These monitors reported MDA8 ozone concentrations of 61 and 58 ppbv, respectively, on the previous day, suggesting ozone enhancements of about 23 and 24 ppbv. Ozone peaked at the Clark County monitors at about 1700 PST on 4 May 2013 and remained high through the following night with exceedances also reported at Joe Neal, Walter Meyer, and Paul Meyer, and Winterwood. This fire closely followed the passage of an upper level low and the FLEXPART and AM3 models suggest that stratospheric air was transported to the surface in Clark County during the first few days of May. This intrusion did not directly cause an exceedance, and was had moved east by the time the smoke plume reached Clark County (**Figure** B7).

Although the O_3 to CO ratio in wildland fire plumes depends on a large number of factors and varies widely in both time and space, a typical ratio of 0.3 would imply an additional O_3 influx of about 10 to 20 ppbv from the fire and could explain the high ozone in Clark County on May 4. The plume moved north and east over the next 12 hours (**Figure** B8) to affect surface O_3 in Great Basin and Zion National Parks the following day.

Finally, **Figures** B9 and B10 show the widespread FLEXPART biomass burning CO distributions on the afternoons of the final two exceedance days (July 3 and 20).

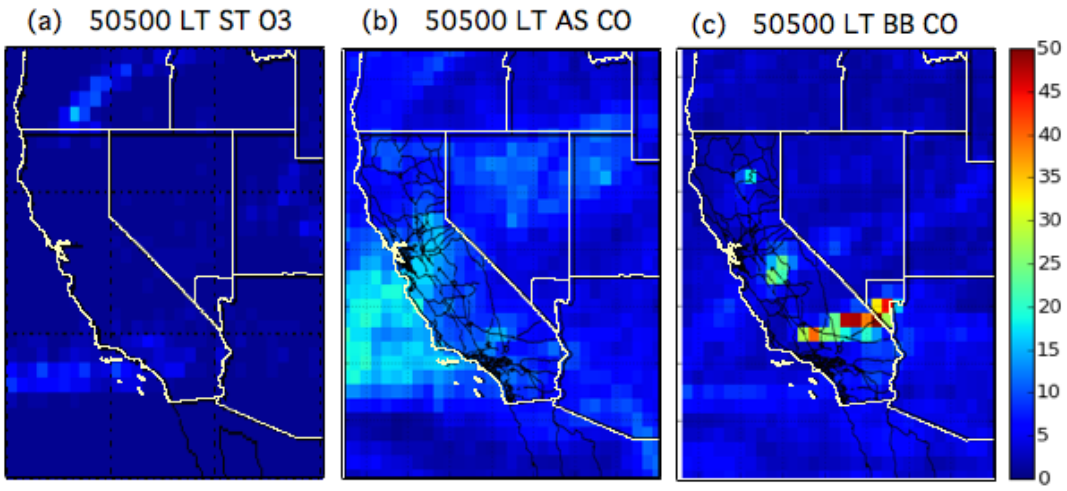

***Figure** B7: FLEXPART ST O_3, AS CO, and BB CO tracer distributions (ppbv) in the lower free troposphere at 0000 UT on May 5.*

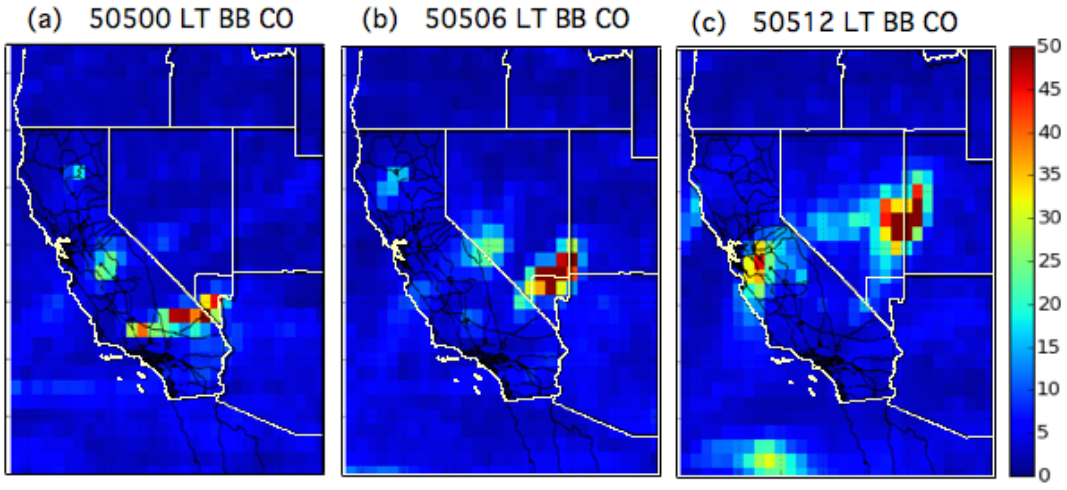

***Figure** B8: FLEXPART biomass burning CO tracer distributions (ppbv) in the boundary layer (<1.5 km) showing the Springs Fire plume at: a) 1200 UT on May 4 (0500 PDT on May 4), (b) 0000 UT on May 5 (1700 PDT on May 4), and (c) 1200 UT on May 5 (0500 PDT on May 5).*

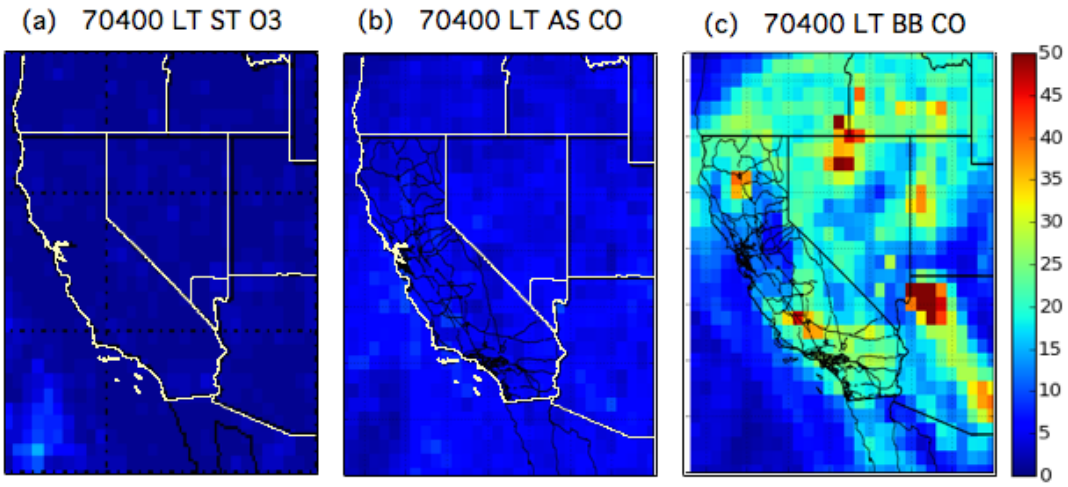

***Figure** B9: FLEXPART biomass burning CO tracer distributions (ppbv) in the lower free troposphere from the multiple fires burning on July 3.*

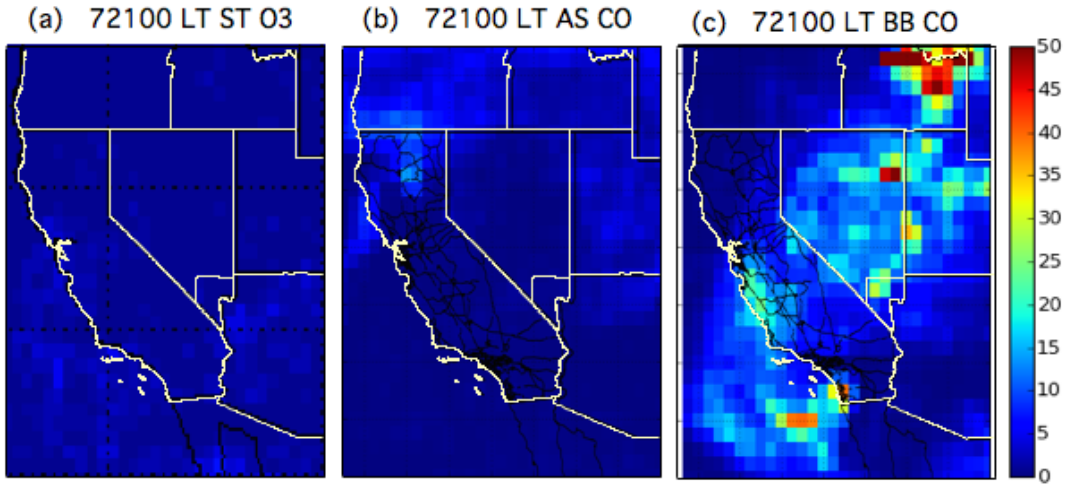

Figure B8

***Figure** B9: FLEXPART biomass burning CO tracer distributions (ppbv) in the lower free troposphere from the multiple fires burning on July 20.*

APPENDIX C: Transport of ozone from the Las Vegas Valley to Angel Peak

The transport patterns above the western U.S. during the last week of June were dominated by a late season stationary low-pressure center over the Gulf of Alaska and a strong (>6000 m at 500 hPa) high-pressure ridge above the desert Southwest (**Figure C1**).

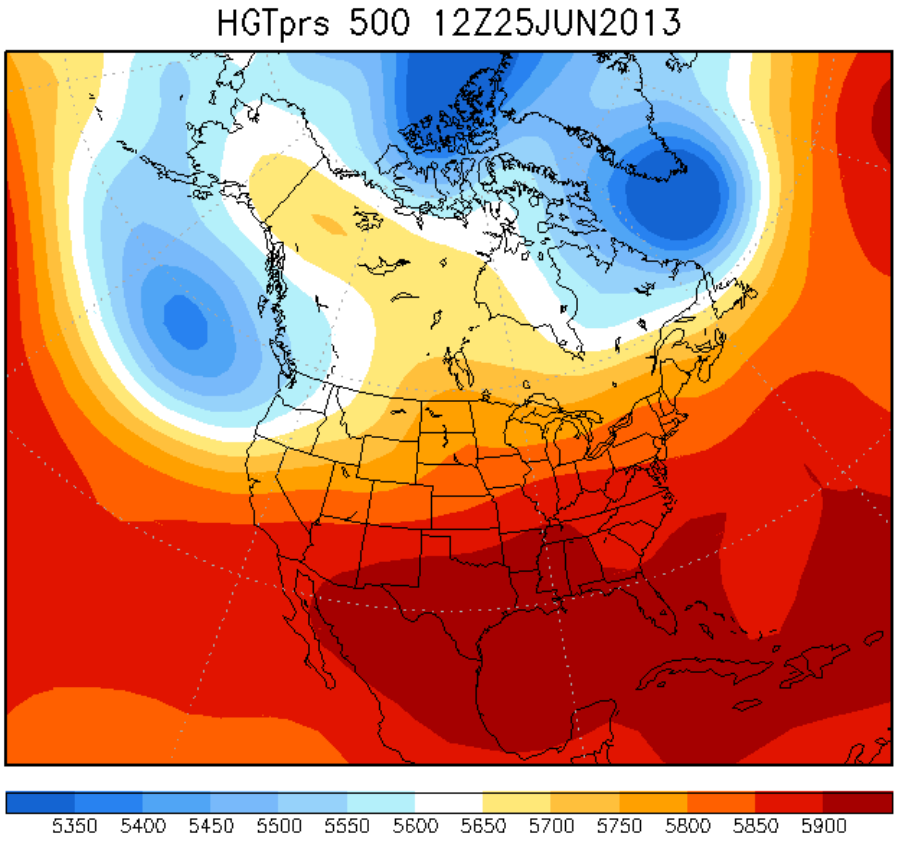

***Figure** C1. NCEP Reanalysis 500 hPa geopotential heights at 1200 UT on June 25, 2013.*

The merged cyclonic and anticyclonic circulations associated with these systems transported subtropical marine air with unusually low O_3 and CO concentrations into the western U.S. between June 22 and 26 (**Figure** C2).

(a) RAQMS O_3

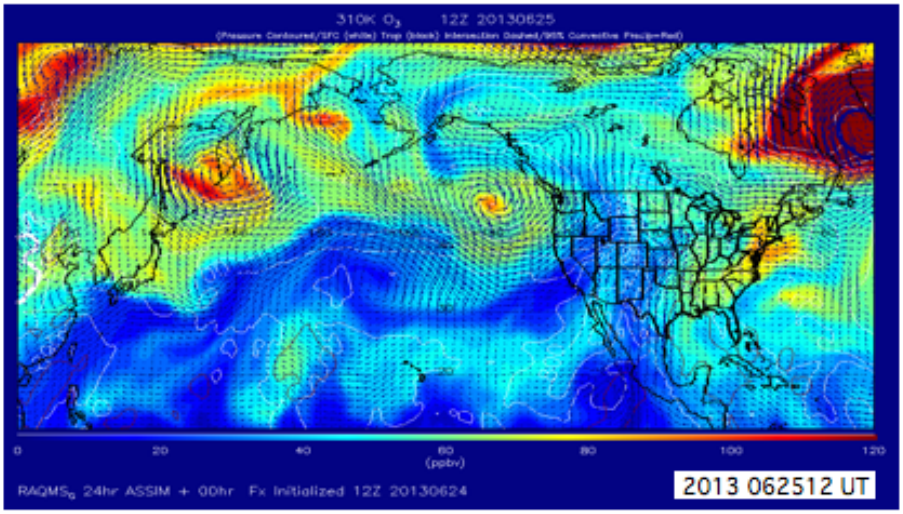

(b) RAQMS CO

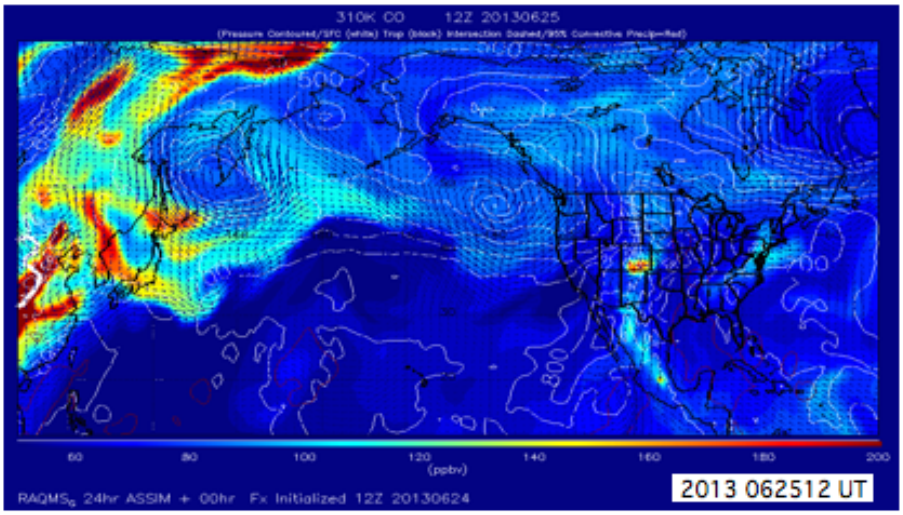

initialized 12UT on June 24, 2013

Figure *C2. RAQMS 310K (a) O_3 and (b) CO distributions at 1200 UT on June 25, 2013 showing the subtropical incursion above the western U.S..*

This moist subtropical air spread across much of the west, decreasing background O_3 and CO concentrations to unusually low values (cf. **Figures** 7 and 8). Between June 22 and 25, the MDA8 O_3 decreased from 48 ppbv to 22 ppbv in Los Angeles (North Main Street), from 42 to 11 ppbv in Sacramento (T-Street), and from 49 to 15 ppbv at Red Bluff in the North Sacramento Valley. The MDA8 O_3 at Jean and Joe Neal decreased to 33 and 37 ppbv, respectively,

on June 25, and the 1-min average O_3 and CO concentrations at Angel Peak were only 22 and 70 ppbv, respectively, on the early morning of June 26.

The unseasonably low regional background O_3 concentrations in Clark County and the surrounding areas provided a unique opportunity to assess local O_3 production and transport within Clark County. Surface temperatures climbed rapidly in the Las Vegas Valley after June 24 as the Gulf of Alaska low weakened and the ridge pushed further north (**Figure** C3). The peak temperatures at Joe Neal increased from about 35°C (95°F) on June 25, to 40°C (105°F) on June 27, and 43°C (110°F) on June 28. Temperatures continued to rise after the LVOS campaign ended with the all time high temperature record (47°C or 117°F) tied at McCarran International Airport on June 30. The relative humidity dropped to single digits under cloudless skies creating ideal conditions for photochemical production of O_3 in the Las Vegas Valley.

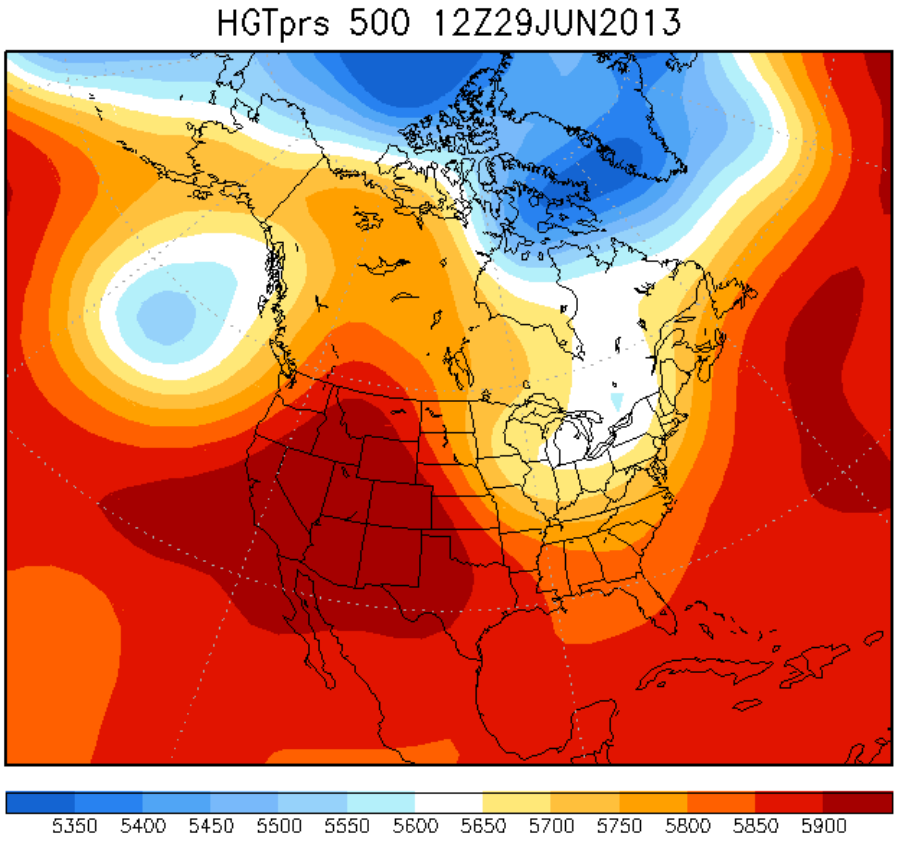

***Figure** C3. NCEP Reanalysis 500 hPa geopotential heights at 1200 UT on June 29, 2013. Note the weaker low and stronger high compared to Figure C1.*

Figure C4 shows that the difference between the MDA8 O_3 at Jean and Joe Neal increased from only 2 ppbv (39 and 41 ppbv, respectively) on June 26, to 16 ppbv on June 27 (46 and 62 ppbv, respectively). The regional concentrations remained low, showing that this rapid change was the result of local photochemical production and transport. The concentrations also remained low at Jerome Mack and Winterwood (not shown) on June 27 as heating of the east facing slopes in the Spring Mountains generated persistent southeasterly upslope flows that transported the O_3 and its photochemical precursors, as well as CO and particulates into the western valley and into the Spring Mountains to Angel Peak. The evening downslope flow redistributed the O_3 across the valley leading to higher concentrations at all of the Clark County monitors on June 28 when Joe Neal recorded an 8-h value of 72 ppbv.

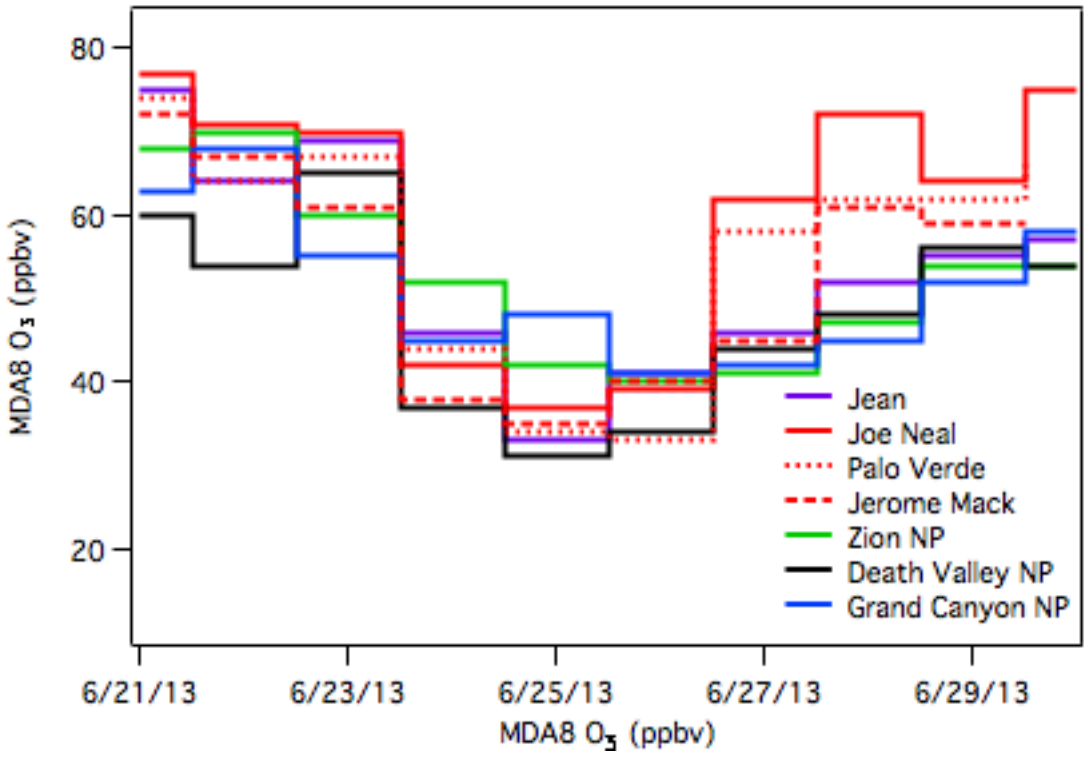

***Figure** C4. MDA8 O_3 measured in Clark County (Jean, Palo Verde, and Joe Neal) and at several nearby National Parks during the last week of June 2013 showing the influence of the subtropical marine air incursion on surface concentrations followed by local photochemical production in the Las Vegas Valley.*

Thee 5-min O_3 concentrations measured on June 27 at several of the valley CAMS located roughly east-to-west across the valley floor and at Angel Peak are plotted in **Figure** C5. This plot shows that the horizontal gradient extended westward well into the Spring Mountains during the late afternoon.

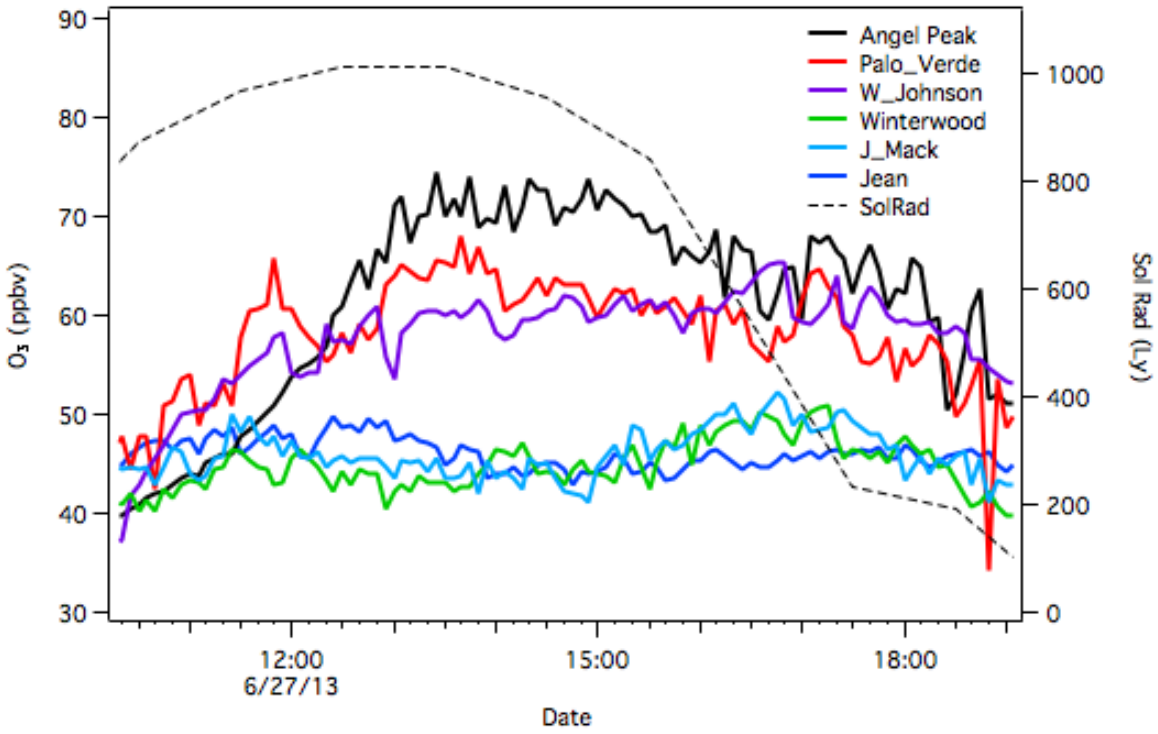

***Figure** C5. Five-minute average O_3 measured in Clark County showing the strong east-to-west concentration gradient from Winterwood and Jerome Mack to Walter Johnson, Palo Verde, and Angel Peak on the afternoon of June 27.*

The upslope transport to Angel Peak is also reflected in the TOPAZ lidar measurements, which show a plume of ozone lofted to more than 2500 m above Angel Peak (i.e. about 5300 m asl) by the upslope flow in the afternoon (**Figure** C6).

Despite the strong surface heating, the 0000 UT (1700 PDT) VEF sounding (not shown) indicated that the subsiding air aloft associated with the strong ridge kept the top of the mixed layer below ~2750 m asl or very nearly at the summit of Angel Peak. Thus the lofting of the ozone plume seen in **Figure** C6a is due to the upslope flow, which remained steady at 2 m/s from the ESE (125°) throughout the measurement period.

The vertical dashed lines at 1300 PDT (1200 PST) in **Figures** C6a and C6b separate the Angel Peak measurements into morning and afternoon regimes. Note the very high specific humidity (red points) from the recent maritime influence. The difference between the morning and afternoon traces in **Figure** C6c suggests production of about 15 ppbv of O_3 in the plume. This estimate is only qualitative, of course, but these data provide an excellent opportunity for comparisons with WRF-Chem or other regional models.

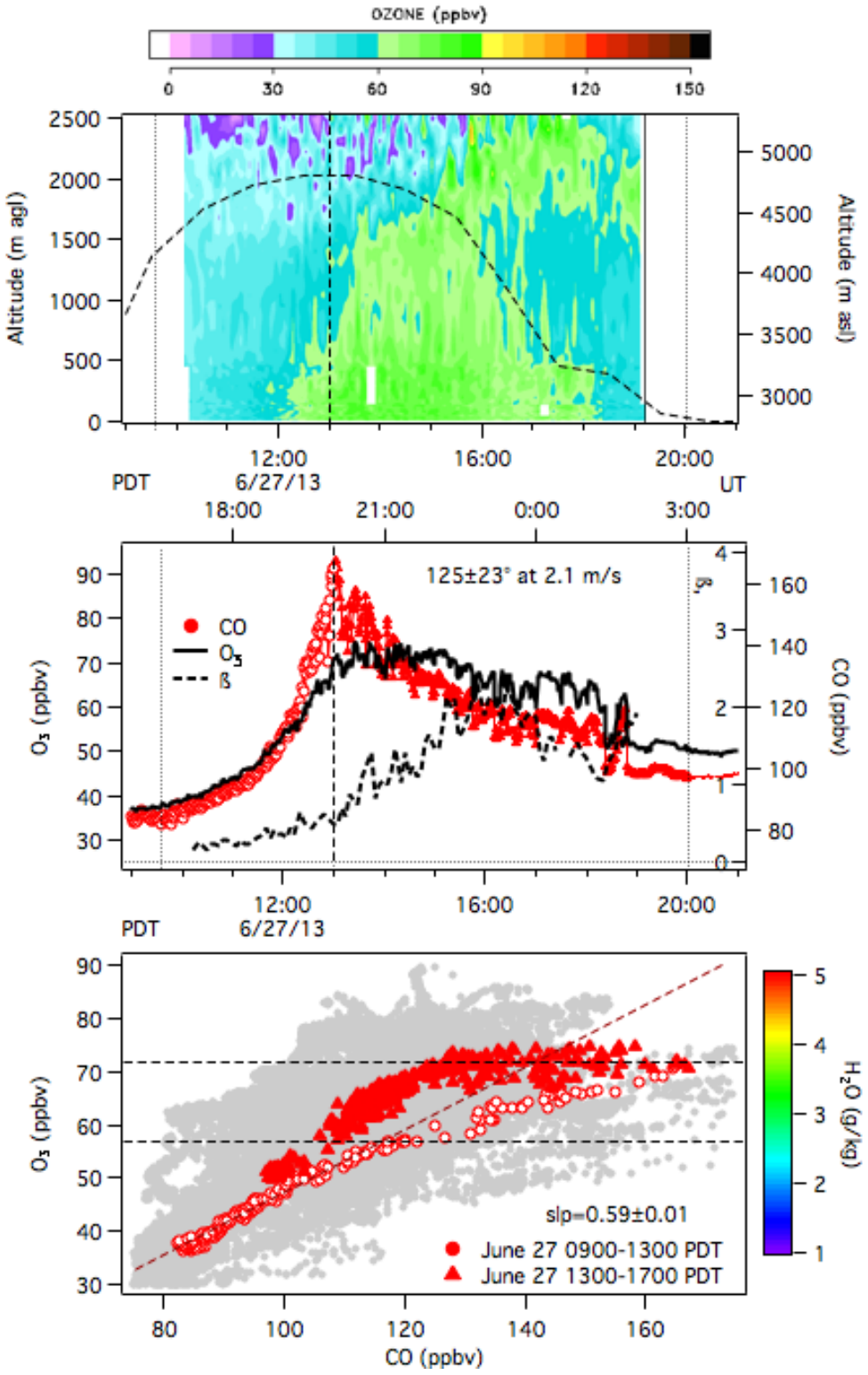

***Figure** C6. (a) TOPAZ O_3 lidar measurements from June 27. (b) time series, and (c) scatter plot showing the corresponding Angel Peak in situ O_3 and CO.*

References

Alvarez II, R. J., et al. (2011), Development and Application of a Compact, Tunable, Solid-State Airborne Ozone Lidar System for Boundary Layer Profiling, *Journal of Atmospheric and Oceanic Technology*, *28*(10), 1258-1272, doi:Doi 10.1175/Jtech-D-10-05044.1.

Ambrose, J. L., D. R. Reidmiller, and D. A. Jaffe (2011), Causes of high O_3 in the lower free troposphere over the Pacific Northwest as observed at the Mt. Bachelor Observatory., *Atmos. Envir.*, *45*, 5302-5315, doi:10.1016/j.atmosenv.2011.06.056.

Brioude, J., et al. (2009), Effect of biomass burning on marine stratocumulus clouds off the California coast, *Atmos. Chem. Phys.*, *9*(22), 8841-8856.

Brioude, J., et al. (2007), Mixing between a stratospheric intrusion and a biomass burning plume, *Atmospheric Chemistry and Physics*, *7*(16), 4229-4235.

Brown-Steiner, B., and P. Hess (2011), Asian influence on surface ozone in the United States: A comparison of chemistry, seasonality, and transport mechanisms, *J. Geophys. Res.-Atmos.*, *116*, doi:Artn D17309, Doi 10.1029/2011jd015846.

Butler, T. J., F. M. Vermeylen, M. Rury, G. E. Likens, B. Lee, G. E. Bowker, and L. McCluney (2011), Response of ozone and nitrate to stationary source NOx emission reductions in the eastern USA, *Atmospheric Environment*, *45*(5), 1084-1094, doi:Doi 10.1016/J.Atmosenv.2010.11.040.

Cooper, O. R., et al. (2004a), On the life cycle of a stratospheric intrusion and its dispersion into polluted warm conveyor belts, *J. Geophys. Res.*, *109*(D23).

Cooper, O. R., et al. (2004b), A case study of trans-Pacific warm conveyor belt transport: The influence of merging airstreams on trace gas import to North America, *J. Geophys. Res.*, *108*(D23S08), doi:10.1029/2003JD003624.

Cooper, O. R., R.-S. Gao, D. Tarasick, T. Leblanc, and C. Sweeney (2012), Long-term ozone trends at rural ozone monitoring sites across the United States, 1990–2010, *J. Geophys. Res*, *117*, doi:10.1029/2012JD018261.

Crutzen, P. J. (1974), Photochemical reactions initiated by and influencing ozone in unpolluted tropospheric air, *Tellus*, *26*, 47-57.

Draxler, R. R., and G. D. Rolph (2003), HYSPLIT (HYbrid Single-Particle Lagrangian Integrated Trajectory) Model access via NOAA ARL READY Website (http://www.arl.noaa.gov/HYSPLIT.php), edited, NOAA Air Resources Laboratory, Silver Spring, MD.

Emanuel, K. A., and M. Zivkovic-Rothman (1999), Development and evaluation of a convective scheme for use in climate models, *J. Atmos. Sci.*, *56*, 1766-1782.

EPA (2012), Our Nation's Air: Status and trends through 2010*Rep.*, U.S. Environmental Protection Agency Research Triangle Park, North Carolina.

Fishman, J., and W. Seiler (1983), Correlative nature of ozone and carbon monoxide in the troposphere: Implications for the tropospheric ozone budget, *J. Geophys. Res.*, *88*, 3662-3670.

Hanna, S. R. (1982), Applications in air pollution modeling, in *Atmospheric Turbulence and Air Pollution Modelling*, edited by F. T. M. Nieuwstadt and H. van Dop, pp. 275–310,, D. Reidel Publishing Company, Dordrecht, Holland.

He, H., et al. (2013), Trends in emissions and concentrations of air pollutants in the lower troposphere in the Baltimore/Washington airshed from 1997 to 2011, *Atmos. Chem. Phys.*, *13*(15), 7859-7874, doi:10.5194/acp-13-7859-2013.

Herman, R. L., et al. (1999), Measurements of CO in the upper troposphere and lower stratosphere, *Chemosphere: Global Change Science*, *1*, 173-183.

Holloway, J. S., R. O. Jakoubek, D. D. Parrish, C. Gerbig, A. Volz-Thomas, S. Schmitgen, A. Fried, B. Wert, B. Henry, and J. R. Drummond (2000), Airborne intercomparison of vacuum ultraviolet fluorescence and tunable

diode laser absorption measurements of tropospheric carbon monoxide, *J. Geophys. Res.-Atmos.*, *105*(D19), 24251-24261, doi:Doi 10.1029/2000jd900237.

Holzer, M., and T. M. Hall (2007), Low-level transpacific transport, *Journal of Geophysical Research*, *112*, D09103.

Jacob, D. J., J. A. Logan, and P. P. Murti (1999), Effect of rising Asian emissions on surface ozone in the United States, *Geophysical Research Letters*, *26*(14), 2175-2178, doi:Doi 10.1029/1999gl900450.

Jaffe, D. A., and N. L. Wigder (2012), Ozone production from wildland fires: A critical review, *Atmospheric Environment*, *51*, 1-10, doi:Doi 10.1016/J.Atmosenv.2011.11.063.

James, P., A. Stohl, C. Forster, S. Eckhardt, P. Seibert, and A. Frank (2003), A 15-year climatology of stratosphere-troposphere exchange with a Lagrangian particle dispersion model 2. Mean climate and seasonal variability *J. Geophys. Res.*, *108*, doi:10.1029/2002JD002639.

Johnson, W. B., and W. Viezee (1981), Stratospheric ozone in the lower troposphere-I. presentation and interpretation of aircraft measurements, *Atmos. Environ.*, *15*, 1309-1323.

Kim, H. S., P. P. Tans, and P. C. Novelli (2008), On the regional background levels of carbon monoxide observed in East Asia during 1991 similar to 2004, *Air Qual Atmos Hlth*, *1*(1), 37-44, doi:Doi 10.1007/S11869-008-0001-3.

Langford, A. O., K. C. Aikin, C. S. Eubank, and E. J. Williams (2009), Stratospheric contribution to high surface ozone in Colorado during springtime, *Geophys. Res. Lett.*, doi:10.1029/2009GL038367.

Langford, A. O., J. Brioude, O. R. Cooper, C. J. Senff, R. J. Alvarez, R. M. Hardesty, B. J. Johnson, and S. J. Oltmans (2012), Stratospheric influence on surface ozone in the Los Angeles area during late spring and early summer of 2010, *J. Geophys. Res.-Atmos.*, *117*, doi:Artn D00v06 Doi 10.1029/2011jd016766.

Langford, A. O., C. J. Senff, R. J. Alvarez, R. M. Banta, and R. M. Hardesty (2010), Long-range transport of ozone from the Los Angeles Basin: A case study, *Geophysical Research Letters*, *37*, doi:Artn L06807
Doi 10.1029/2010gl042507.

Lefohn, A. S., D. Shadwick, and S. J. Oltmans (2010), Characterizing changes in surface ozone levels in metropolitan and rural areas in the United States for 1980-2008 and 1994-2008, *Atmospheric Environment*, *44*(39), 5199-5210, doi:Doi 10.1016/J.Atmosenv.2010.08.049.

Lefohn, A. S., H. Wernli, D. Shadwick, S. Limbach, S. J. Oltmans, and M. Shapiro (2011), The importance of stratospheric-tropospheric transport in affecting surface ozone concentrations in the western and northern tier of the United States, *Atmospheric Environment*, *45*(28), 4845-4857, doi:Doi 10.1016/J.Atmosenv.2011.06.014.

Liang, Q., L. Jaeglé, D. Jaffe, P. Weiss-Penzias, A. Heckman, and J. A. Snow (2004), Long-range transport of Asian pollution to the northeast Pacific: Seasonal variations and transport pathways of carbon monoxide, *Journal of Geophysical Research*, *109*, doi:10.1029/2003JD004402.

Liang, Q., L. Jaegle, and J. M. Wallace (2005), Meteorological indices for Asian outflow and transpacific transport on daily to interannual timescales, *Journal of Geophysical Research*, *110*(D18), D18308.

Lin, M. Y., A. M. Fiore, O. R. Cooper, L. W. Horowitz, A. O. Langford, H. Levy, B. J. Johnson, V. Naik, S. J. Oltmans, and C. J. Senff (2012a), Springtime high surface ozone events over the western United States: Quantifying the role of stratospheric intrusions, *J. Geophys. Res.-Atmos.*, *117*, doi:Artn D00v22
Doi 10.1029/2012jd018151.

Lin, M. Y., et al. (2012b), Transport of Asian ozone pollution into surface air over the western United States in spring, *J. Geophys. Res.-Atmos.*, *117*, doi:Artn D00v07
Doi 10.1029/2011jd016961.

Neuman, J. A., et al. (2011), Ozone transport from the free troposphere to the Los Angeles basin, *J. Geophys. Res.*, doi:10.1029/2011JD016919.

Olivier, J. G. J., J. A. Van Aardenne, F. Dentener, L. Ganzeveld, and J. A. H. W. Peters (2005), Recent trends in global greenhouse gas emissions: regional trends and spatial distribution of key sources, in *Non-CO2 Greenhouse Gases (NCGG-4)* edited by A. v. Amstel, pp. 325-330, Millpress, Rotterdam.

Parrish, D. D., J. S. Holloway, M. Trainer, P. C. Murphy, G. L. Forbes, and F. C. Fehsenfeld (1993), Export of North American ozone pollution to the North Atlantic Ocean, *Science*, *259*, 1436-1439.

Parrish, D. D., M. Trainer, J. S. Holloway, J. E. Yee, M. S. Warshawsky, F. C. Fehsenfeld, G. L. Forbes, and J. L. Moody (1998), Relationships between ozone and carbon monoxide at surface sites in the North Atlantic region, *J. Geophys. Res.-Atmos.*, *103*(D11), 13357-13376, doi:Doi 10.1029/98jd00376.

Pierce, R. B., et al. (2003), Regional Air Quality Modeling System (RAQMS) predictions of the tropospheric ozone budget over east Asia, *J. Geophys. Res.-Atmos.*, *108*(D21), doi:Artn 8825

Doi 10.1029/2002jd003176.

Pierce, R. B., et al. (2007), Chemical data assimilation estimates of continental US ozone and nitrogen budgets during the Intercontinental Chemical Transport Experiment-North America, *J. Geophys. Res.-Atmos.*, *112*(D12), doi:Artn D12s21

Doi 10.1029/2006jd007722.

Prather, M. J., X. Zhu, Q. Tang, J. N. Hsu, and J. L. Neu (2011), An atmospheric chemist in search of the tropopause, *J. Geophys. Res.-Atmos.*, *116*, doi:Artn D04306

Doi 10.1029/2010jd014939.

Seiler, W., and J. Fishman (1981), The Distribution of Carbon-Monoxide and Ozone in the Free Troposphere, *Journal of Geophysical Research-*

Oceans and Atmospheres, *86*(Nc8), 7255-7265, doi:Doi 10.1029/Jc086ic08p07255.

Sprenger, M., and H. Wernli (2003), A northern hemisphere climatology of cross-tropopause exchange for the ERA15 time period (1979-1993), *J. Geophys. Res.*, *108*, doi:10.1029/2002JD002636.

Stohl, A. (2001), A 1-year Lagrangian "climatology" of airstreams in the Northern Hemisphere troposphere and lowermost stratosphere, *J. Geophys. Res.*, *106*, 7263-7279.

Stohl, A., et al. (2007), Arctic smoke - record high air pollution levels in the European Arctic due to agricultural fires in Eastern Europe in spring 2006, *Atmos. Chem. Phys.*, *7*, 511-534.

Stohl, A., C. Forster, A. Frank, P. Seibert, and G. Wotawa (2005), Technical note: The Lagrangian particle dispersion model FLEXPART version 6.2, *Atmos. Chem. Phys.*, *5*, 2461-2474.

Stohl, A., and T. Trickl (1999), A textbook example of long-range transport: Simultaneous observation of ozone maxima of stratospheric and North American origin in the free troposphere over Europe, *J. Geophys. Res.*, *104*, 30445-30462.

Warneck, P. (1988), *Chemistry of the Natural Atmosphere*, 753 pp., Academic Press, San Diego.

Wernli, H., and M. Bourqui (2002), A Lagrangian "1-year climatology" of (deep) cross-tropopause exchange in the extratropical Northern Hemisphere, *J. Geophys. Res.*, *107*(D1-D2), doi:10.1029/2001JD000812.

White, A. B., C. J. Senff, and R. M. Banta (1999), A comparison of mixing depths observed by ground-based wind profilers and an airborne lidar, *J. Atmos. Oceanic Technol.*, *16*, 584-590.

Williams, E. J., F. C. Fehsenfeld, B. T. Jobson, W. C. Kuster, P. D. Goldan, J. Stutz, and W. A. McClenny (2006), Comparison of ultraviolet absorbance, chemiluminescence, and DOAS instruments for ambient ozone monitoring, *Environmental Science and Technology*, *40*(18), doi:10.1021/es0523542.

Wofsy, S. C., et al. (1992), Atmospheric Chemistry in the Arctic and Sub-Arctic - Influence of Natural Fires, Industrial Emissions, and Stratospheric Inputs, *J. Geophys. Res.-Atmos.*, *97*(D15), 16731-16746.

Zhang, L., D. J. Jacob, N. V. Downey, D. A. Wood, D. Blewitt, C. C. Carouge, A. van Donkelaar, D. B. A. Jones, L. T. Murray, and Y. X. Wang (2011), Improved estimate of the policy-relevant background ozone in the United States using the GEOS-Chem global model with 1/2 degrees x 2/3 degrees horizontal resolution over North America, *Atmospheric Environment*, *45*(37), 6769-6776, doi:Doi 10.1016/J.Atmosenv.2011.07.054.